Using Method of Characteristics for Aerospike Nozzle Contour Design

Stephen A. Whitmore
Mechanical and Aerospace Engineering Department

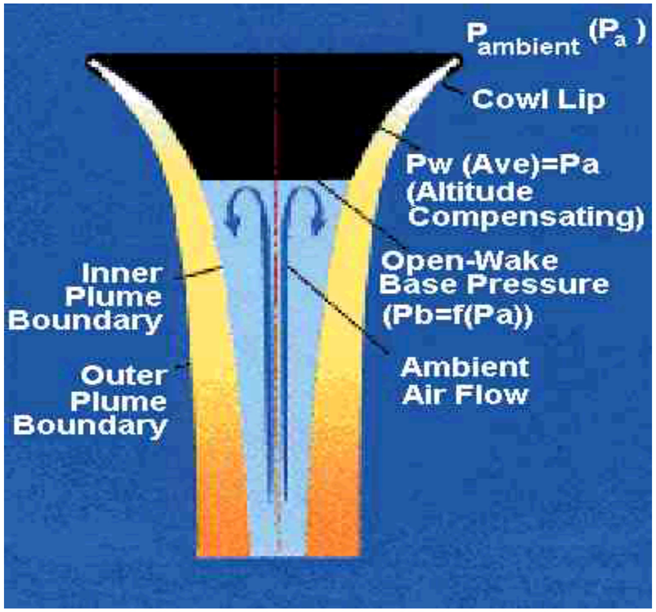

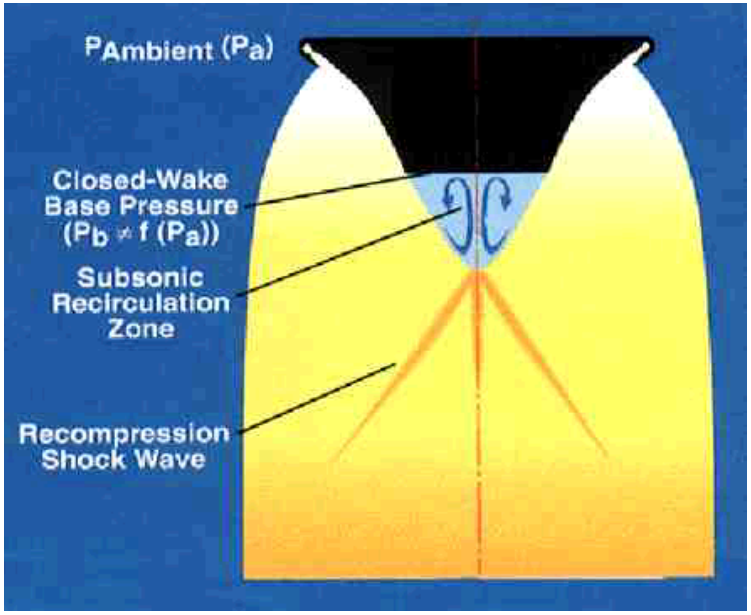

Apply Method of Characteristics to Aerospike Nozzle

NASA TECHNICAL MEMORANDUM

NASA TM X-53019

NASA TM X-53019

FACILITY FORM 602

N69-71654
(ACCESSION NUMBER)

(THRU)

57
(PAGES)

NONE
(CODE)

NASA-TMX#-53019
(NASA CR OR TMX OR AD NUMBER)

(CATEGORY)

July 6, 1964

FORTRAN PROGRAM FOR PLUG NOZZLE DESIGN

by CHE-CHING LEE AND DONALD D. THOMPSON
Propulsion and Vehicle Engineering Laboratory

Apply Method of Characteristics to Aerospike Nozzle (1)

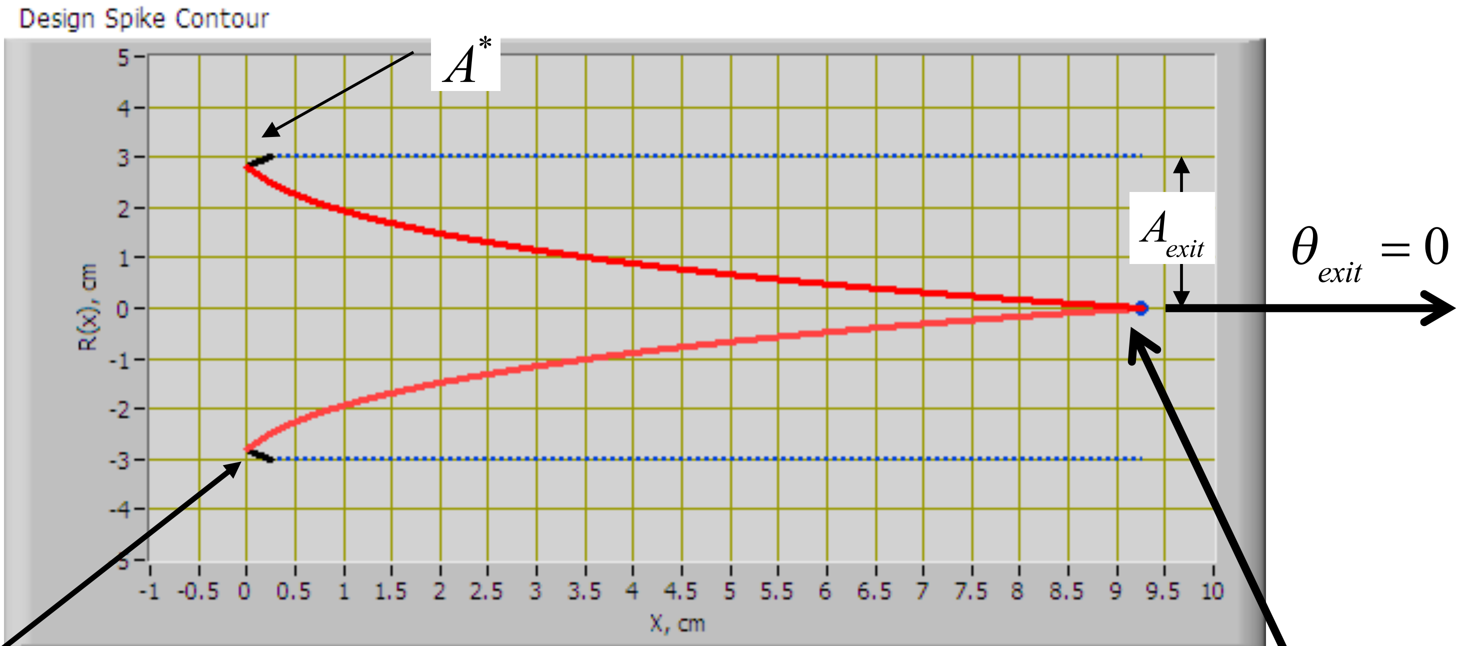

$$\nu_{throat} = \sqrt{\frac{\gamma+1}{\gamma-1}}\tan^{-1}\left\{\sqrt{\frac{\gamma-1}{\gamma+1}\left(1^2-1\right)}\right\} - \tan^{-1}\sqrt{1^2-1} = 0$$

$$\frac{A_{exit}}{A^*} = \left[\frac{1}{M_{exit}}\left[\left(\frac{2}{\gamma+1}\right)\left(1+\frac{(\gamma-1)}{2}M_{exit}{}^2\right)\right]^{\frac{\gamma+1}{2(\gamma-1)}}\right]$$

Apply Method of Characteristics to Aerospike Nozzle (2)

$$\theta_{throat} + \nu_{throat} = \theta_x + \nu_x = \theta_{exit} + \nu_{exit}$$

$$\delta = 90^\circ - \theta_{throat} = 90^\circ - \left(\theta_{exit} + \nu_{exit} - \nu_{throat}\right) \rightarrow$$

$$\rightarrow \nu_{throat} = 0,\ \theta_{exit} = 0$$

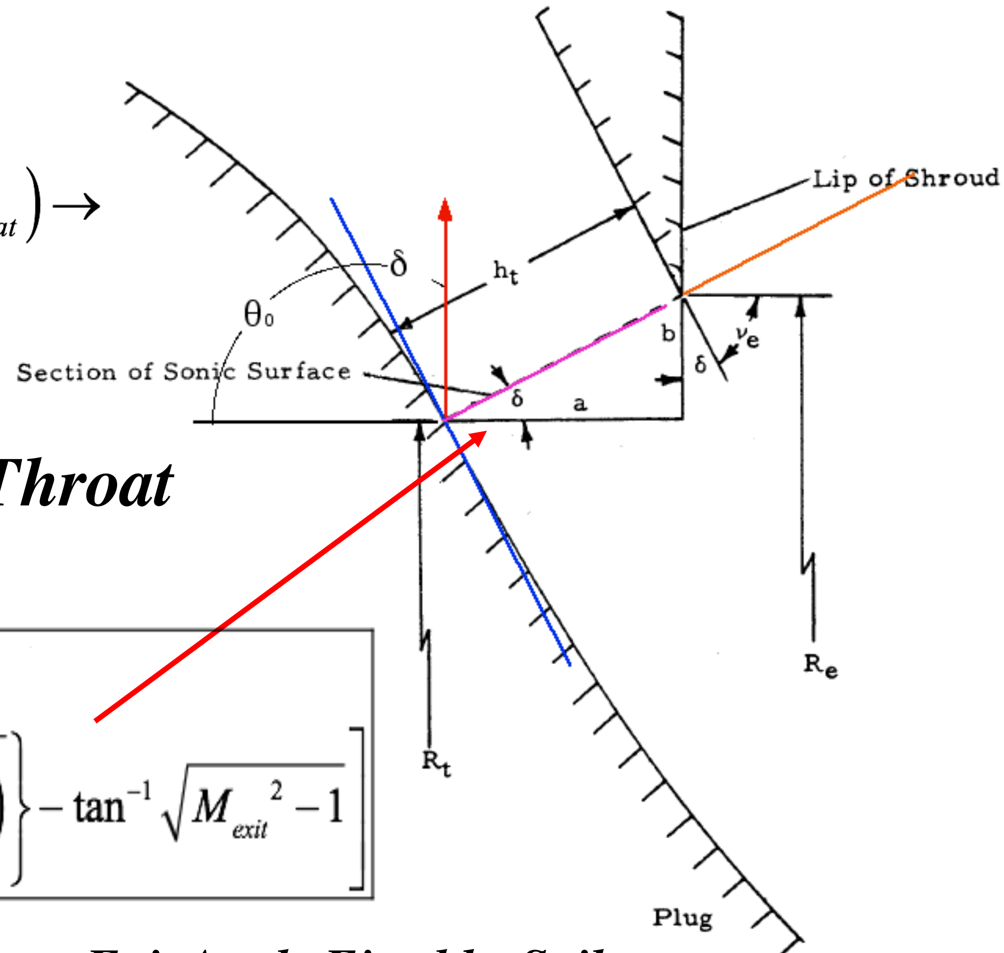

Throat

$$\delta = 90^\circ - \left(\nu_{exit}\right) =$$

$$\text{pi/2} - \left[\sqrt{\frac{\gamma+1}{\gamma-1}}\tan^{-1}\left\{\sqrt{\frac{\gamma-1}{\gamma+1}\left(M_{exit}^{\ 2}-1\right)}\right\} - \tan^{-1}\sqrt{M_{exit}^{\ 2}-1}\right]$$

Throat Exit Angle Fixed by Spike Design expansion ratio

Apply Method of Characteristics to Aerospike Nozzle (3)

$$\theta_x + \nu_x = \nu_{exit}$$

$$\rightarrow \theta_x = \left[\sqrt{\frac{\gamma+1}{\gamma-1}}\tan^{-1}\left\{\sqrt{\frac{\gamma-1}{\gamma+1}\left(M_{exit}^2-1\right)}\right\} - \tan^{-1}\sqrt{M_{exit}^2-1}\right] - \left[\sqrt{\frac{\gamma+1}{\gamma-1}}\tan^{-1}\left\{\sqrt{\frac{\gamma-1}{\gamma+1}\left(M_x^2-1\right)}\right\} - \tan^{-1}\sqrt{M_x^2-1}\right]$$

Along spike surface

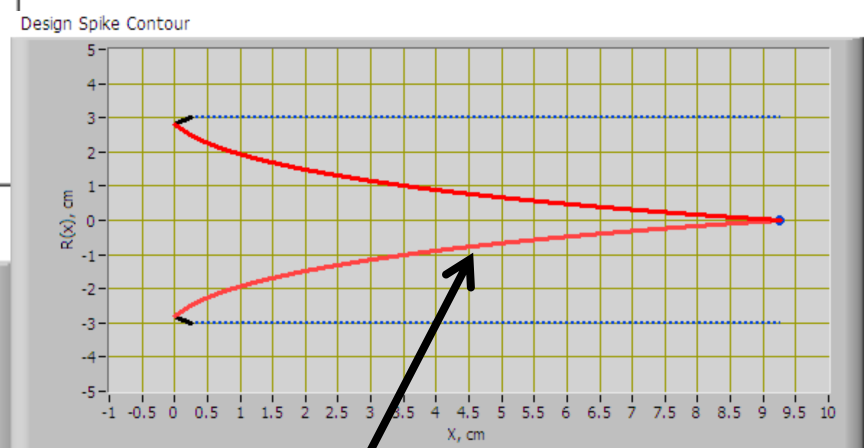

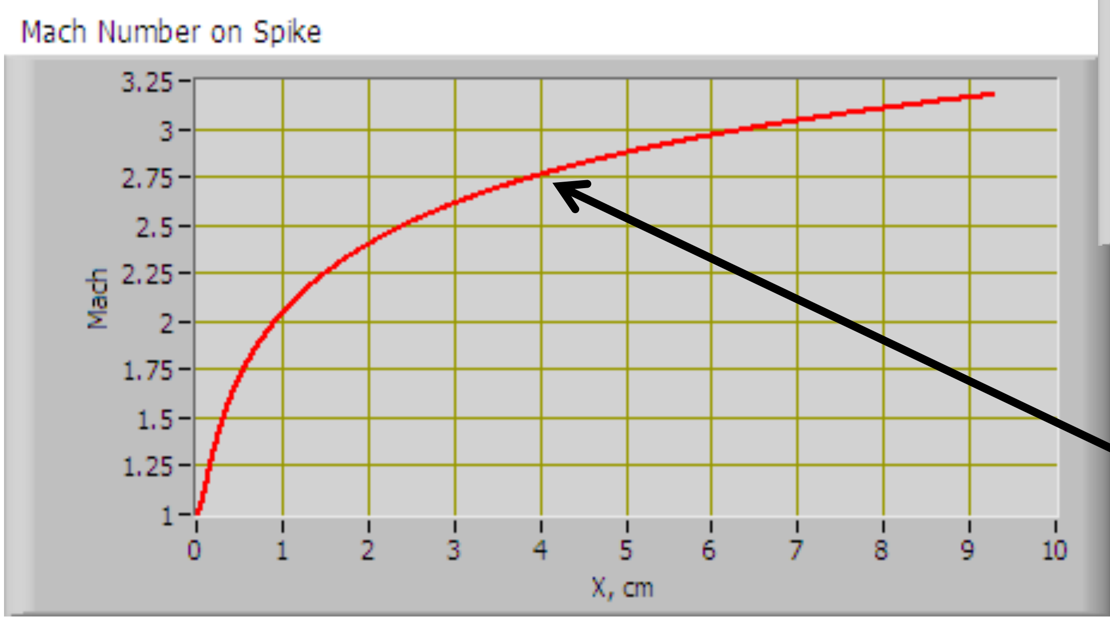

Plug Geometry At position X

$$A_x \sin\phi_x = \pi\left[R_e^{\,2} - R_x^{\,2}\right]$$

$$\left.\begin{array}{l}\phi_x = \theta_x + \mu_x \\ \theta_x = \nu_e - \nu_x\end{array}\right| \Rightarrow \phi_x = \nu_e - \nu_x + \mu_x$$

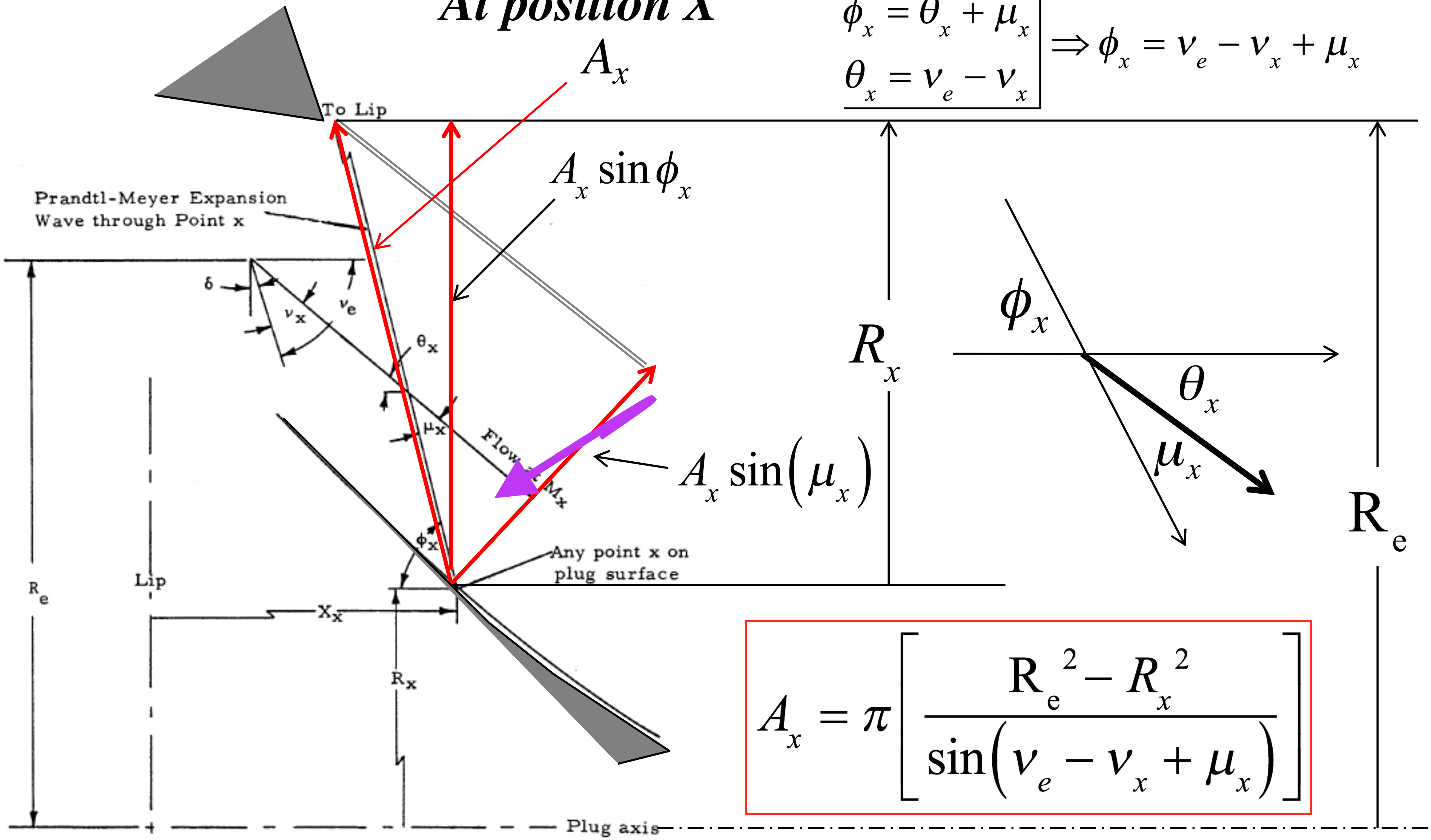

$$A_x = \pi\left[\frac{R_e^{\,2} - R_x^{\,2}}{\sin\left(\nu_e - \nu_x + \mu_x\right)}\right]$$

Apply Continuity equation

$$\dot{m} = \rho_x A_x V_x \sin(\mu_x) = \rho_t A_t V_t$$

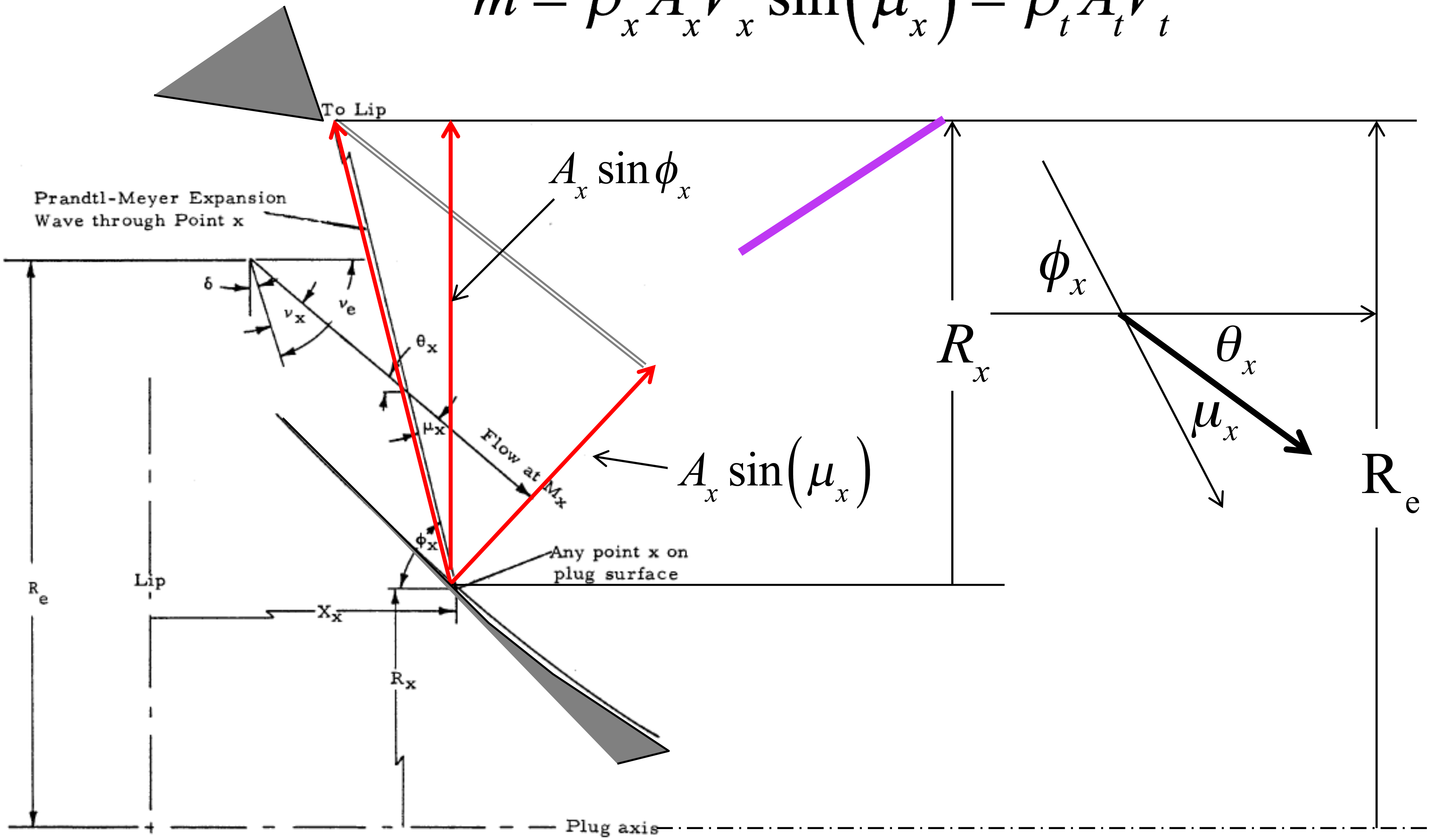

Apply Method of Characteristics to Aerospike Nozzle (5)

- Solving for A_x

$$A_x = \frac{\rho_t A_t}{\rho_x \frac{V_x}{V_t}\sin\left(\mu_x\right)} = \frac{P_t A_t}{T_t \frac{P_x}{T_x}\frac{V_x}{V_t}\sin\left(\mu_x\right)} =$$

$$\frac{P_t A_t}{P_x\sqrt{\frac{T_t}{T_x}}\sqrt{\frac{T_t}{T_x}}\frac{V_x}{V_t}\sin\left(\mu_x\right)} = \frac{P_t A_t}{P_x\sqrt{\frac{T_t}{T_x}}\frac{\sqrt{T_t}}{V_t}\frac{V_x}{\sqrt{T_x}}\sin\left(\mu_x\right)} = \frac{P_t A_t}{P_x\sqrt{\frac{T_t}{T_x}}\frac{M_x}{M_t}\sin\left(\mu_x\right)}$$

- Divide by throat area

$$\frac{A_x}{A_t} = \frac{\frac{P_0}{P_x}\sqrt{\frac{T_x}{T_0}}}{\frac{P_0}{P_t}\sqrt{\frac{T_t}{T_0}}\frac{M_x}{M_t}\sin\left(\mu_x\right)} = \frac{\left[1+\frac{\gamma-1}{2}M_x^{\,2}\right]^{\frac{\gamma}{\gamma-1}}\cdot\left[1+\frac{\gamma-1}{2}M_x^{\,2}\right]^{-1/2}\frac{1}{M_x}}{\left[1+\frac{\gamma-1}{2}M_t^{\,2}\right]^{\frac{\gamma}{\gamma-1}}\cdot\left[1+\frac{\gamma-1}{2}M_t^{\,2}\right]^{-1/2}\cdot\frac{1}{M_t}\cdot\sin\left(\mu_x\right)}$$

Apply Method of Characteristics to Aerospike Nozzle (6)

- Simplifying

$$\frac{A_x}{A_t} = \frac{\left[1+\frac{\gamma-1}{2}M_x^{\,2}\right]^{\frac{\gamma+1}{2(\gamma-1)}}\cdot\frac{1}{M_x}}{\left[1+\frac{\gamma-1}{2}M_t^{\,2}\right]^{\frac{\gamma+1}{2(\gamma-1)}}\cdot\frac{1}{M_t}\cdot\sin(\mu_x)} = \frac{\left[\left(\frac{2}{\gamma+1}\right)\cdot\left(1+\frac{\gamma-1}{2}M_x^{\,2}\right)\right]^{\frac{\gamma+1}{2(\gamma-1)}}\cdot\frac{1}{M_x}}{\left[\left(\frac{2}{\gamma+1}\right)\cdot\left(1+\frac{\gamma-1}{2}M_t^{\,2}\right)\right]^{\frac{\gamma+1}{2(\gamma-1)}}\cdot\frac{1}{M_t}\cdot\sin(\mu_x)} =$$

$$\frac{\left[\left(\frac{2}{\gamma+1}\right)\cdot\left(1+\frac{\gamma-1}{2}M_x^{\,2}\right)\right]^{\frac{\gamma+1}{2(\gamma-1)}}\cdot\frac{1}{M_x}}{\frac{A_t}{A^*}\cdot\sin(\mu_x)} \rightarrow \boxed{\frac{A_x}{A_t}\cdot\frac{A_t}{A^*} = \frac{\left[\left(\frac{2}{\gamma+1}\right)\cdot\left(1+\frac{\gamma-1}{2}M_x^{\,2}\right)\right]^{\frac{\gamma+1}{2(\gamma-1)}}\cdot\frac{1}{M_x}}{\sin(\mu_x)}}$$

Apply Method of Characteristics to Aerospike Nozzle (7)

- Simplifying again

$$A_x = A^* \frac{\left[\left(\frac{2}{\gamma+1}\right)\cdot\left(1+\frac{\gamma-1}{2}M_x^{\ 2}\right)\right]^{\frac{\gamma+1}{2(\gamma-1)}}\cdot\frac{1}{M_x}}{\sin(\mu_x)} \rightarrow \sin(\mu_x) = \frac{1}{M_x}$$

$$A_x = A^*\left[\left(\frac{2}{\gamma+1}\right)\cdot\left(1+\frac{\gamma-1}{2}M_x^{\ 2}\right)\right]^{\frac{\gamma+1}{2(\gamma-1)}} = \frac{A_e}{\varepsilon}\left[\left(\frac{2}{\gamma+1}\right)\cdot\left(1+\frac{\gamma-1}{2}M_x^{\ 2}\right)\right]^{\frac{\gamma+1}{2(\gamma-1)}} =$$

$$\frac{\pi \mathrm{R_e}^2}{\varepsilon}\left[\left(\frac{2}{\gamma+1}\right)\cdot\left(1+\frac{\gamma-1}{2}M_x^{\ 2}\right)\right]^{\frac{\gamma+1}{2(\gamma-1)}}$$

thus

$$A_x = \frac{\pi\left(\mathrm{R_e}^2 - R_x^{\ 2}\right)}{\sin\left(\nu_e - \nu_x + \mu_x\right)} = \frac{\pi \mathrm{R_e}^2}{\varepsilon}\left[\left(\frac{2}{\gamma+1}\right)\cdot\left(1+\frac{\gamma-1}{2}M_x^{\ 2}\right)\right]$$

Apply Method of Characteristics to Aerospike Nozzle (8)

- Solve for R_x

$$\left(1-\left(\frac{R_x}{\mathrm{R_e}}\right)^2\right)=\frac{\sin\left(\nu_e-\nu_x+\mu_x\right)}{\varepsilon}\left[\left(\frac{2}{\gamma+1}\right)\cdot\left(1+\frac{\gamma-1}{2}M_x^{\ 2}\right)\right]^{\frac{\gamma+1}{2(\gamma-1)}}$$

$$\rightarrow\frac{R_x}{\mathrm{R_e}}=\sqrt{1-\frac{\sin\left(\nu_e-\nu_x+\mu_x\right)}{\varepsilon}\left[\left(\frac{2}{\gamma+1}\right)\cdot\left(1+\frac{\gamma-1}{2}M_x^{\ 2}\right)\right]^{\frac{\gamma+1}{2(\gamma-1)}}}$$

Apply Method of Characteristics to Aerospike Nozzle (9)

- and since by geometry of the surface

$$\tan\phi_x = \frac{R_e - R_x}{X_x} \rightarrow \phi_x = \nu_e - \nu_x + \mu_x \rightarrow$$

$$X_x = \frac{R_{exit} - R_x}{\tan\left(\nu_e - \nu_x + \mu_x\right)}$$

$$R_x = R_{exit}\sqrt{1 - \frac{\sin\left(\nu_e - \nu_x + \mu_x\right)}{\varepsilon}\left[\left(\frac{2}{\gamma+1}\right)\cdot\left(1 + \frac{\gamma-1}{2}M_x^{\,2}\right)\right]^{\frac{\gamma+1}{2(\gamma-1)}}}$$

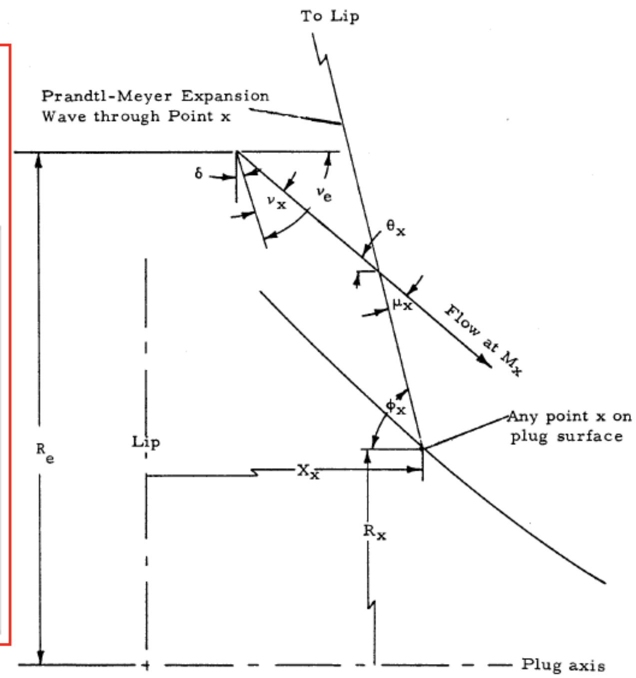

$$\sin\left(\mu_x\right) = \frac{1}{M_x}$$

- These equations define the isentropic spike profile

Aerospike Contour Computational Algorithm(9)

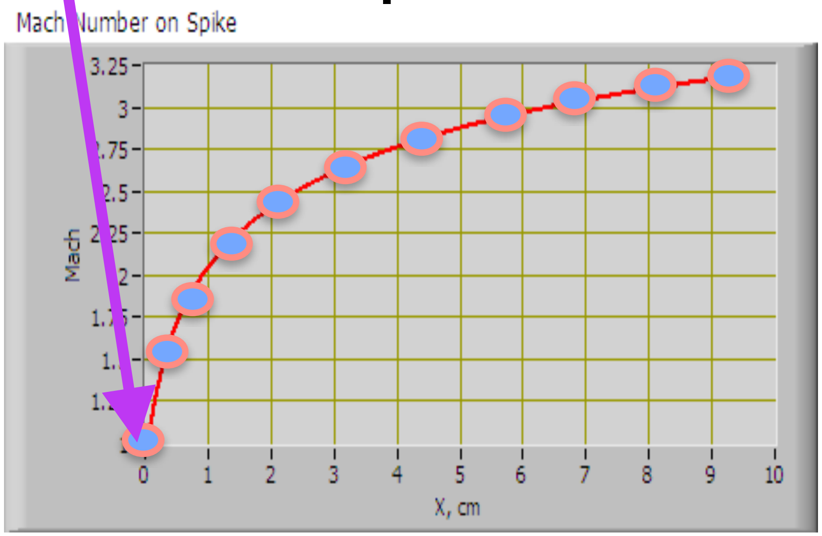

- Step up in M from $M=1 \ldots M_{exit}$

$$\nu_{exit} = \sqrt{\frac{\gamma+1}{\gamma-1}} \tan^{-1}\left[\sqrt{\frac{\gamma-1}{\gamma+1}\left(M_{exit}^{2}-1\right)}\right] - \tan^{-1}\left[\sqrt{M_{exit}^{2}-1}\right]$$

$$\nu_{x} = \sqrt{\frac{\gamma+1}{\gamma-1}} \tan^{-1}\left[\sqrt{\frac{\gamma-1}{\gamma+1}\left(M_{x}^{2}-1\right)}\right] - \tan^{-1}\left[\sqrt{M_{x}^{2}-1}\right]$$

$$\mu_x = \sin^{-1} M_x$$

$$R_x = R_{exit}\sqrt{1-\left(\frac{\sin\left(\nu_{exit}-\nu_x+\mu_x\right)}{\varepsilon}\right)\cdot\left[\left(\frac{2}{\gamma+1}\left(1+\frac{\gamma-1}{2}M_x^2\right)\right)^{\frac{\gamma+1}{2(\gamma-1)}}\right]}$$

$$X_x = \frac{R_{exit}-R_x}{\tan\left(\nu_{exit}-\nu_x+\mu_x\right)}$$

Apply Method of Characteristics to Aerospike Nozzle (10)

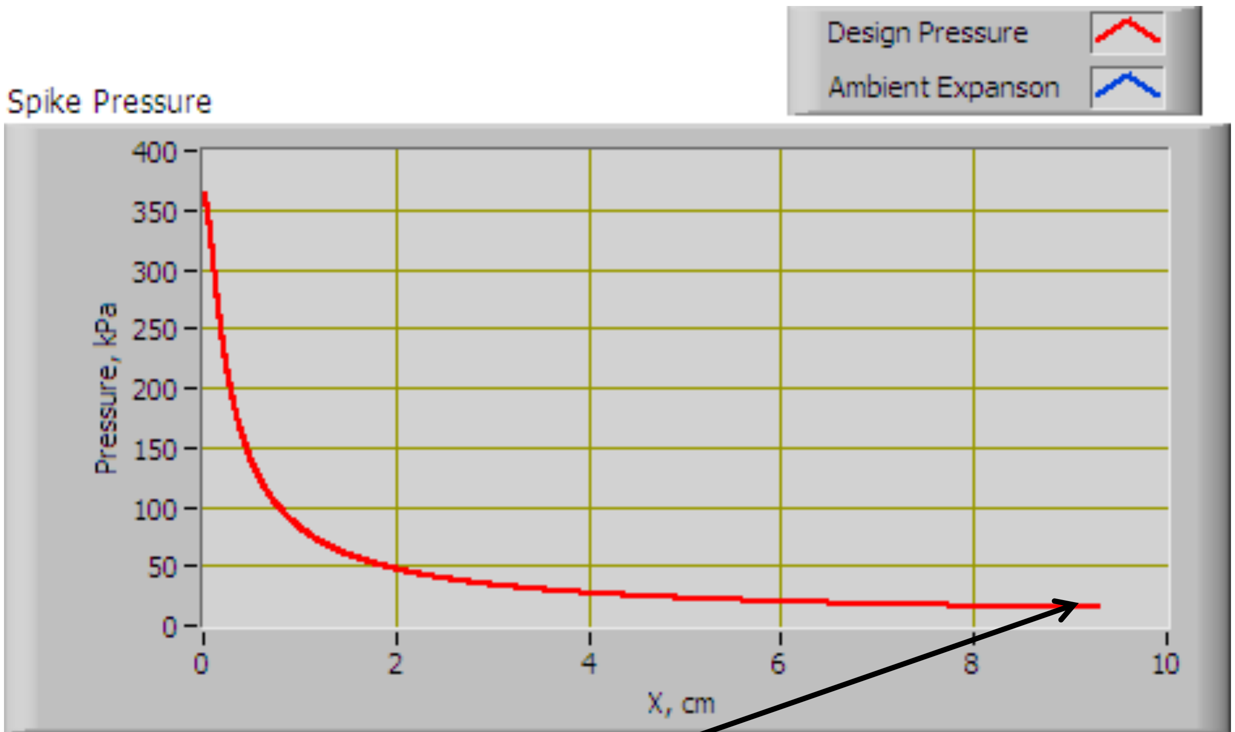

Exit pressure expands to ambient condition

Apply Method of Characteristics to Aerospike Nozzle (11)

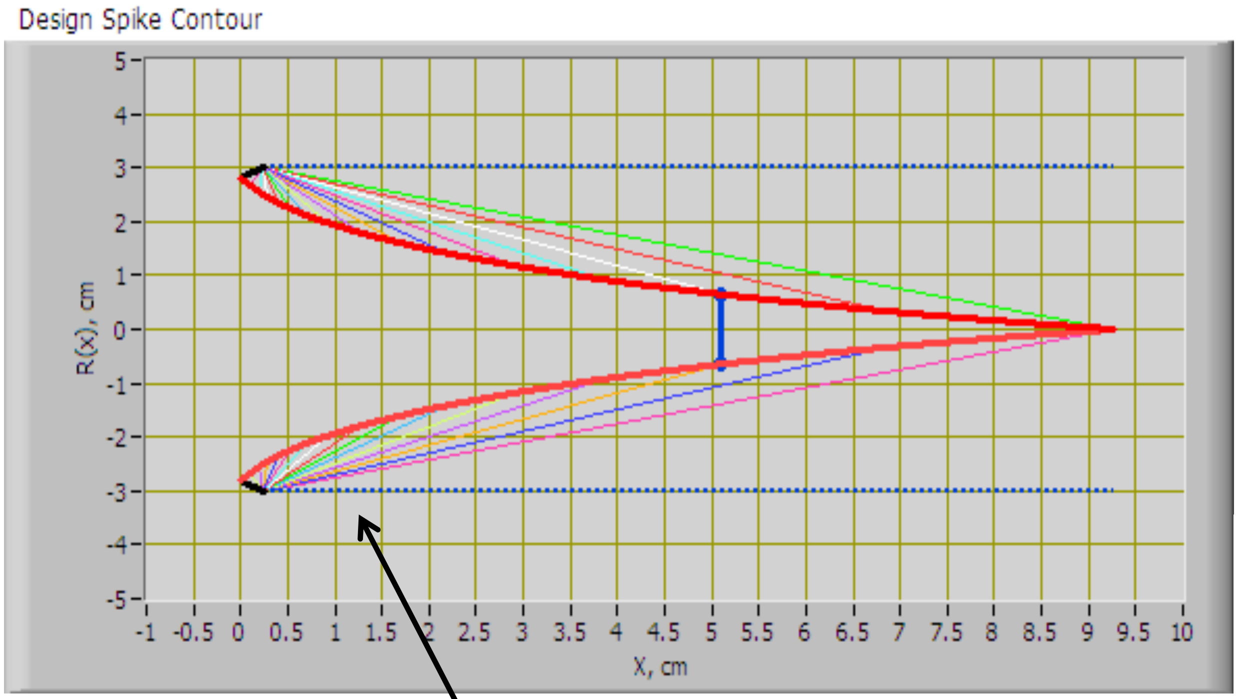

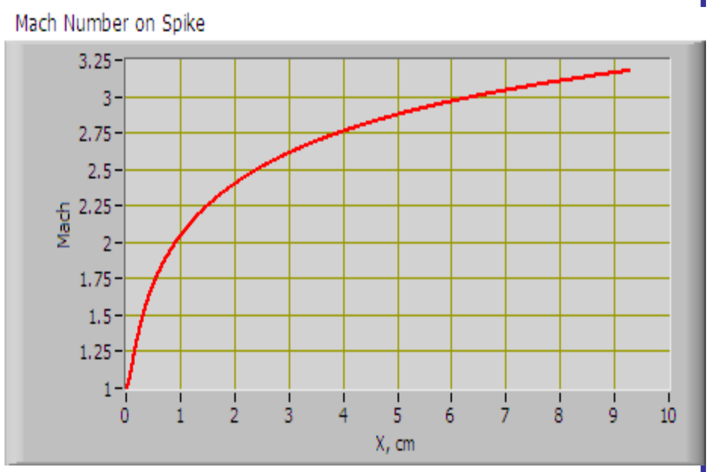

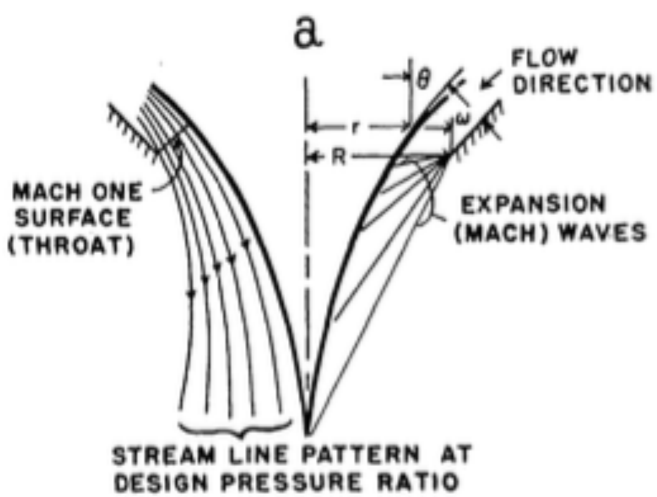

$$\mu_x = \sin^{-1}\left(\frac{1}{M_x}\right)$$

"Mach lines" converge on cowl lip

Thrust Calculation

• This algorithm works for both Design and Off-design configuration where Altitude Greater than Design Condition (8)

$$F_{total} = F_{throat} + F_{spike}$$

$$F_{throat} = \left[\dot{m} \cdot V_{throat} + \left(p_{throat} - p_{\infty}\right) \cdot A^{*}\right] \cdot \sin\delta_{throat}$$

$$\rightarrow F_{throat} = \left[\dot{m} \cdot \sqrt{\gamma \cdot R_{g} \cdot T^{*}} + \left(p^{*} - p_{\infty}\right) \cdot A^{*}\right] \cdot \sin\delta_{throat}$$

$$T^{*} = \frac{T_{0}}{\left(\gamma+1\right)/2} \rightarrow p^{*} = \frac{P_{0}}{\left[\left(\gamma+1\right)/2\right]^{\frac{\gamma}{\gamma-1}}}$$

Thrust Calculation

- Impulse Thrust at Throat exit

Lift off

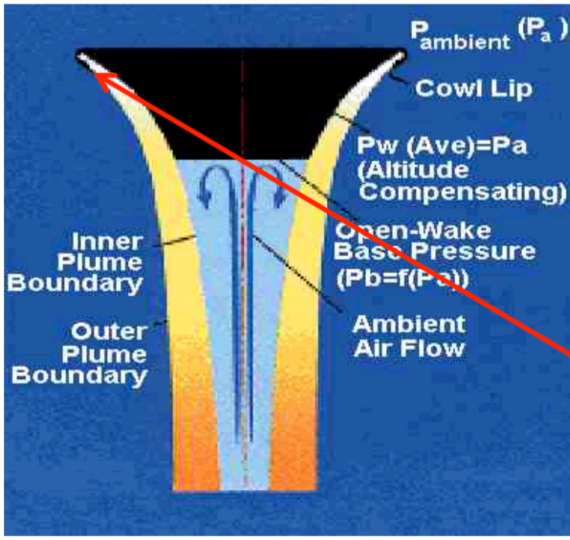

Vacuum (Space)

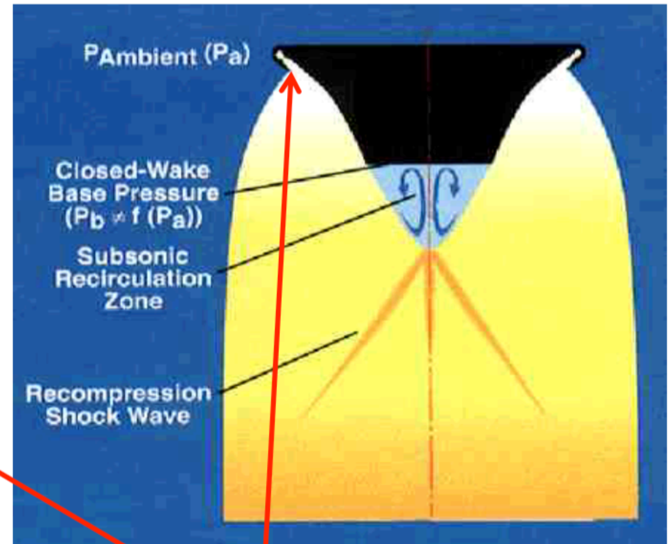

Thrust from throat exit

$$F_{throat} = \left[\dot{m} \cdot V_{throat} + \left(p_{throat} - p_{\infty}\right) \cdot A^*\right] \cdot \sin\delta_{throat}$$

$$\rightarrow F_{throat} = \left[\dot{m} \cdot \sqrt{\gamma \cdot R_g \cdot T^*} + \left(p^* - p_{\infty}\right) \cdot A^*\right] \cdot \sin\delta_{throat}$$

$$T^* = \frac{T_0}{(\gamma+1)/2} \rightarrow p^* = \frac{P_0}{\left[(\gamma+1)/2\right]^{\frac{\gamma}{\gamma-1}}}$$

Thrust Calculation (2)

Calculate ramp pressure force

$$\delta F_j = \left(\frac{p_j + p_{j+1}}{2} - p_\infty\right) \cdot dA_j \cdot \sin\theta$$

From geometry

$$dA_j = \frac{\left(X_{j+1} - X_j\right)}{\cos\theta_j} \cdot 2\pi \cdot \left(\frac{R_j + R_{j+1}}{2}\right)$$

Substitute

$$\delta F_j = \left(\frac{p_j + p_{j+1}}{2} - p_\infty\right) \cdot dA_j \cdot \sin\theta = \left(\frac{p_j + p_{j+1}}{2} - p_\infty\right) \cdot \frac{\left(X_{j+1} - X_j\right)}{\cos\theta_j} \cdot \pi \cdot \left(R_j + R_{j+1}\right) \cdot \sin\theta_j$$

$$= \left(\frac{p_j + p_{j+1}}{2} - p_\infty\right) \cdot \left(X_{j+1} - X_j\right) \cdot \tan\theta_j \cdot \pi \cdot \left(R_j + R_{j+1}\right)$$

Pressure Thrust Force Increment Across Surface Element

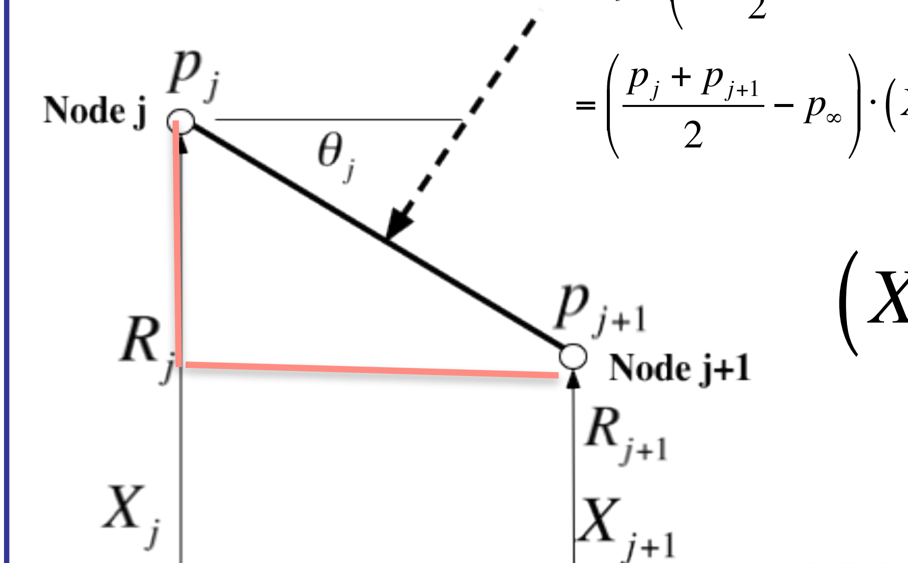

From Geometry

$$\left(X_{j+1} - X_j\right) \cdot \tan\theta_j = \left(R_j - R_{j+1}\right)$$

→

Thrust Calculation (3)

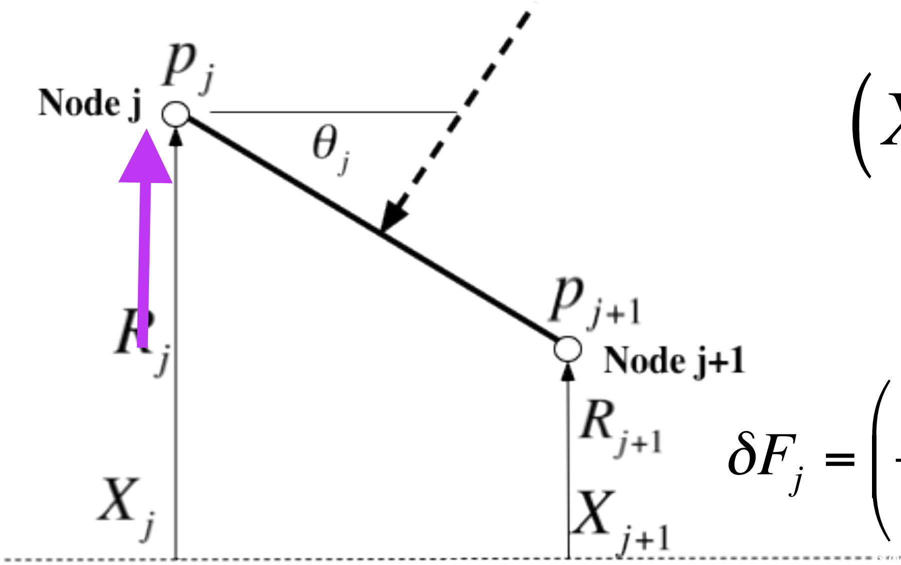

$$\left(X_{j+1} - X_j\right) \cdot \tan\theta_j = \left(R_j - R_{j+1}\right)$$

→Difference of squares

$$\delta F_j = \left(\frac{p_j + p_{j+1}}{2} - p_\infty\right) \cdot \pi \cdot \left(R_j - R_{j+1}\right)\left(R_j + R_{j+1}\right) =$$

$$\left(\frac{p_j + p_{j+1}}{2} - p_\infty\right) \cdot \pi \cdot \left(R_j^2 - R_{j+1}^2\right)$$

$$F_{ramp} = \sum_{j=0}^{N} \left(\frac{p_j + p_{j+1}}{2} - p_\infty\right) \cdot \pi \cdot \left(R_j^2 - R_{j+1}^2\right)$$

Ramp Pressure Thrust

Lift off

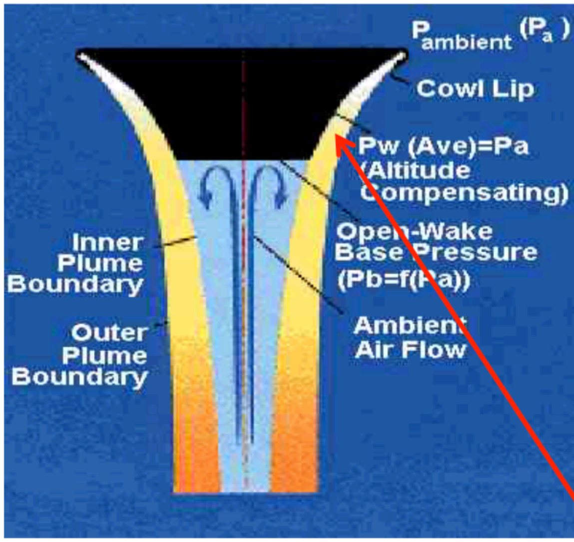

Vacuum (Space)

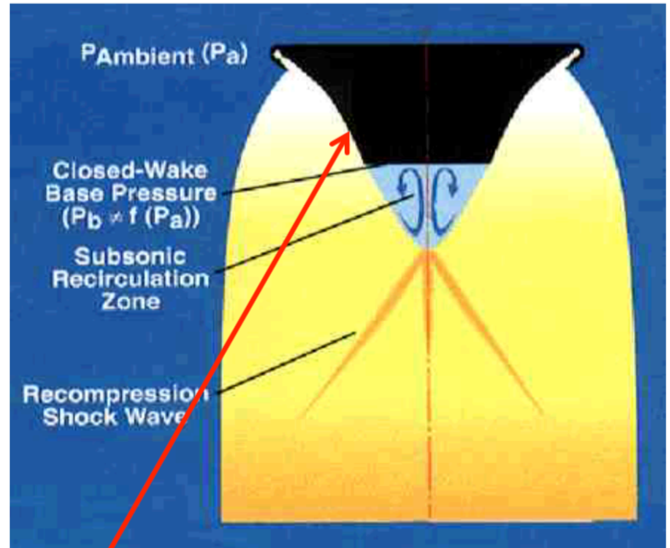

$$F_{ramp} = \sum_{j=0}^{N} \left(\frac{p_j + p_{j+1}}{2} - p_{\infty} \right) \cdot \pi \cdot \left(R_j^2 - R_{j+1}^2 \right)$$

Collected Thrust Calculation

Lift off

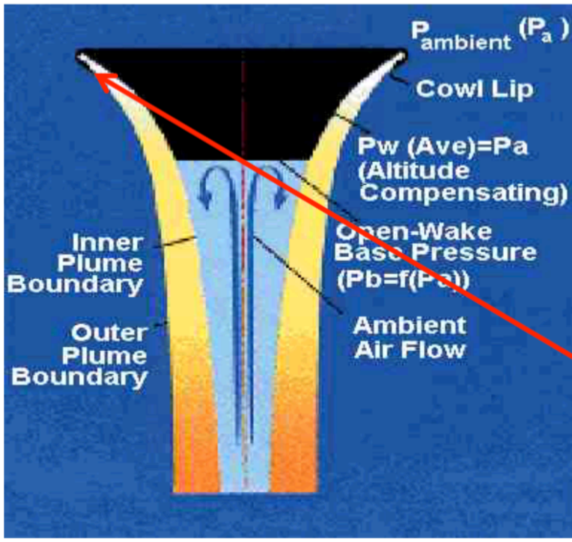

Vacuum (Space)

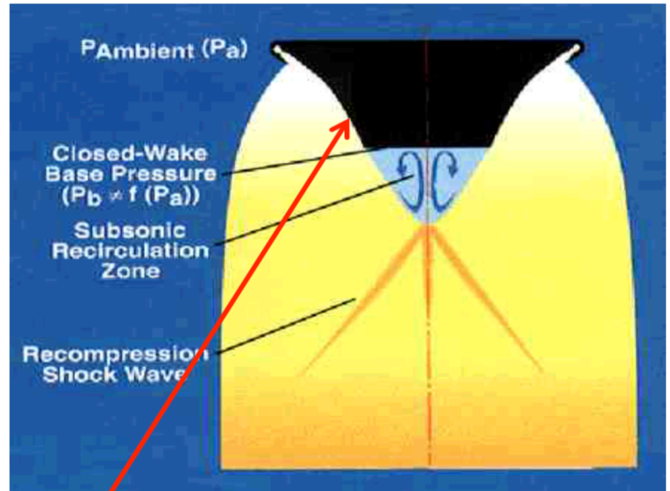

$$F_{ramp} = \sum_{j=0}^{N} \left(\frac{p_j + p_{j+1}}{2} - p_\infty \right) \cdot \pi \cdot \left(R_j^2 - R_{j+1}^2 \right)$$

Thrust from throat exit

$$F_{throat} = \left[\dot{m} \cdot V_{throat} + \left(p_{throat} - p_\infty \right) \cdot A^* \right] \cdot \sin \delta_{throat}$$

$$\rightarrow F_{throat} = \left[\dot{m} \cdot \sqrt{\gamma \cdot R_g \cdot T^*} + \left(p^* - p_\infty \right) \cdot A^* \right] \cdot \sin \delta_{throat}$$

$$T^* = \frac{T_0}{(\gamma+1)/2} \rightarrow p^* = \frac{P_0}{\left[(\gamma+1)/2\right]^{\frac{\gamma}{\gamma-1}}}$$

Off Design Operation

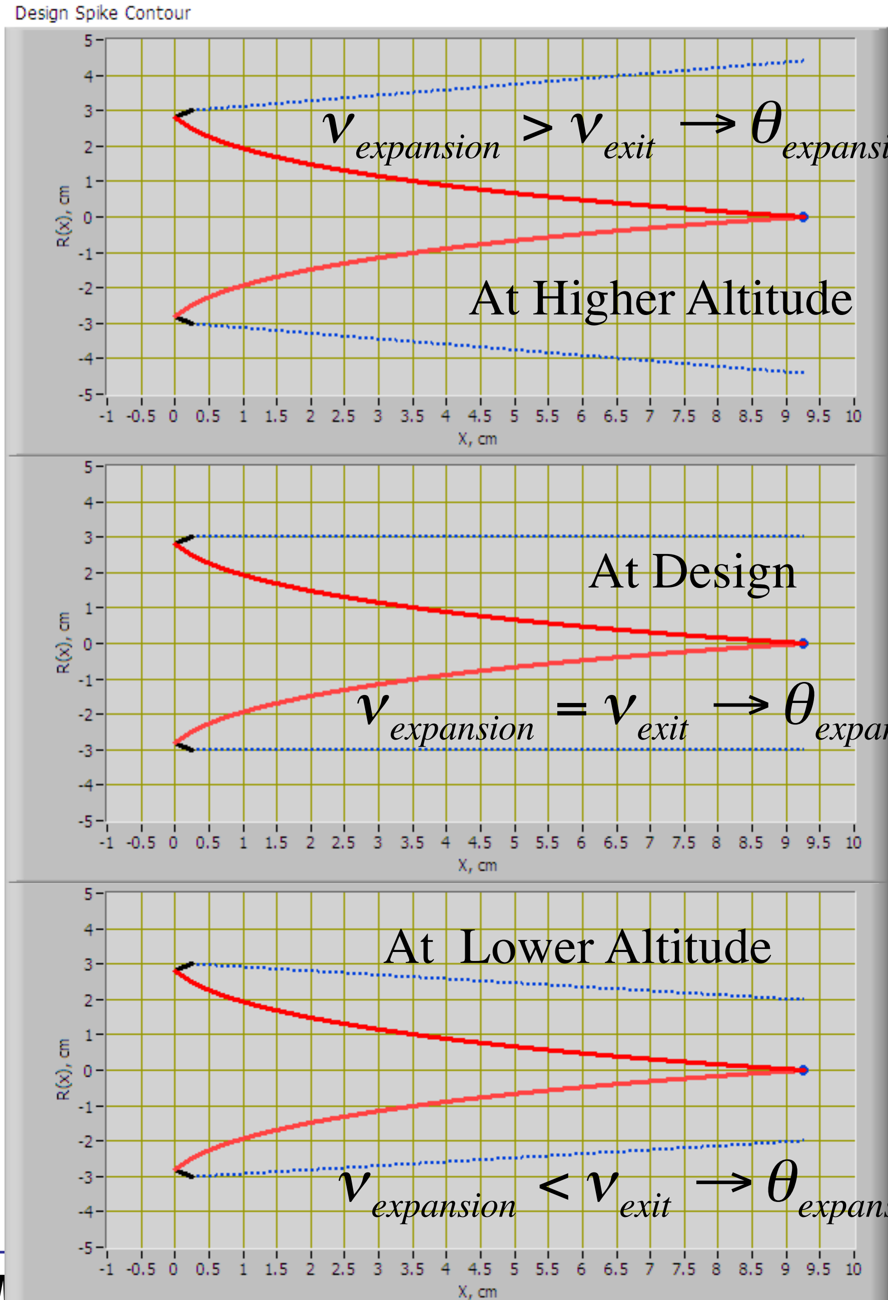

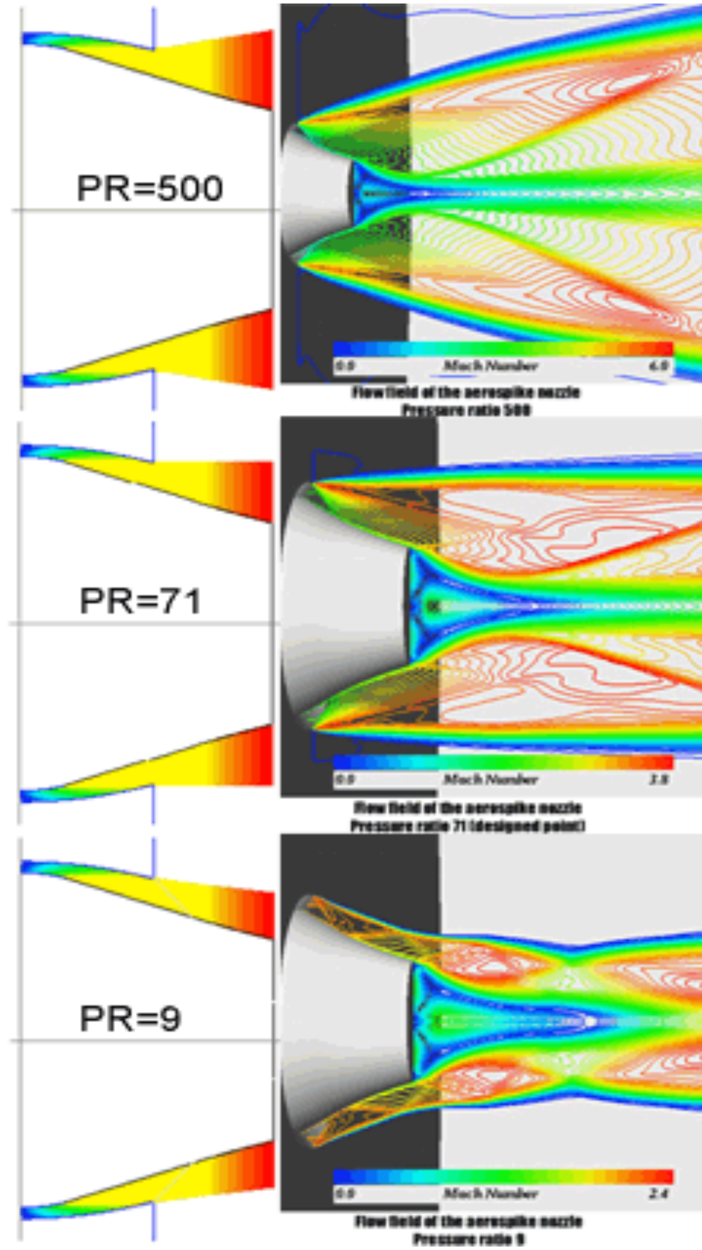

At Higher Altitude

$$\nu_{expansion} > \nu_{exit} \rightarrow \theta_{expansion} > 0$$

At Design

$$\nu_{expansion} = \nu_{exit} \rightarrow \theta_{expansion} = 0$$

At Lower Altitude

$$\nu_{expansion} < \nu_{exit} \rightarrow \theta_{expansion} < 0$$

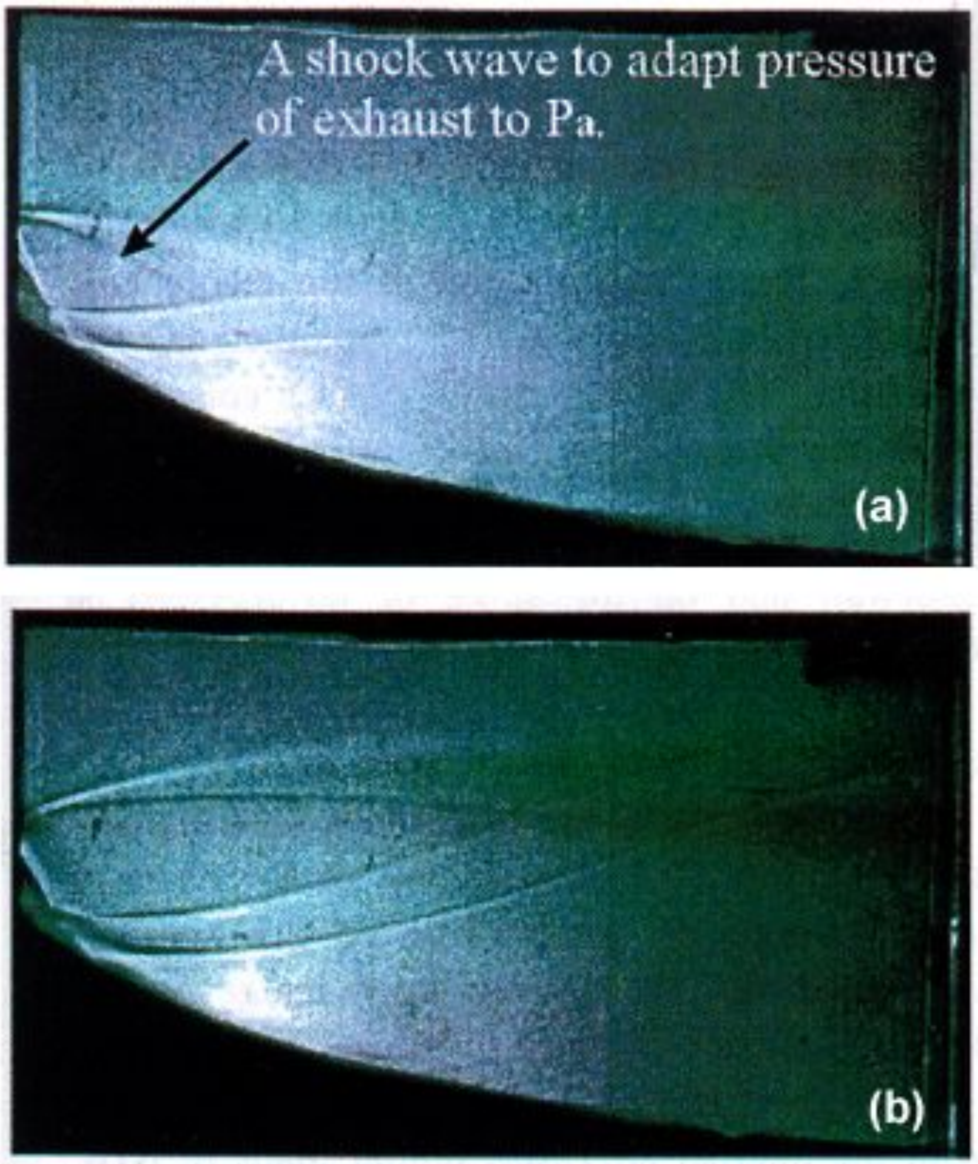

Credit: Aerospace web

- Shadowgraph flow visualization of an ideal isentropic spike at

(a) low altitude and
(b) high altitude conditions

[from Tomita et al, 1998]

Off Design Operation (1)
Altitude Greater than Design Condition

Calculating the Off-design conditions

Design Spike Contour

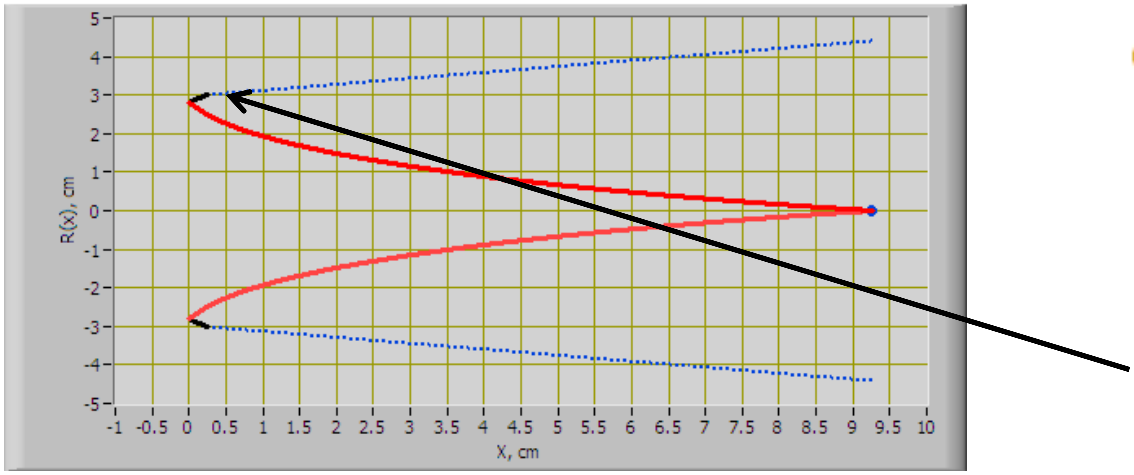

Design Altitude, km

13.8263

Operating Altitude, km

21.254

- Throat exit expands to ambient conditions' due to unconstrained flow

- Use Isentropic Flow laws to calculate effective expansion Mach number .. as flow "turns corner"

$$M_{expansion} = \sqrt{\left(\frac{2}{\gamma - 1}\right)\left[\left(\frac{P_0}{p_{amb}}\right)^{\frac{(\gamma-1)}{\gamma}} - 1\right]}$$

Off Design Operation (2)
Altitude Greater than Design Condition

- calculate turning angle

$$M_{expansion} = \sqrt{\left(\frac{2}{\gamma - 1}\right)\left[\left(\frac{P_0}{p_{amb}}\right)^{\frac{(\gamma-1)}{\gamma}} - 1\right]}$$

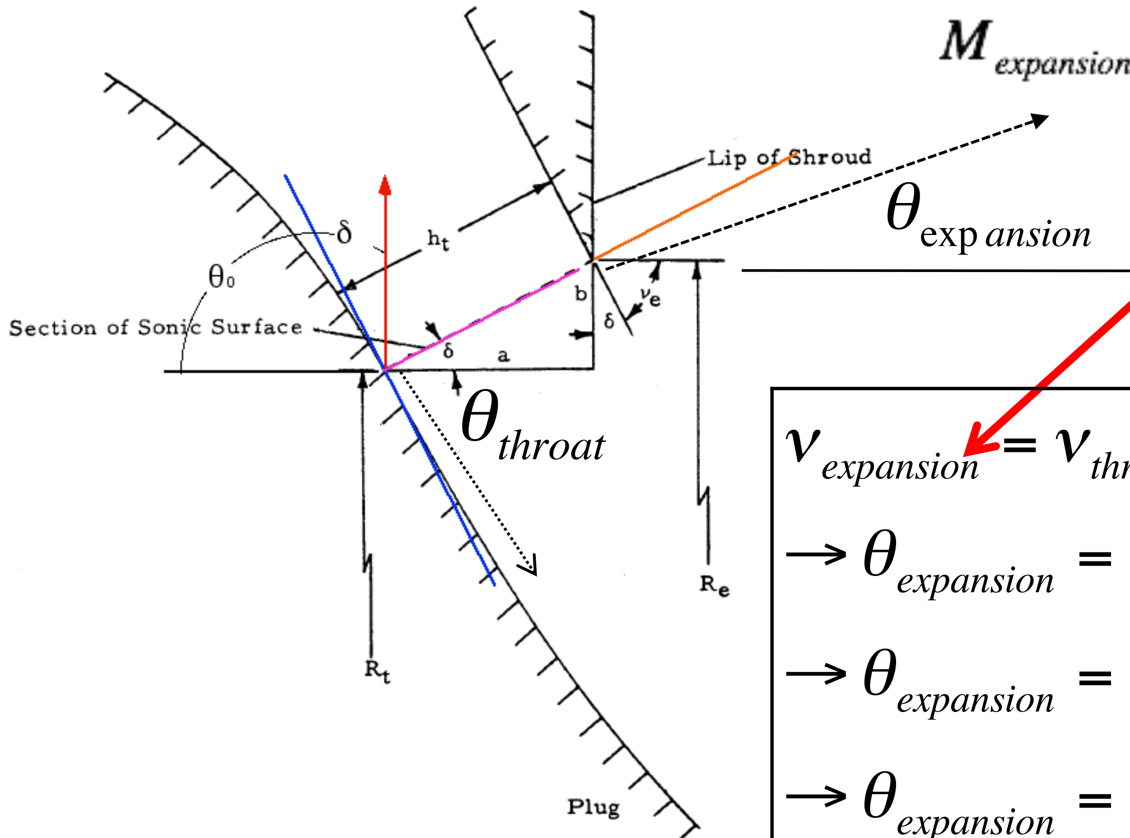

$$\nu_{expansion} = \nu_{throat} + \left(\theta_{expansion} - \theta_{throat}\right)$$

$$\rightarrow \theta_{expansion} = \nu_{expansion} + \theta_{throat}$$

$$\rightarrow \theta_{expansion} = \nu_{expansion} + \delta_{throat} - 90^0$$

$$\rightarrow \theta_{expansion} = \nu_{expansion} + \left(90^0 - \nu_{exit}\right) - 90^0$$

$$\rightarrow \boxed{\theta_{expansion} = \nu_{expansion} - \nu_{exit}}$$

@ design condition

Off Design Operation

Altitude Greater than Design Condition (3)

$$\theta_{expansion} = \nu_{expansion} - \left(\nu_{exit}\right)_{\substack{design \\ condition}}$$

Design Altitude, 13.8263

Operating Altitude, km 21.254

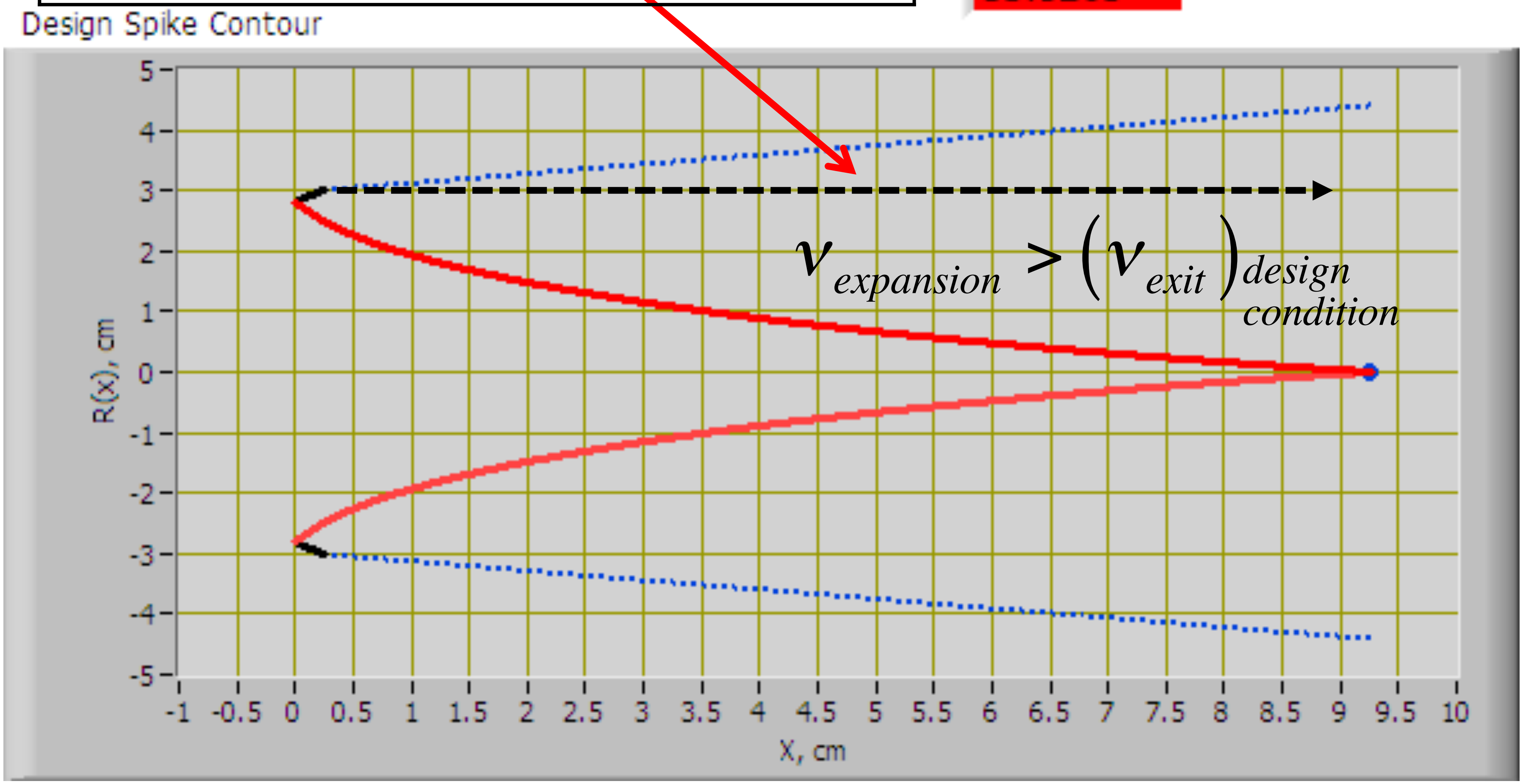

Off Design Operation Altitude Greater than Design Condition (4)

"Left" characteristics lines … intersect expansion slip line

$$\begin{bmatrix} \theta \\ M \\ \nu \end{bmatrix}_{expansion}$$

$$\rightarrow \theta_x - \nu_x = \theta_{expansion} - \nu_{expansion}$$

$$\rightarrow \boxed{\nu_x = \nu_{expansion} - \theta_{expansion} + \theta_x}$$

Expansion slip line

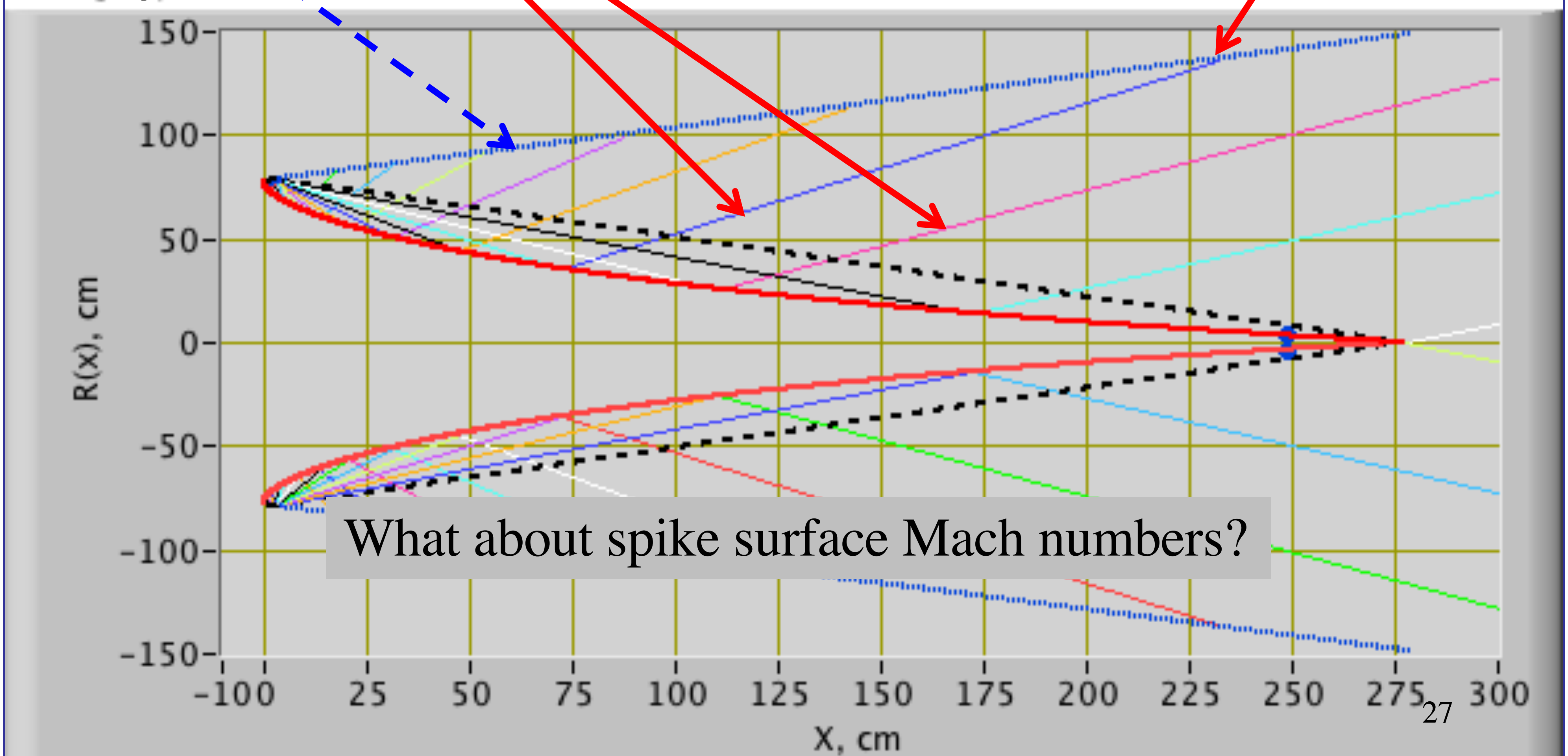

What about spike surface Mach numbers?

Off Design Operation Altitude Greater than Design Condition (5)

"Left" characteristics lines … Intersect expansion line

$$\rightarrow \theta_x - \nu_x = \theta_{expansion} - \nu_{expansion}$$

$$\rightarrow \boxed{\nu_x = \nu_{expansion} - \theta_{expansion} + \theta_x}$$

$$\rightarrow \nu_x = \nu_{expansion} - \left(\nu_{expansion} - \left(\nu_{exit}\right)_{\substack{design\\condition}}\right) + \theta_x$$

$$\rightarrow \boxed{\nu_x = \left(\nu_{exit}\right)_{\substack{design\\condition}} + \theta_x}$$

- … *Which is our original spike contour prescription!* !

See … Slide 5

Off Design Operation Altitude Greater than Design Condition (5)

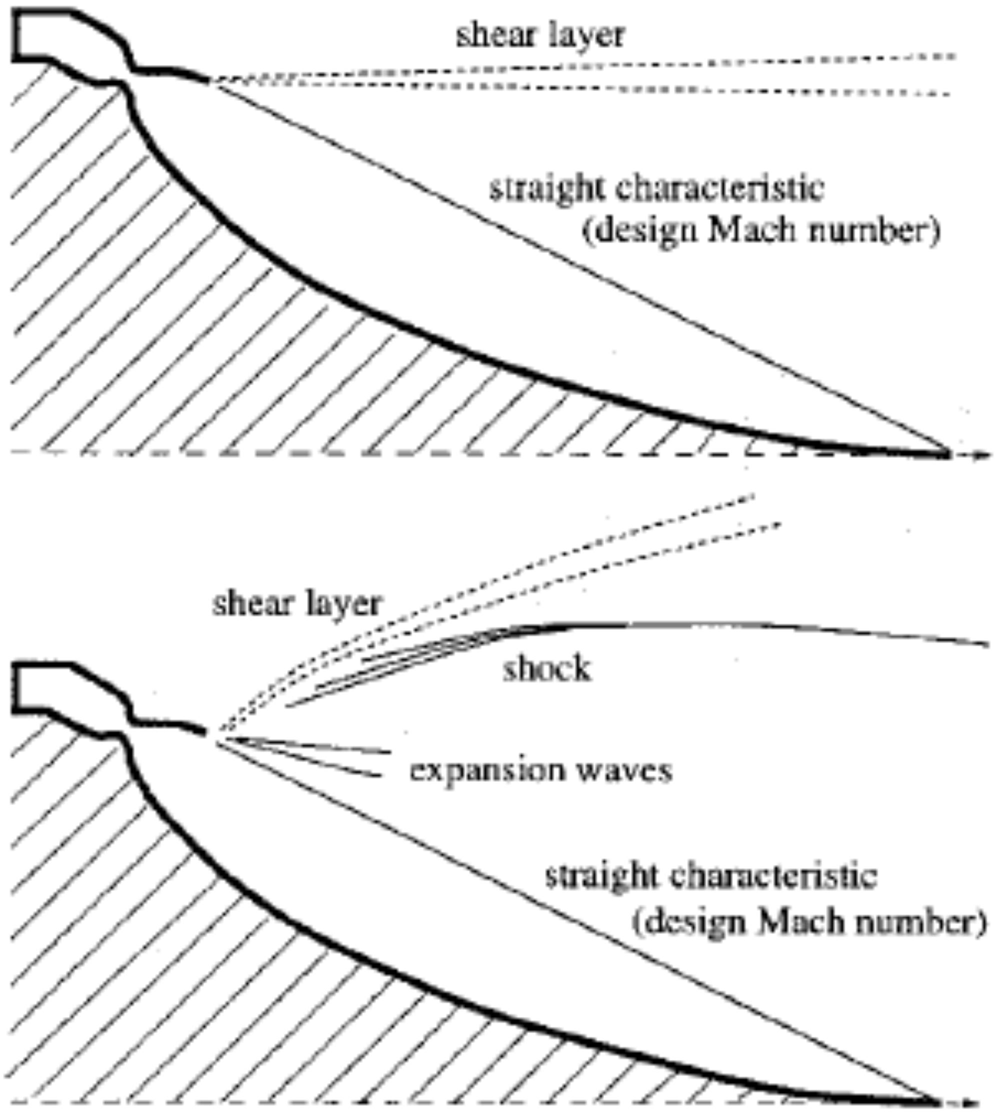

…Ramp Surface Pressure and Mach Numbers Unaffected by nozzle operating at higher-than-design altitude

Off-Design Algorithm Summary
Altitude Greater than Design Condition (6)

$$\begin{bmatrix} P_0 = operating\ chamber\ pressure \\ p_{amb} = ambient\ pressure\ at\ operating\ altitude \end{bmatrix}$$

… Expansion Line Mach Number and Flow Angle

$$M_{expansion} = \sqrt{\left(\frac{2}{\gamma - 1}\right)\left[\left(\frac{P_0}{p_{amb}}\right)^{\frac{(\gamma-1)}{\gamma}} - 1\right]}$$

$$\theta_{expansion} = \nu_{expansion} - \left(\nu_{exit}\right)_{\substack{design \\ condition}}$$

$$\nu_x = \nu_{expansion} - \theta_{expansion} + \theta_x \rightarrow \boxed{\begin{matrix} M_x \\ p_x \end{matrix}}$$

Aerospike Nozzle Endo-Atmospheric Compensation (2)

High Altitude Aerodynamics

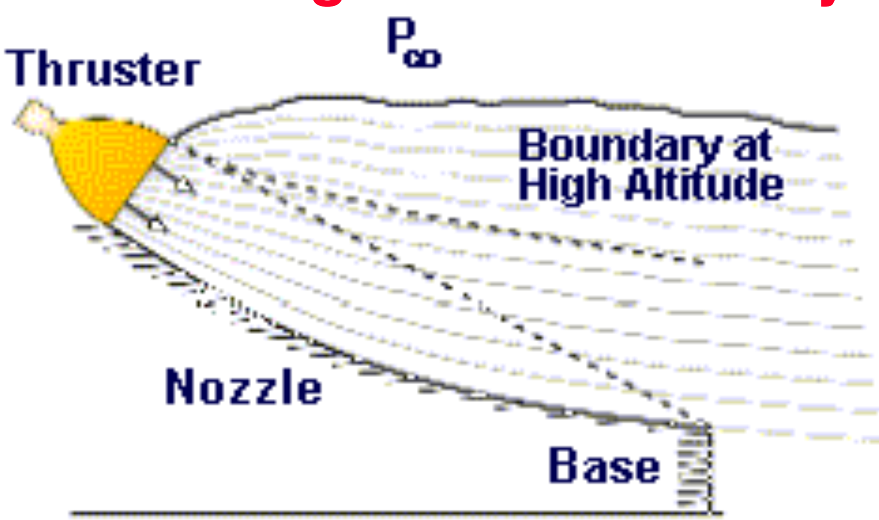

Pressure, Mach Distribution on Spike is Unchanged

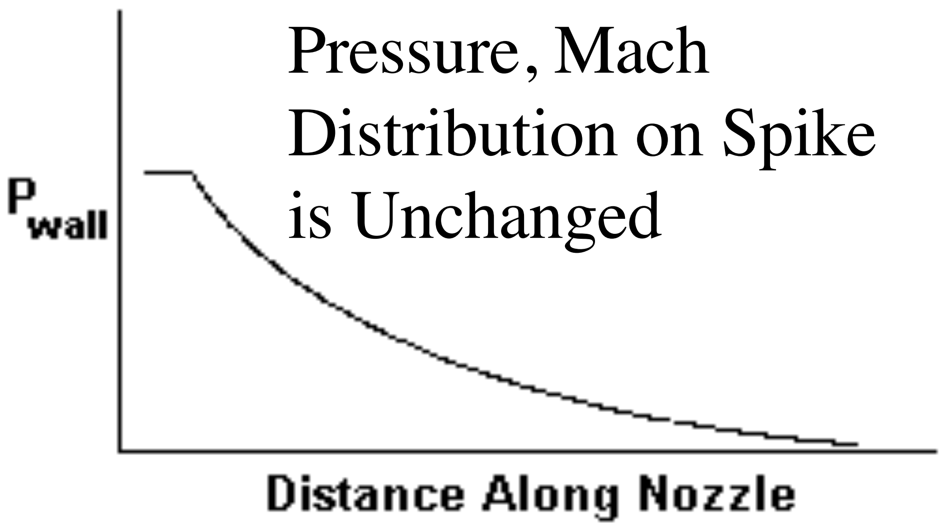

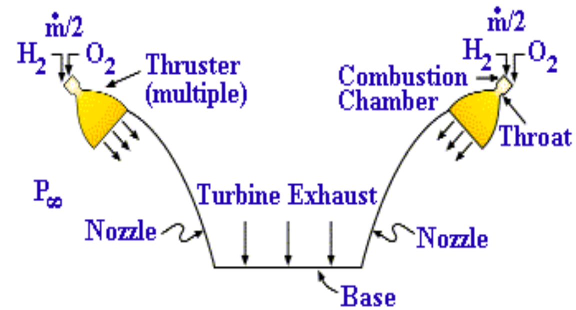

- Thruster flow discharges to ramp
- Expansion waves turn flow axially
- No compression waves exist - all flow turning done by expansion waves
- Nozzle behaves likes a bell

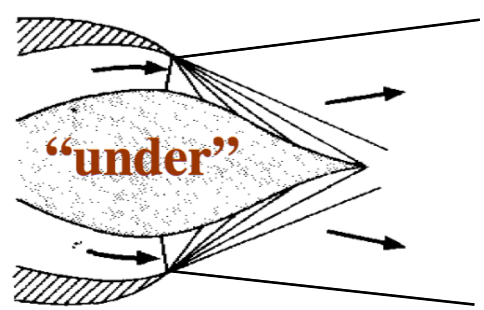

Altitude Greater than Design Condition (7)

$$\rightarrow \boxed{\nu_x = \left(\nu_{exit}\right)_{\substack{design\\condition}} + \theta_x}$$

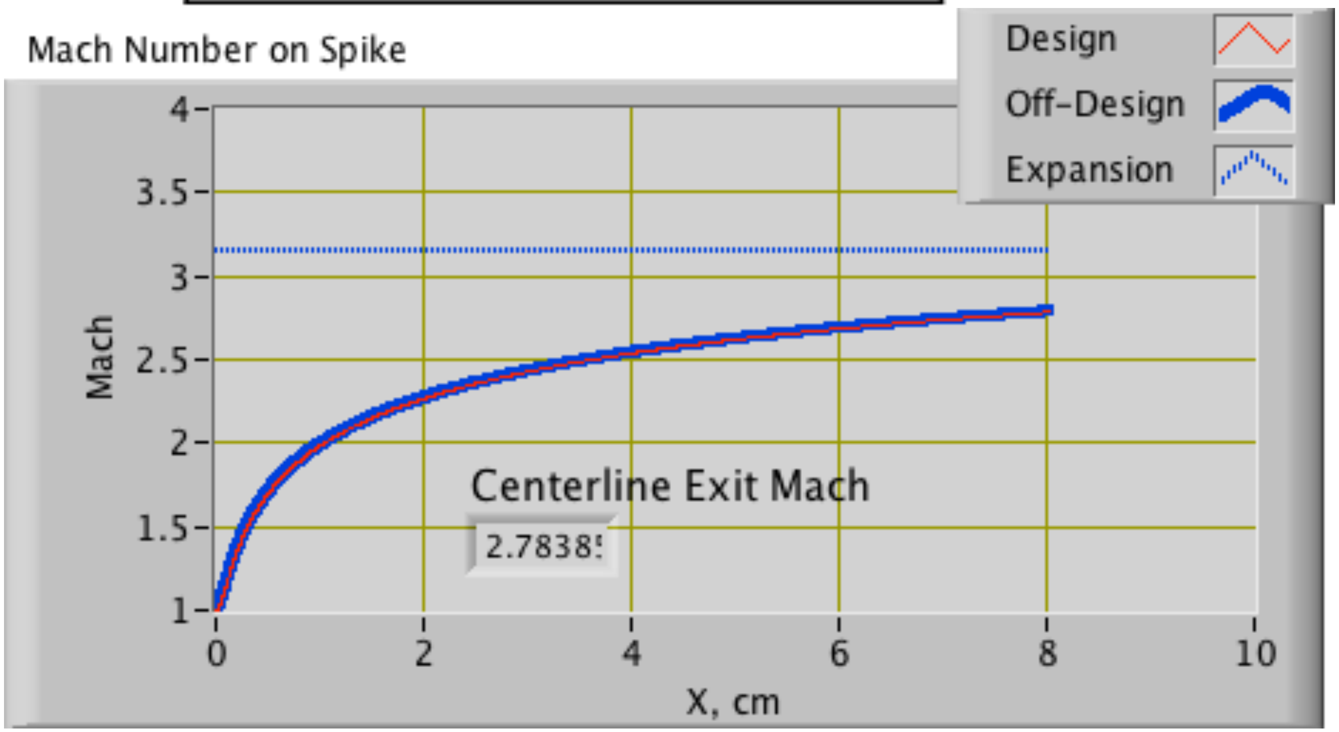

Mach Number Along Spike is Unaltered From Design Condition

Altitude Greater than Design Condition (8)

Spike Pressure

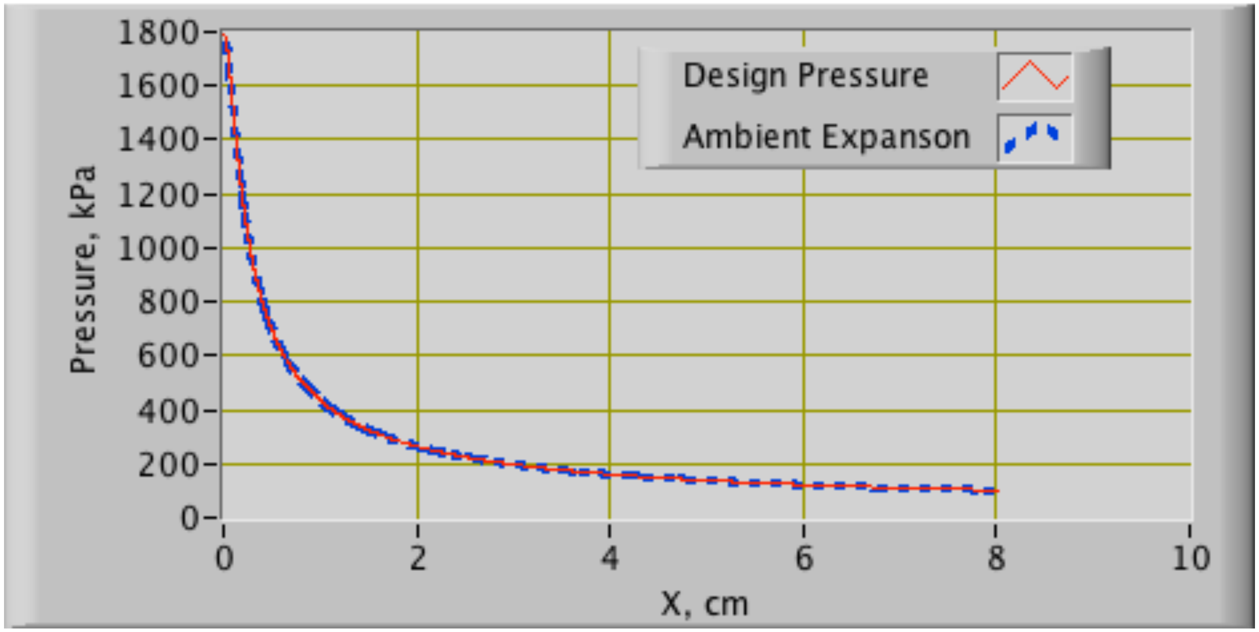

Spike Differential Pressure from Ambient

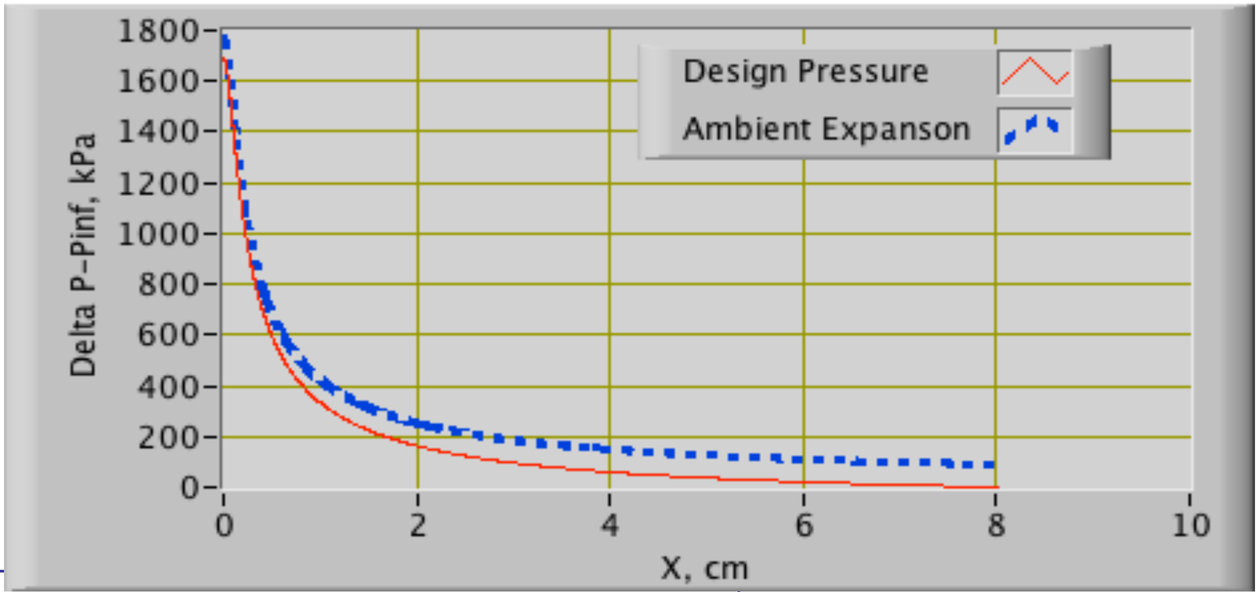

Significant gain in pressure thrust

Altitude Greater than Design Condition (9)

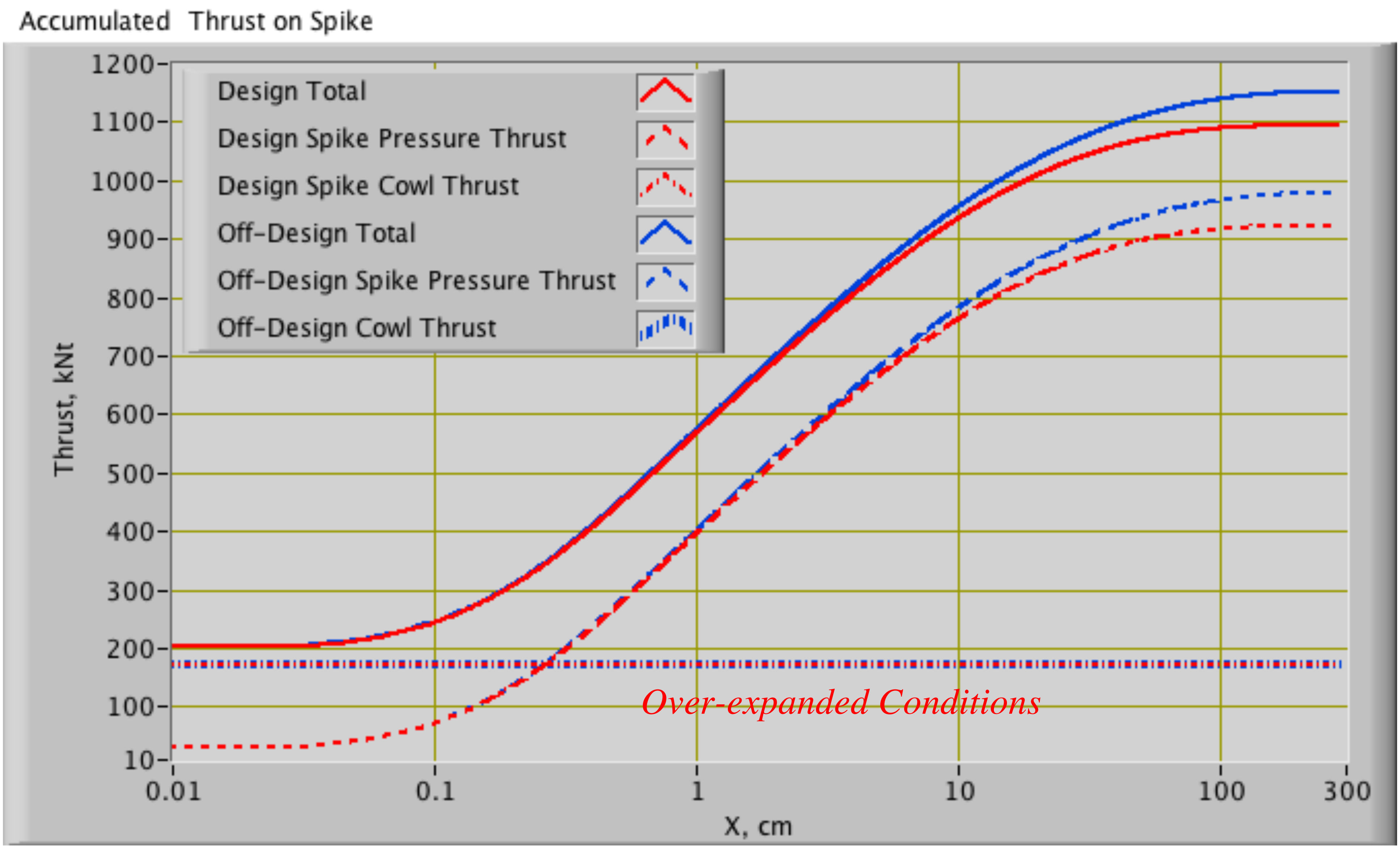

Altitude Greater than Design Condition (10)

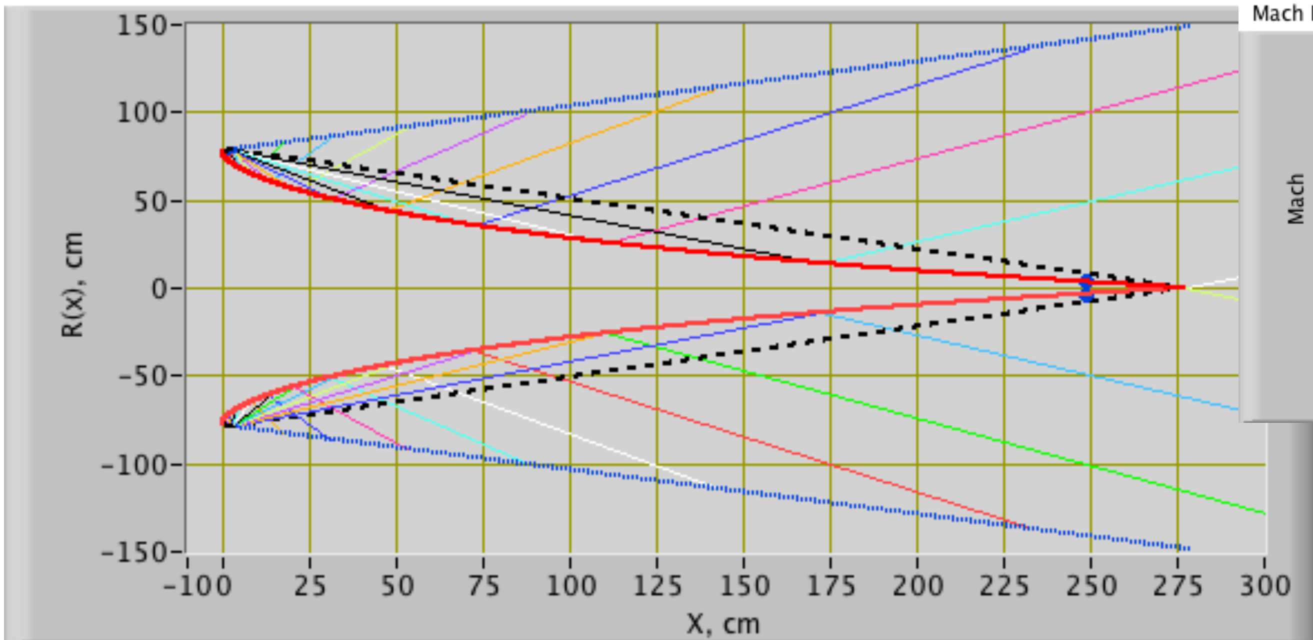

Mach Number on Spike

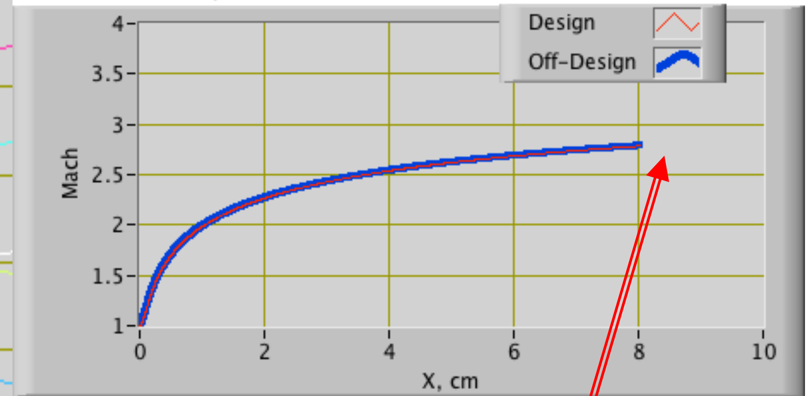

- **Mach Numbers on Spike Surface Unaffected**

Design Spike Contour , aft view

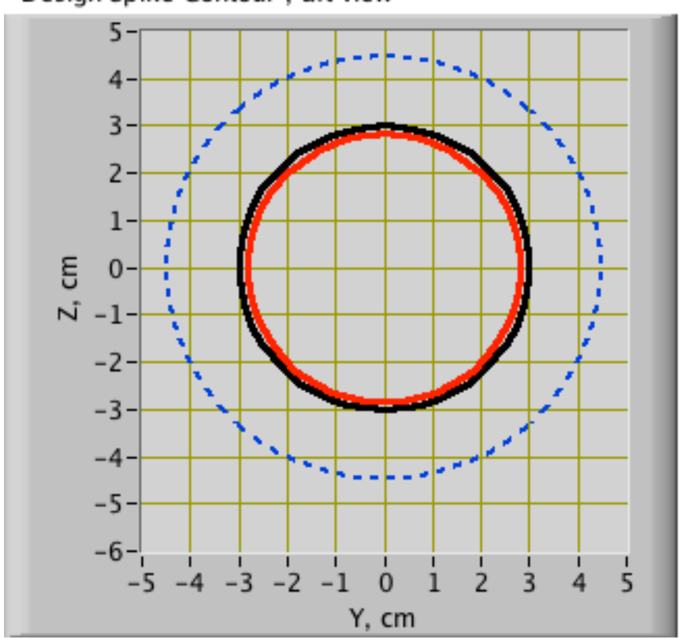

P-Pinf aLONG EXIT PLANE

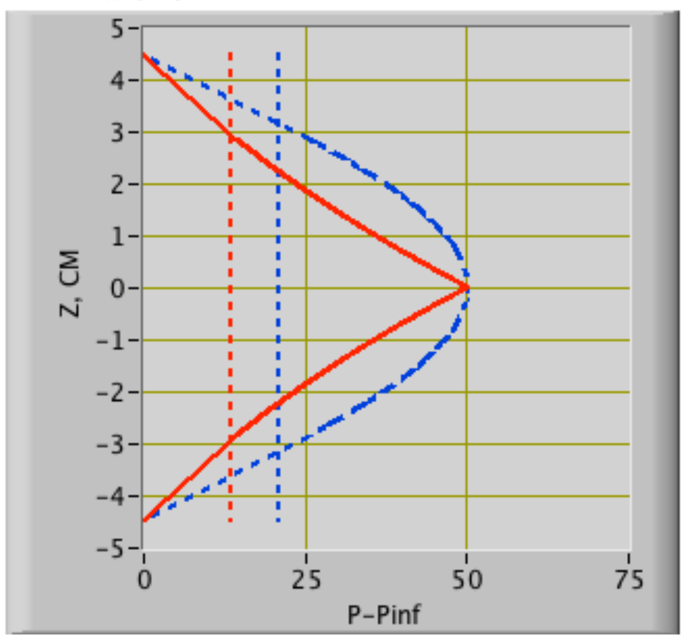

Mach Profile aLONG EXIT PLANE

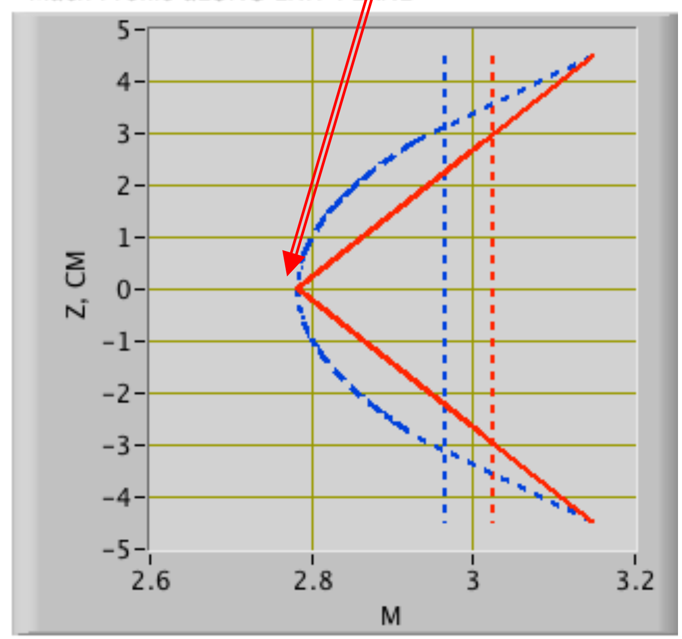

Utah State University

Mechanical & Aerospace Engineering

Off Design Operation
@ Altitude Lower than Design Condition

External Pressure Compresses Flow Field Resulting in Higher Spike Pressures

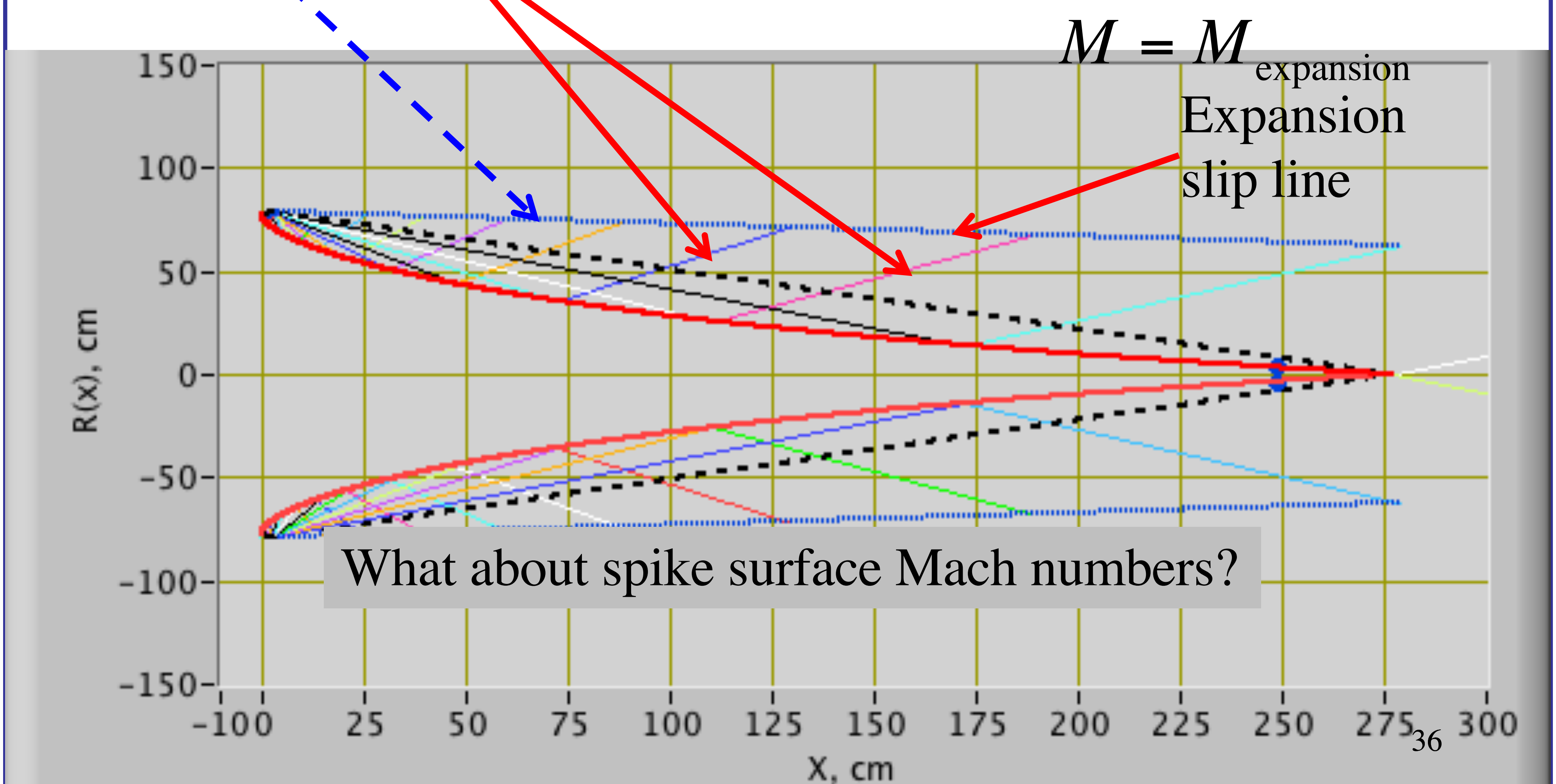

Off Design Operation
Altitude Lower than Design Condition (2)

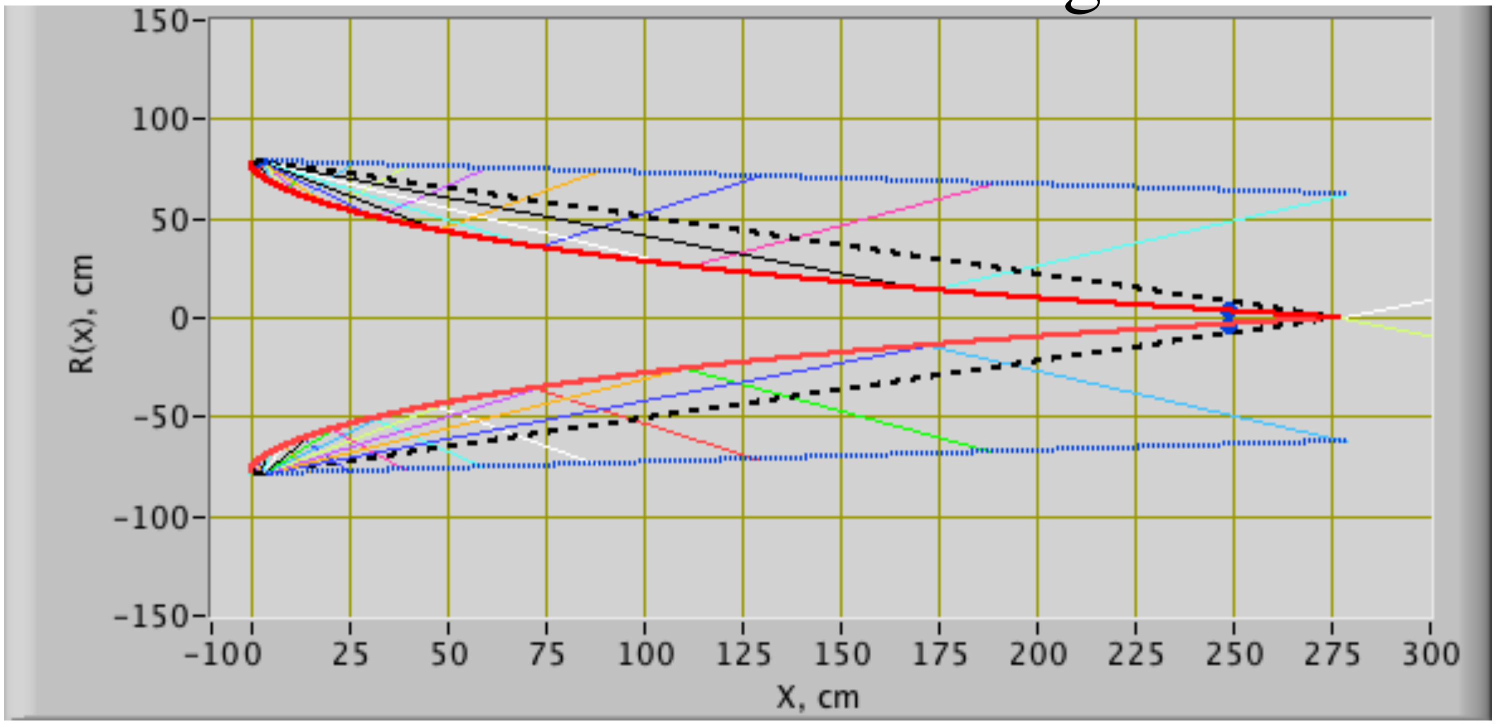

- At below design pressure ratio, the flow in the plug nozzle is radically different from that in a conventional nozzle. The expansion occurring at the cowl-lip would proceed only up to the ambient pressure p_a and not all the way down to the design exit pressure p_e.

Off Design Operation
Altitude Lower than Design Condition (2)

$p_\infty > p_{\infty,design}$ (overexpanded)

– $p_{spike} = p_\infty$ before plug ends

– ***weak*** shocks and expansions downstream

Average Nozzle Pressure greater Than Freestream, No suction effects or separation like on conventional nozzle

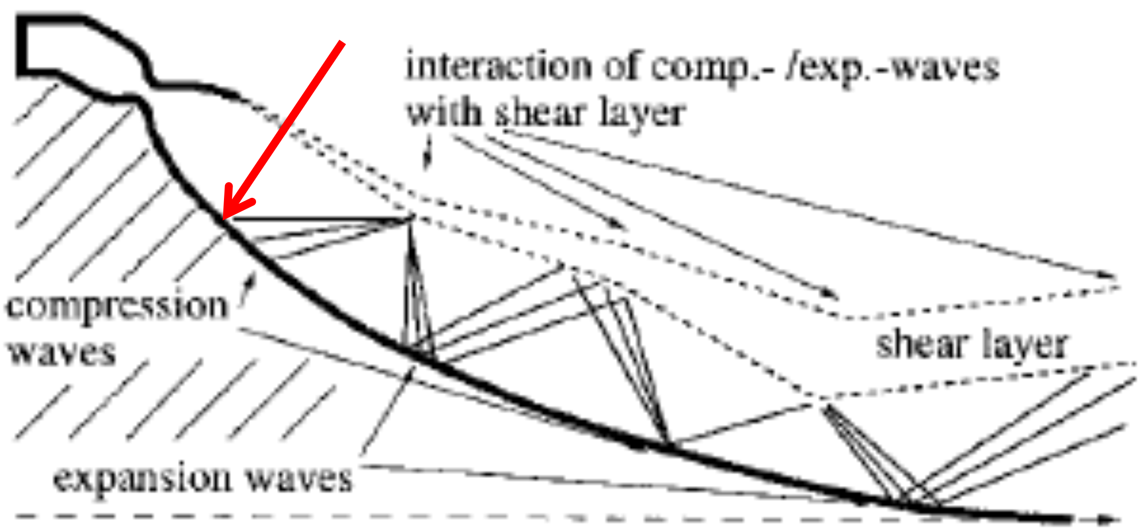

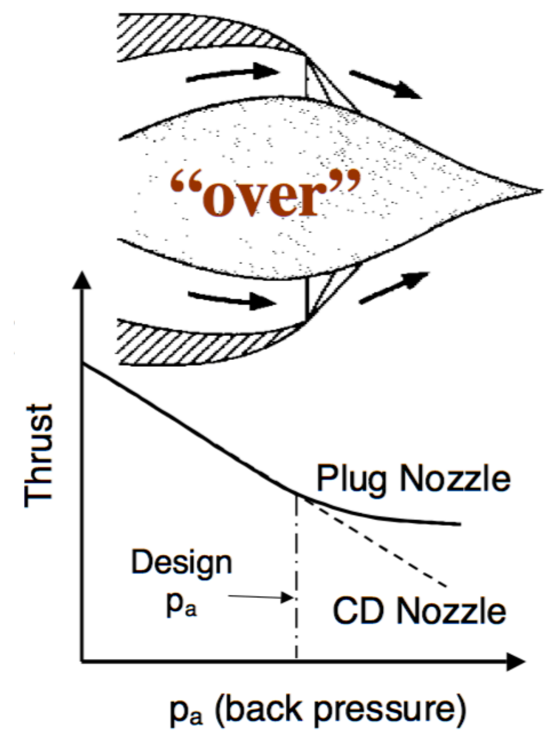

Aerospike Nozzle Endo-Atmospheric Compensation

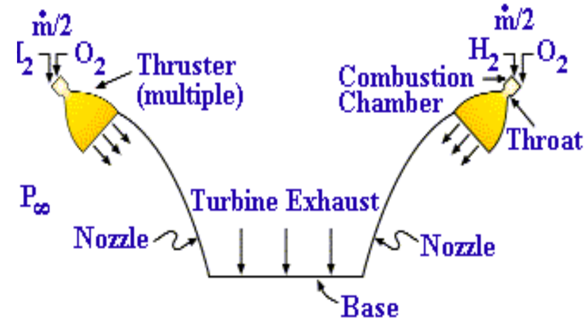

Low Altitude Aerodynamics

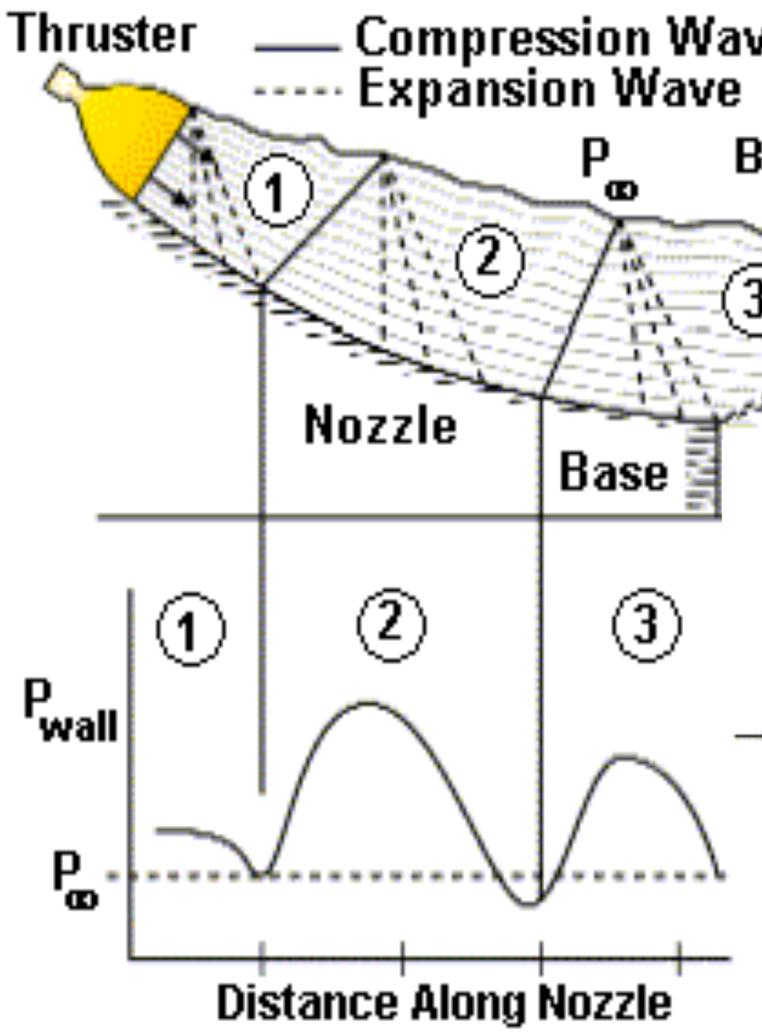

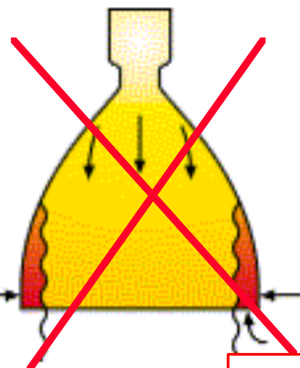

- Thruster flow discharges to ramp
- Expansion waves turn flow axially
- Ramp curves, turns flow axially (at low altitudes)
- Turning causes compression wave from (1) to (2) - nozzle pressure increases
- Compression wave reflects off boundary causing expansion waves
- Flow crosses expansion waves in (2) - nozzle pressure decreases
- Ramp continues to curve and turn flow
- Process repeats (2) to (3)

Averaged ramp pressure > P∞
… no losses or separation of flow, even with high expansion ratio nozzle

Wave Reflection Rules for Solid and Free Boundaries

- Anderson,
  Chapter 4 pp. 152-164

1. Waves Incident on a Solid Boundary Reflect in a Like manner;
   Compression wave reflects as compression wave, expansion wave reflects as expansion wave

2. Waves Incident on a Free Boundary Reflect in an Opposite manner;
   Compression wave reflects as expansion wave, expansion wave reflects as compression wave

Wave reflections from solid/free boundary

- Solid Boundary

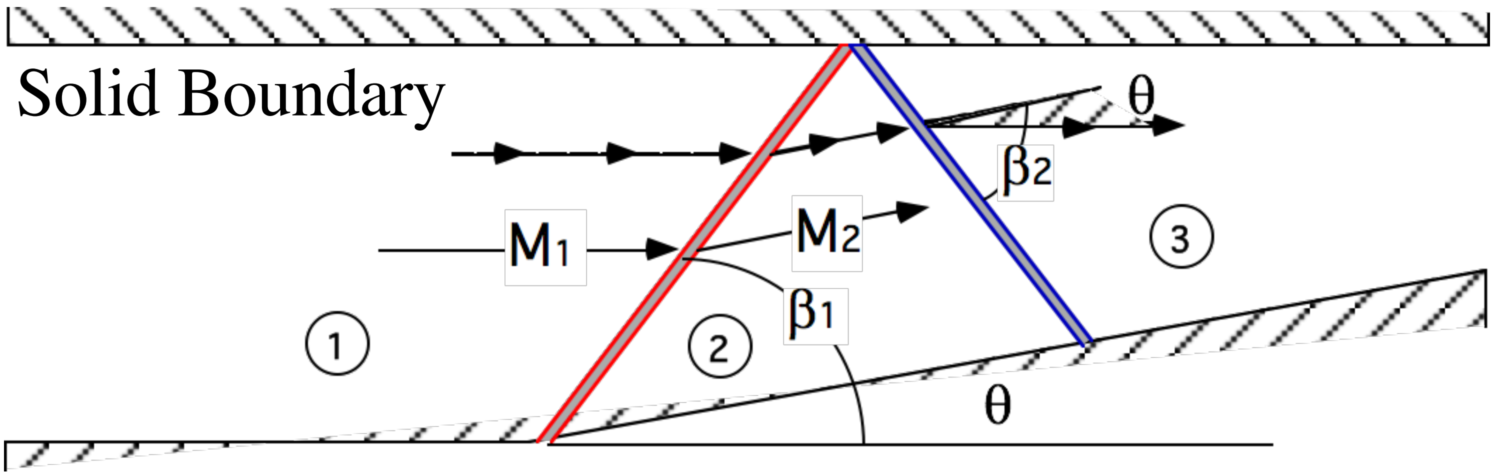

- Free Boundary

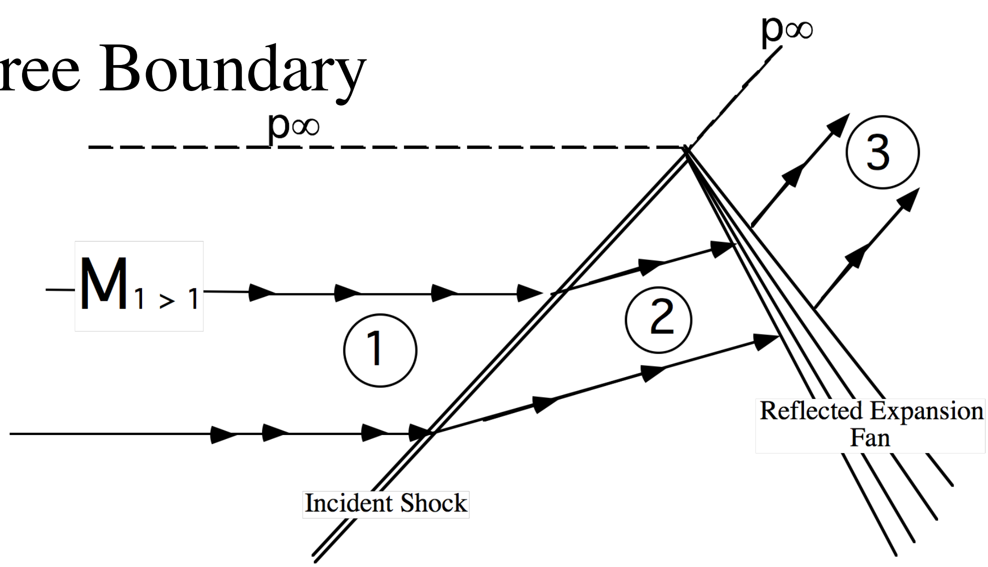

Shock Wave Incident on Constant Pressure Boundary

Wave reflections from a free boundary

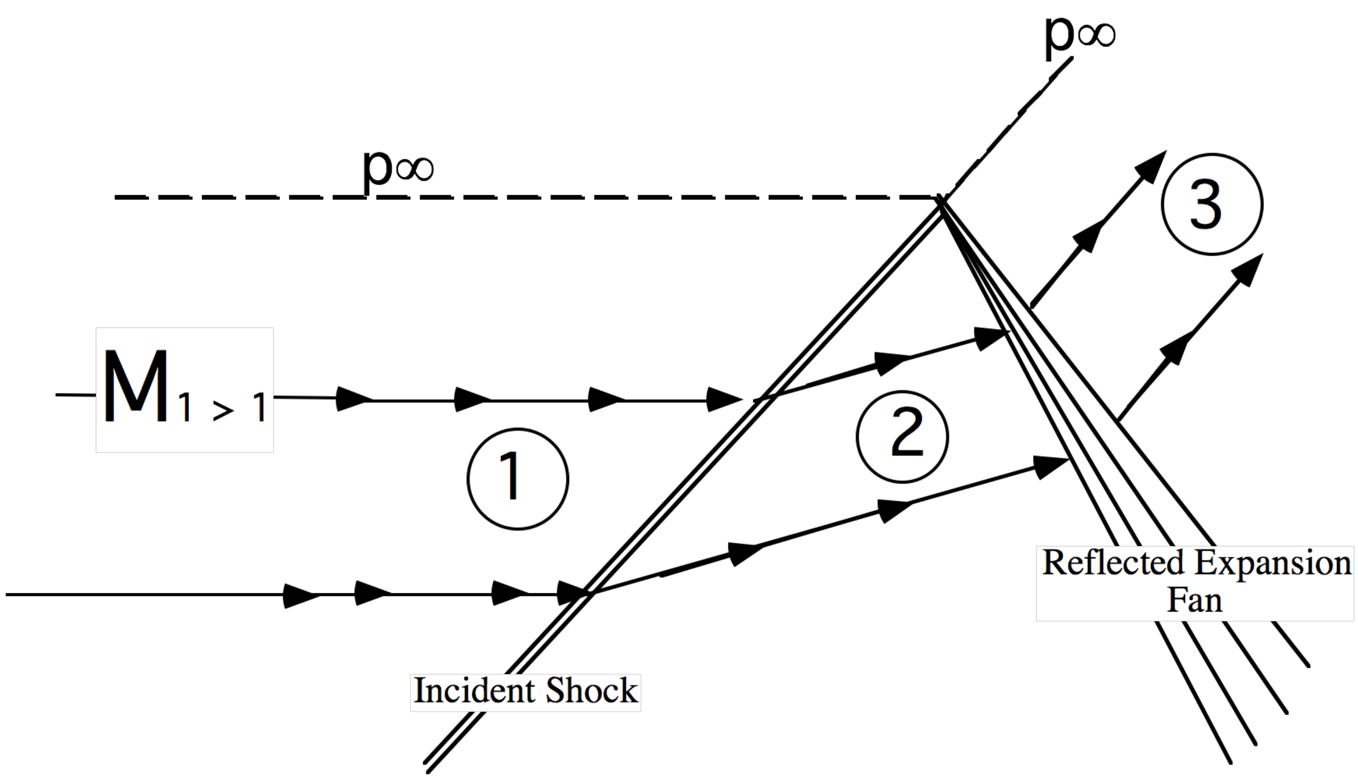

Shock Wave Incident on Constant Pressure Boundary

Wave reflections from a free boundary

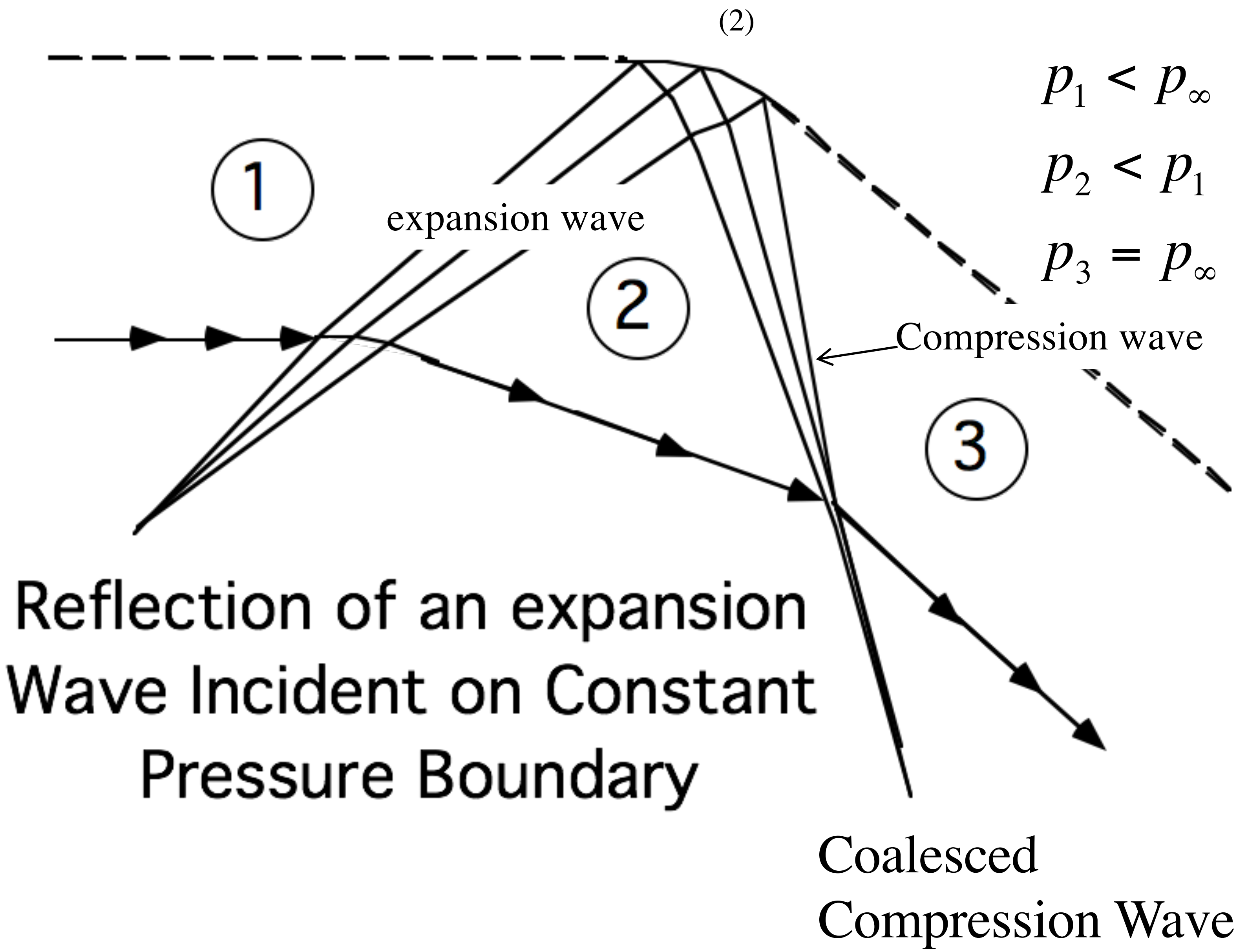

$p_1 < p_\infty$

$p_2 < p_1$

$p_3 = p_\infty > p_2$

Off Design Operation

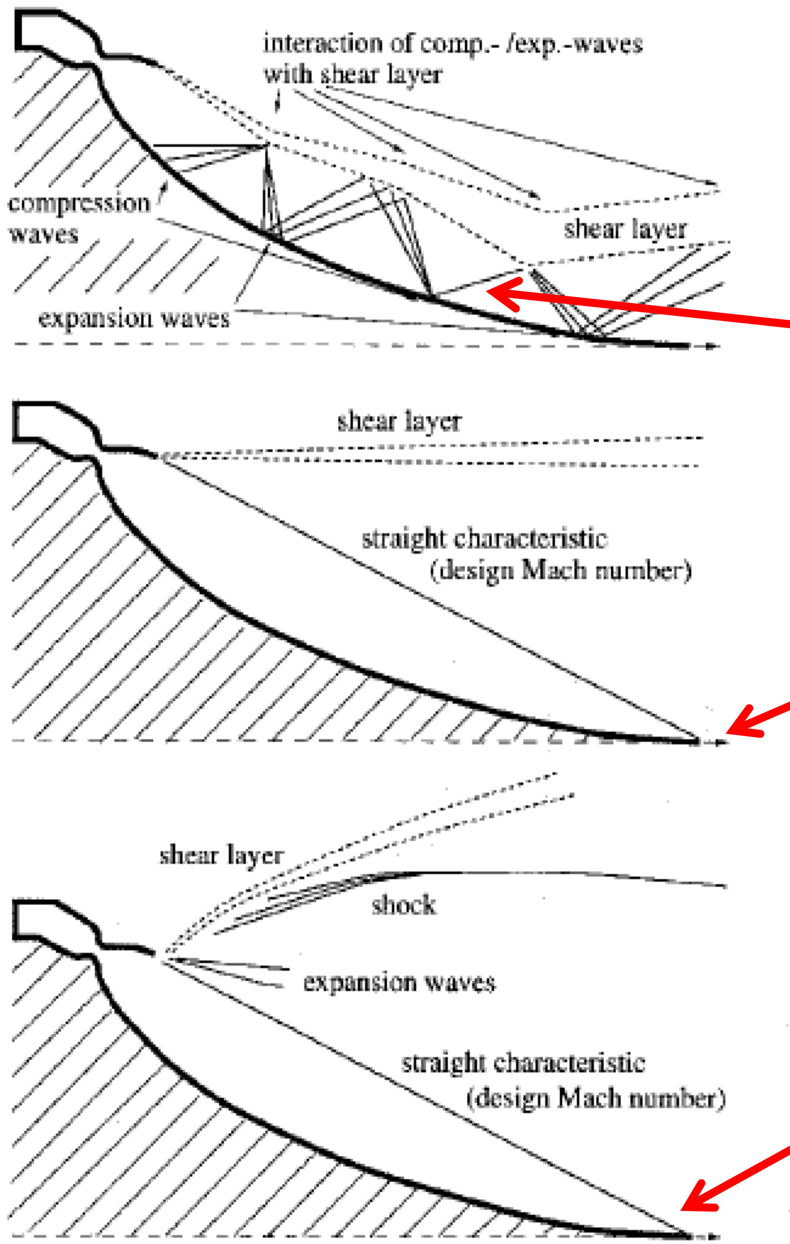

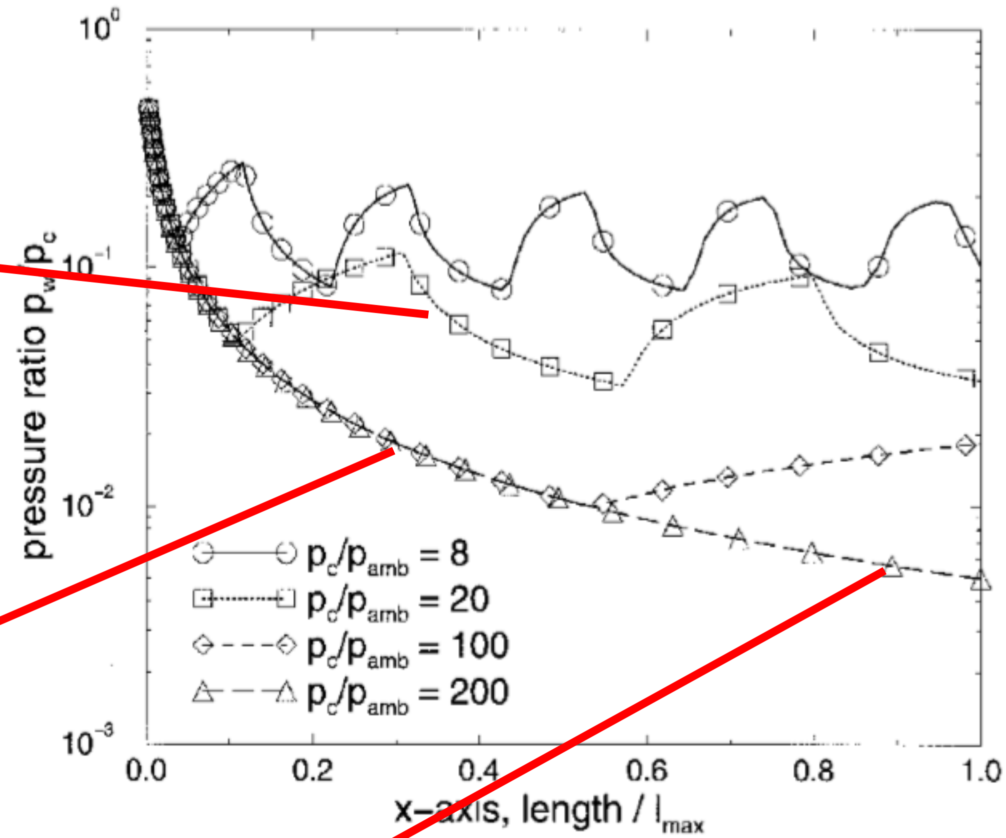

Flow phenomena of a plug nozzle with full length at different pressure ratios *pc* / *p*am b, off-design (top, bottom) and design (center) pressure ratio.

Off Design Operation

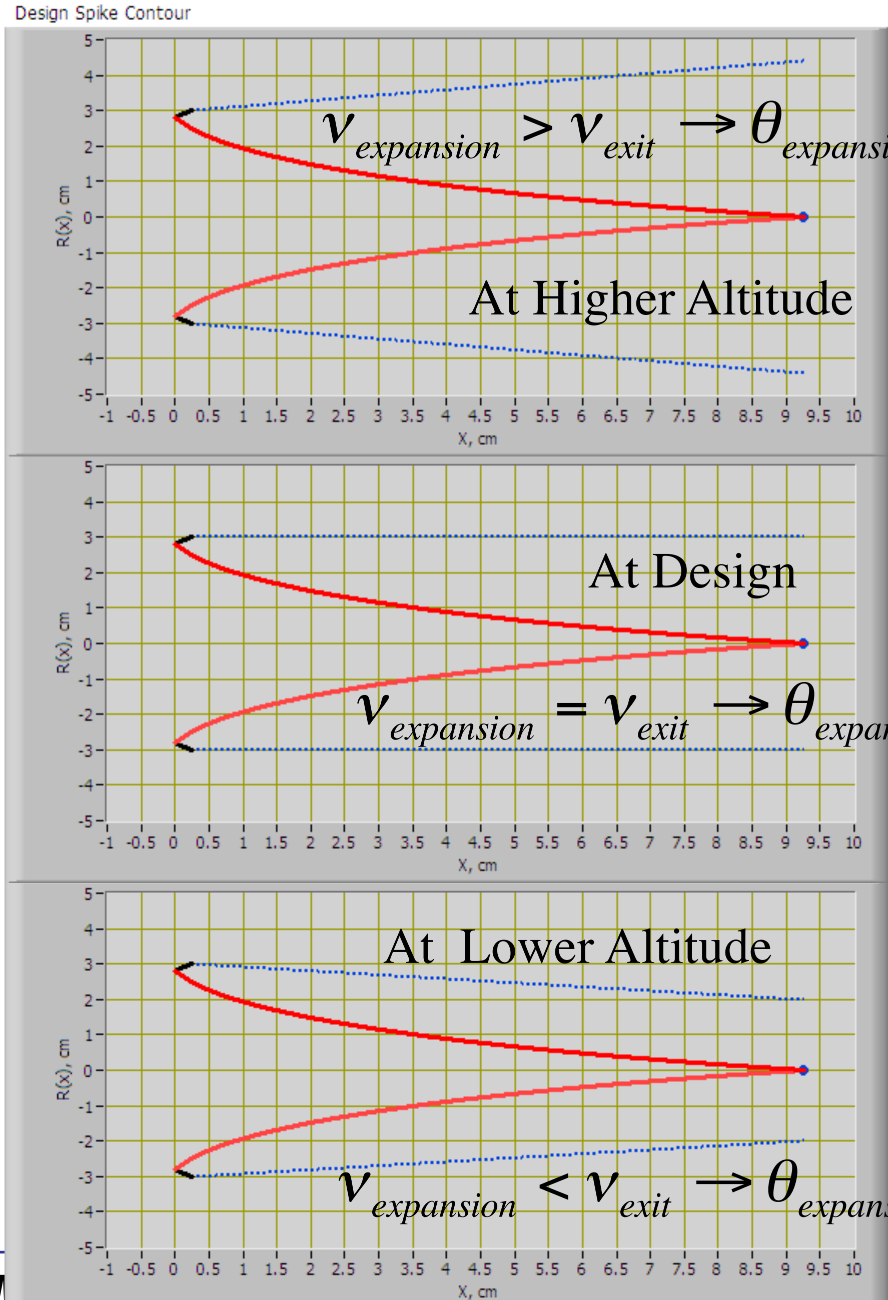

$$\nu_{expansion} > \nu_{exit} \rightarrow \theta_{expansion} > 0$$

$$\nu_{expansion} = \nu_{exit} \rightarrow \theta_{expansion} = 0$$

$$\nu_{expansion} < \nu_{exit} \rightarrow \theta_{expansion} < 0$$

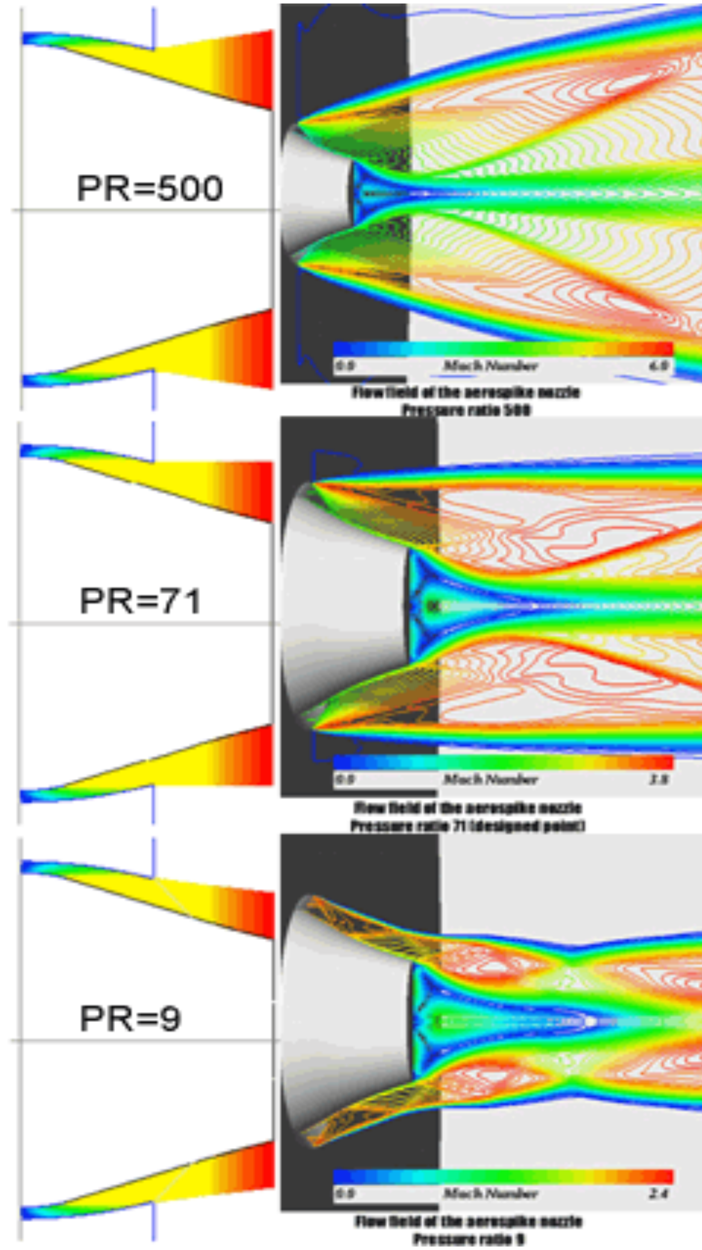

Aerospike Nozzle With Shock Diamonds

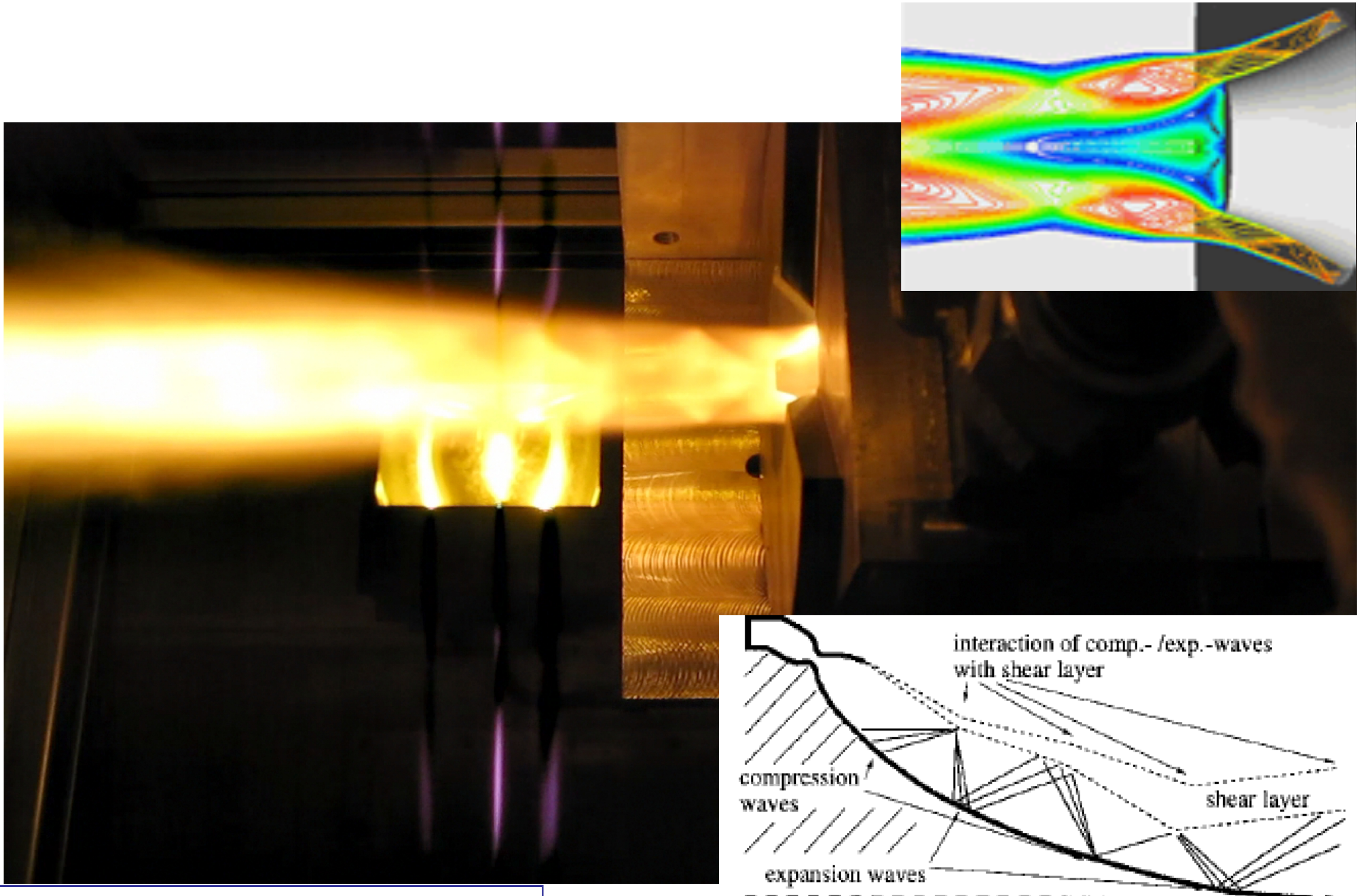

Aerospike Nozzle Endo-Atmospheric Compensation (3)

SlipStream effects

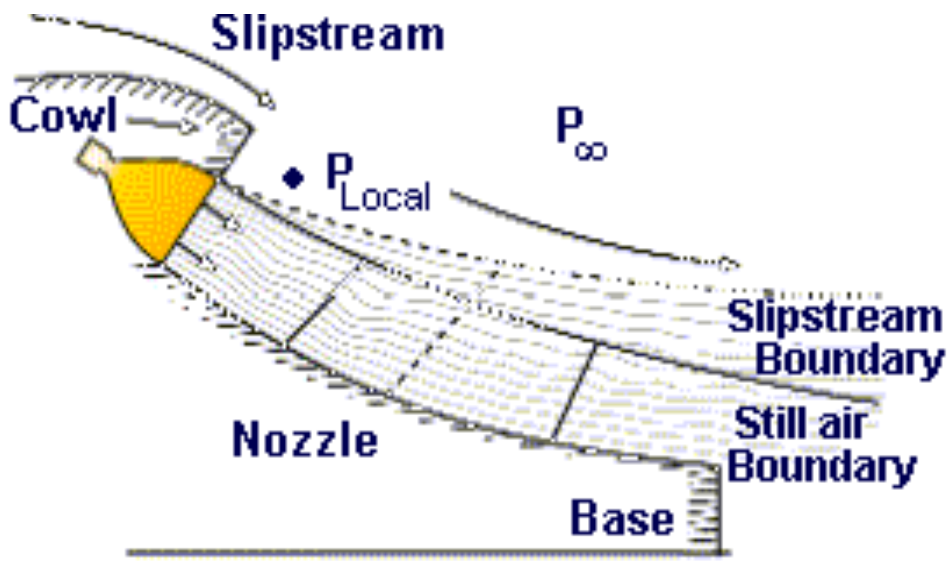

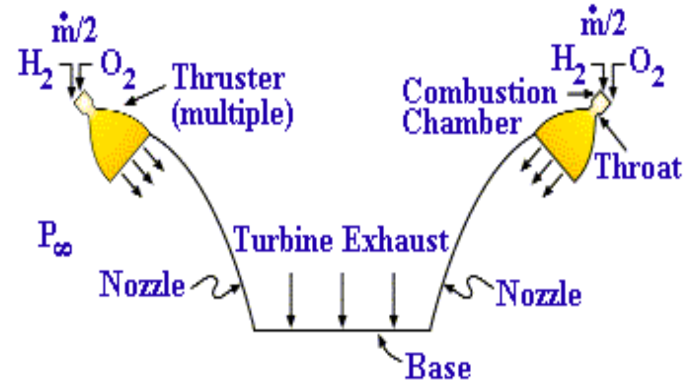

- Air streaming over cowl lowers local pressure - $P_{Local} < P_{infinity}$
- Exhaust plume expands beyond still air case
- Expansion and compression wave systems move aft from still air case

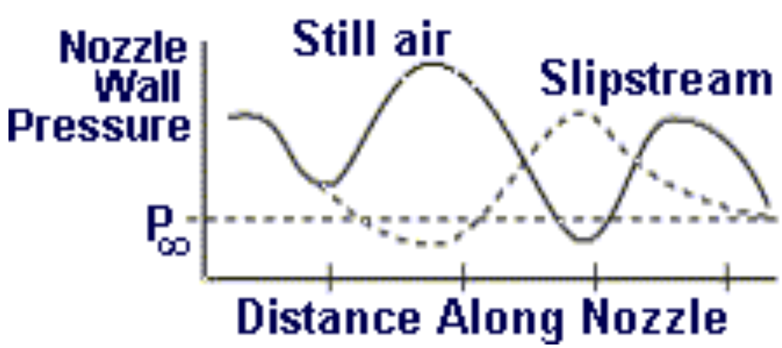

- Resulting recompression Delays Nozzle separation

Averaged ramp pressure > P∞
… no losses or separation of flow, even with high expansion ratio nozzle

Compare Aerospike to Minimum Length Nozzle with Same Expansion Ratio

Input Cowl Gemetry

Cowl Lip Mach Number

1

Radius of Cowl upper Lip from CL, cm

3

Geometric Aerospike Expansion Ratio (spike area/Cowl exit)

5

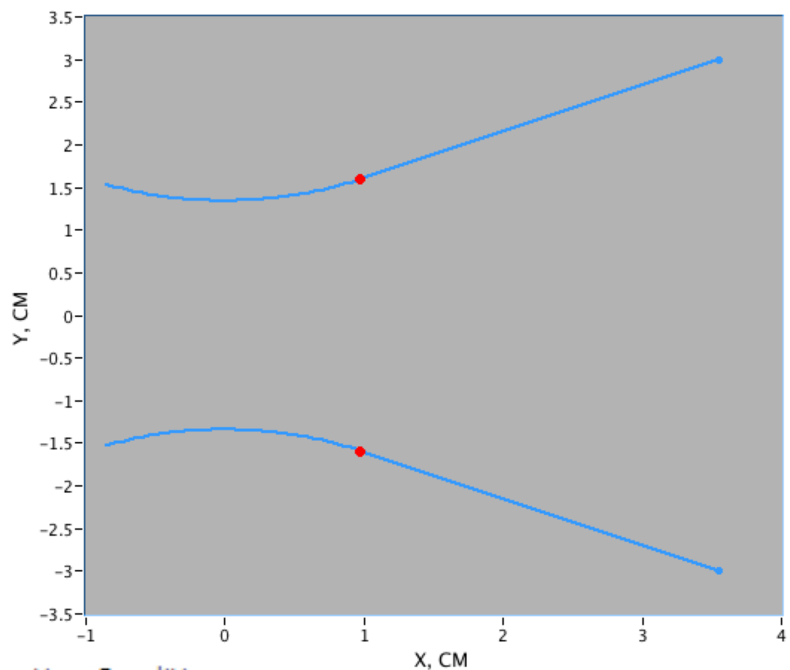

Minimum Length Nozzle 4.546 cm
(including convergent section)

Design Altitude, km

0.000339217

Gas Properties

Gamma

1.2

MWght, kg/kg-mol

16

Operating Conditions

P0, kPa

3175.7

T0, K

3200

Pa, kPa

101.321

Design Spike Contour

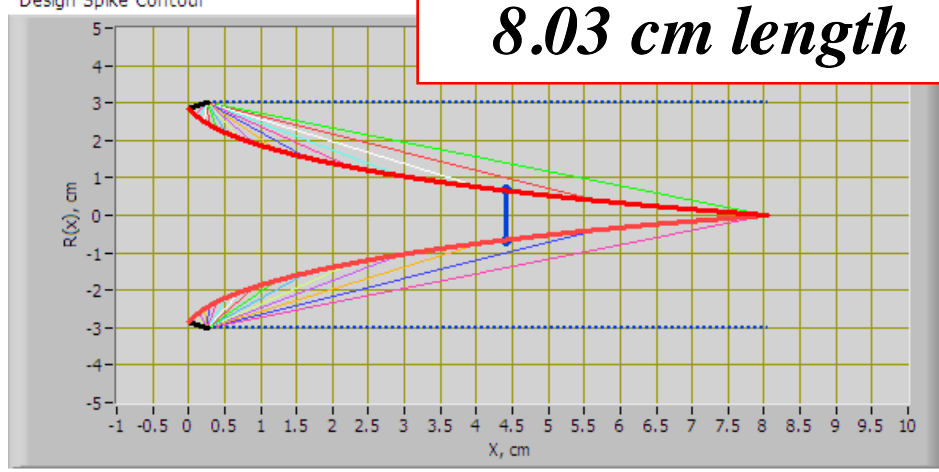

Full Conical Aerospike Nozzle 8.03 cm length

Compare Aerospike to Minimum Length Nozzle with Same Expansion Ratio (2)

At design condition

Aerospike

Design Thrust/Force Data

Parameter	Value
Design Pressure Thrust (Spike), kNt	1.49459
Massflow, kg/sec	0.903154
Throat Exit (kPa) Momentum Thrust	2.17283
Design Isp, sec	301.058
Throat Exit Momentum, Axial Direction	1.17188
Design Base Area Thrust, kNt	0
Design Total Thrust, kNt	2.66646

Superior Aerospike Performance at Design Condition

Conventional

Minimum length Nozzle
Isentropic
Output parameters

Parameter	Value
Exit mach Number	2.785045
Pexit, kPa	101.32
Texit, deg. K	1802.1
Vexit, m/sec	2952.4
Mdot, kg/sec	0.90316
Thrust, kNt	2.50291
Isp, sec	282.59
Exit Area, M^2	0.002827
Cstar, m/sec	1988.38
Max Isp, sec	455.511
Max Thrust, Kn	4.03446
Ce, m/.sec	2771.28
Volumetric flow rate, m^3/sec	0.01456
Chamber density kg/m^2	62.0254
Rg, J/kg-deg-K	519.65079
Lambda, divergence	0.9386531

UtahState UNIVERSITY

Mechanical & Ae

Compare Aerospike to Minimum Length Nozzle with Same Expansion Ratio (3)

Expanded (non Ideal) Operating Exit Flow Properties

Flow Area, cm^2	Temperature, K	Thrust, kNt
145.018	1262.91	2.91902
Mach number	**Pressure, kPa**	**Isp, Sec**
3.91641	12	322.98
massflow, kg/sec	**Velocity, m/sec**	**mdot, ve (kNt)**
0.92159	3475.53	3.20302

Off-design Cowl Thrust, kNt: 1.19912

Operating Conditions

- P0, kPa: 3175.7
- T0, K: 3200
- Pa, kPa: 12

Conventional

Operating Altitude, km: 15.0246

Minimum length Nozzle
Isentropic
Output parameters

- Exit mach Number: 2.785045
- Pexit, kPa: 101.32
- Texit, deg. K: 1802.1
- Vexit, m/sec: 2952.4
- Mdot, kg/sec: 0.90316
- Thrust, kNt: 2.75546
- Isp, sec: 311.10
- Exit Area, M^2: 0.002827
- Cstar, m/sec: 1988.38
- Max Isp, sec: 455.511
- Max Thrust, Kn: 4.03446
- Ce, m/.sec: 3050.91
- Volumetric flow rate, m^3/sec: 0.01456
- Chamber density kg/m^2: 62.0254
- Rg, J/kg-deg-K: 519.65079
- Lambda, divergence: 0.9386531

Design Spike Contour

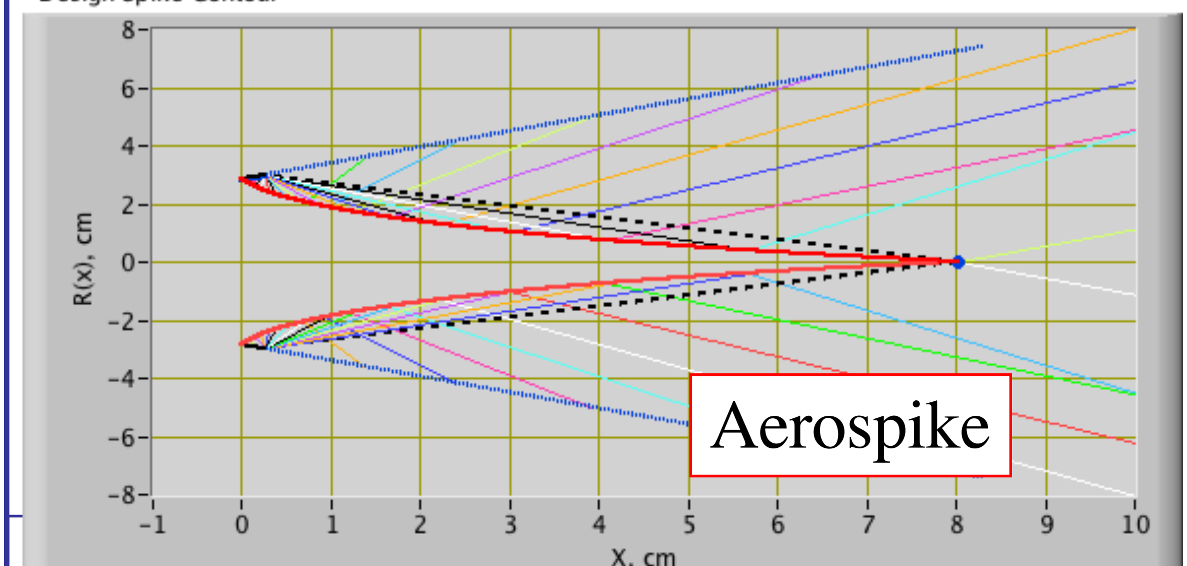

Even more improved aerospike performance at Altitude

Compare Aerospike to Minimum Length Nozzle …. (4)

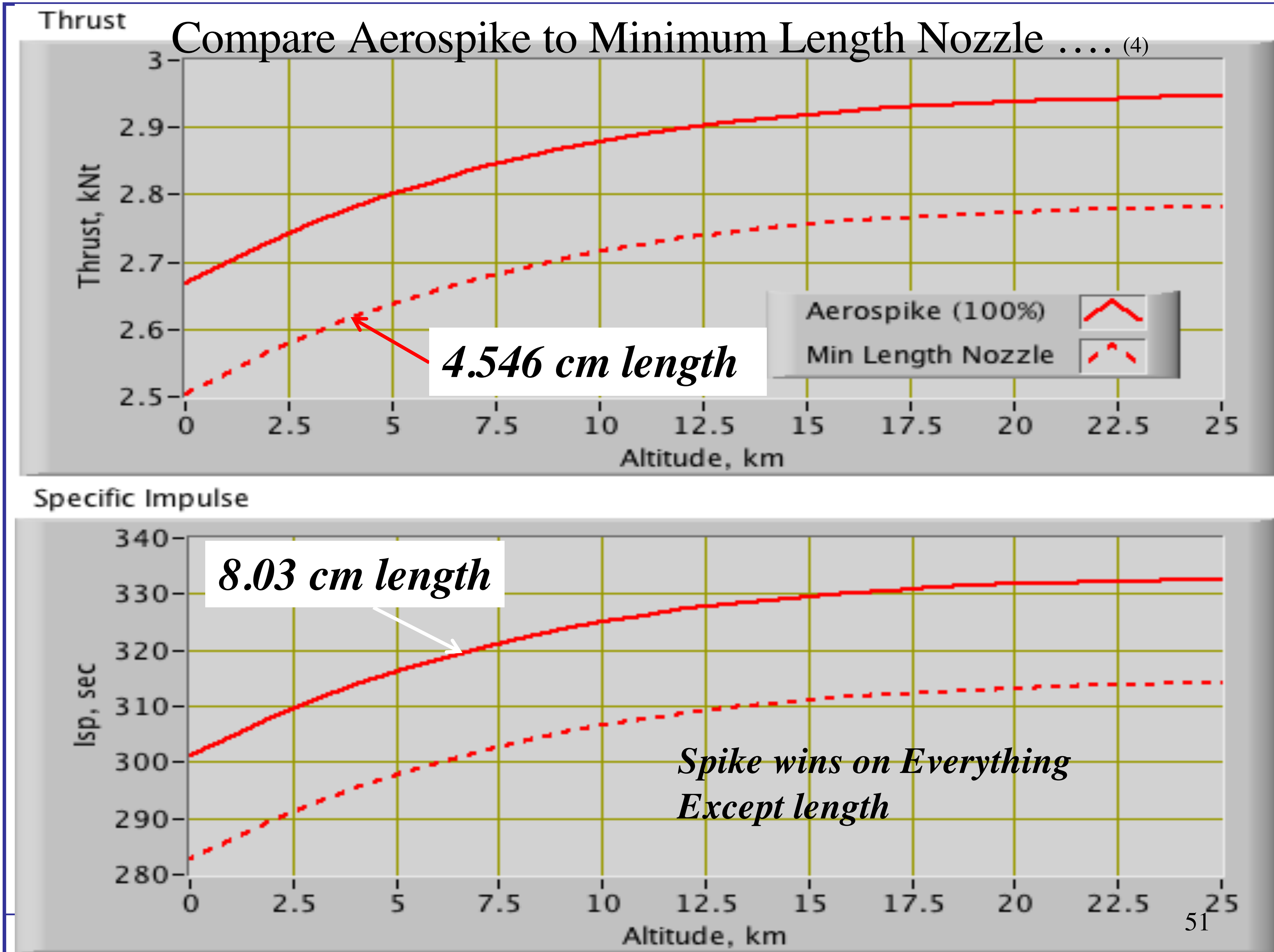

Effects of Spike Truncation

NASA DFRC (Trong Bui)

Example Base Integration

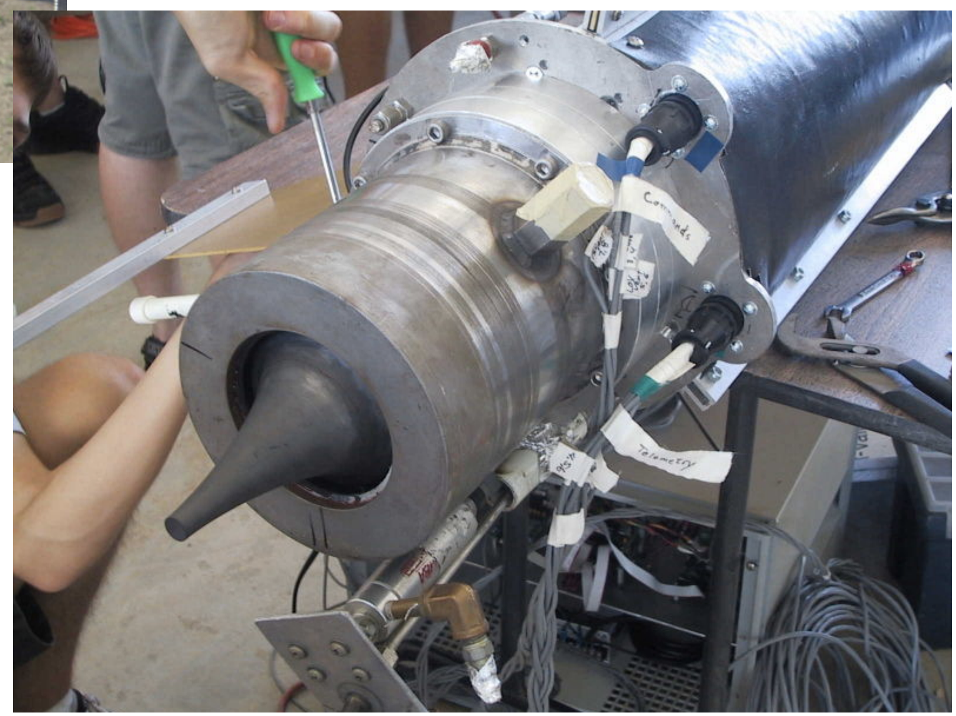

- Long Beach State

(Eric Besnard)

Effects of Spike Truncation (2)

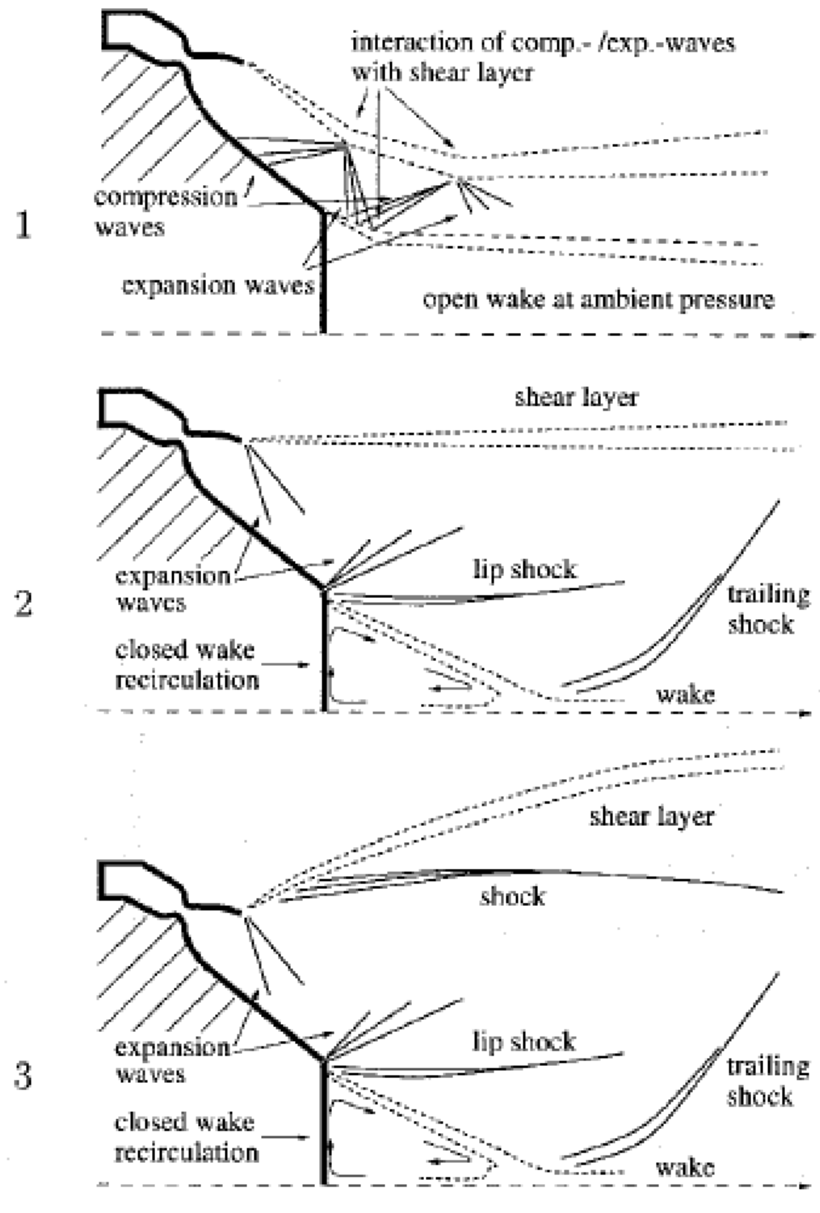

Flow phenomena of a plug nozzle truncated central body (right column) at different pressure ratios *pc* / *p*am b, off-design (top, bottom) and design (center) pressure ratio.

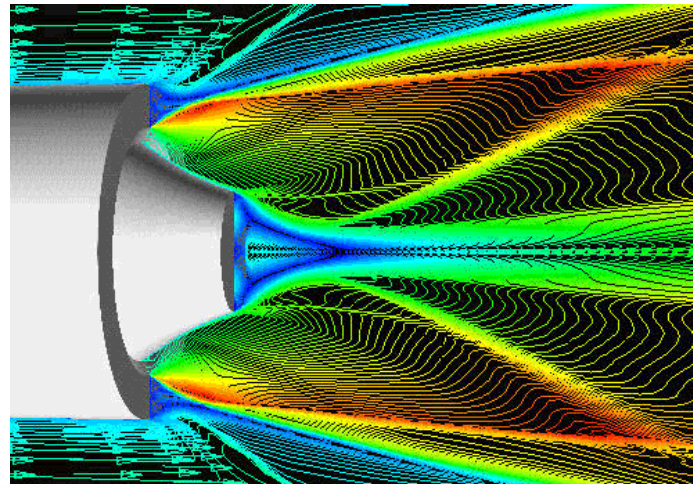

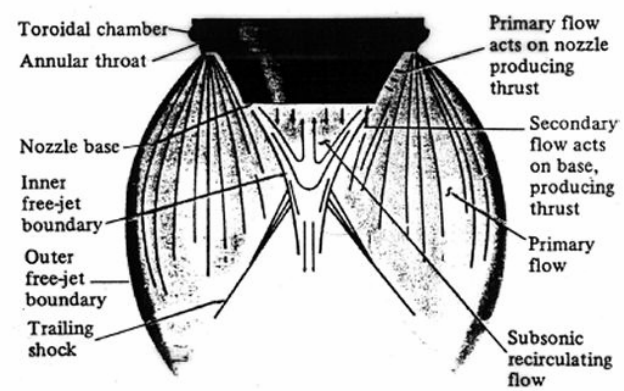

Separated Base Area
(low pressure produces drag)

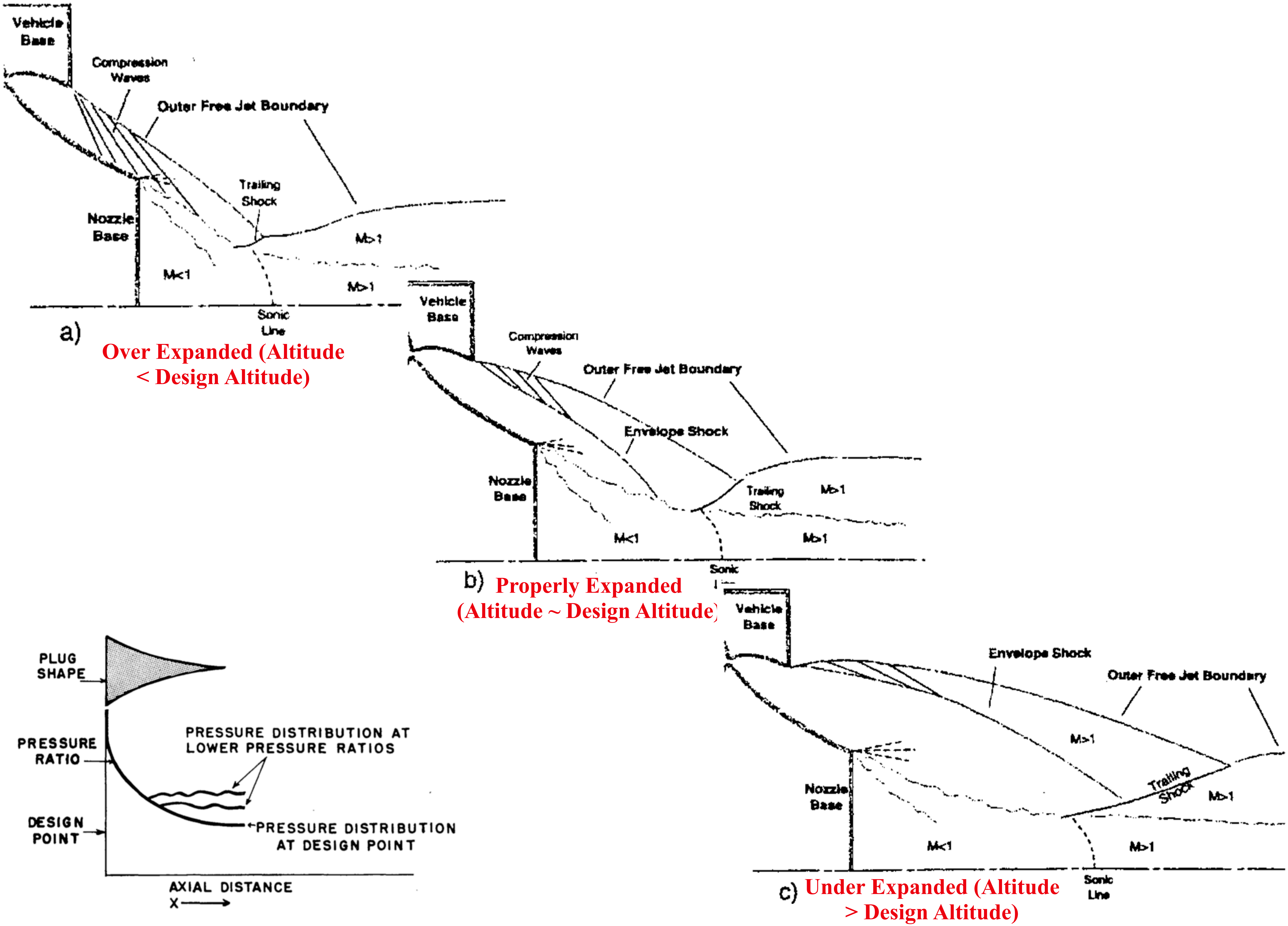
Vehicle Base
Compression Waves
Outer Free Jet Boundary
Trailing Shock
Nozzle Base
M>1
M<1
M>1
Sonic Line
a)
Over Expanded (Altitude < Design Altitude)
Vehicle Base
Compression Waves
Outer Free Jet Boundary
Envelope Shock
Nozzle Base
Trailing Shock
M>1
M<1
M>1
Sonic
b)
Properly Expanded (Altitude ~ Design Altitude)
Vehicle Base
Envelope Shock
Outer Free Jet Boundary
M>1
Trailing Shock
M>1
Nozzle Base
M<1
M>1
Sonic Line
c)
Under Expanded (Altitude > Design Altitude)
PLUG SHAPE
PRESSURE RATIO
PRESSURE DISTRIBUTION AT LOWER PRESSURE RATIOS
DESIGN POINT
PRESSURE DISTRIBUTION AT DESIGN POINT
AXIAL DISTANCE
X

Effects of Spike Truncation (7)

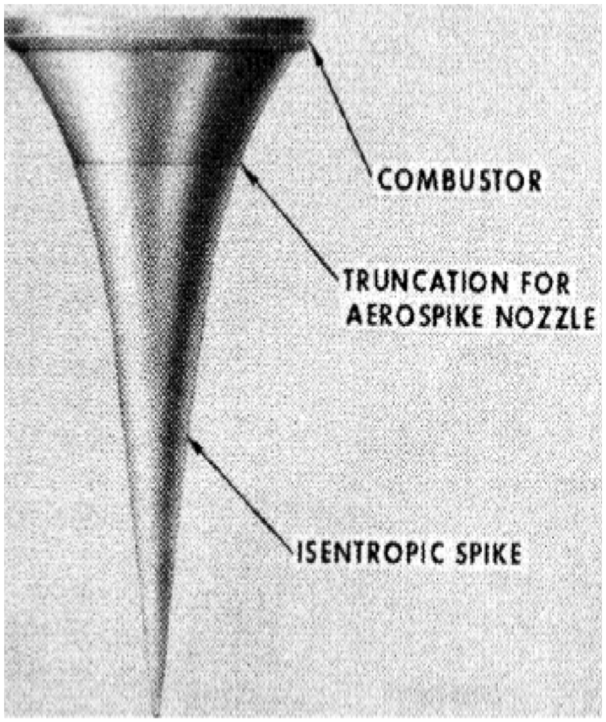

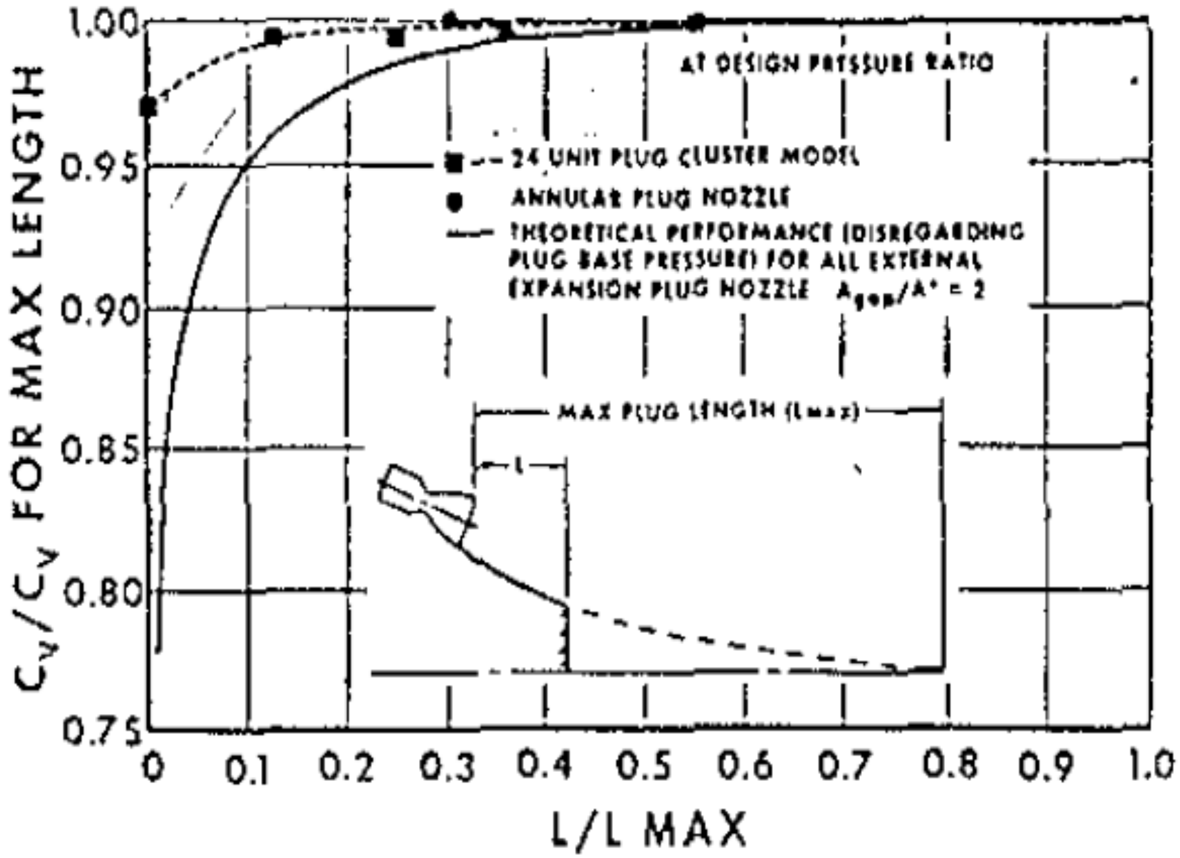

Effects are not as dramatic as one would think!

… At higher altitudes truncation hurts you less

Effects of Spike Truncation (6)

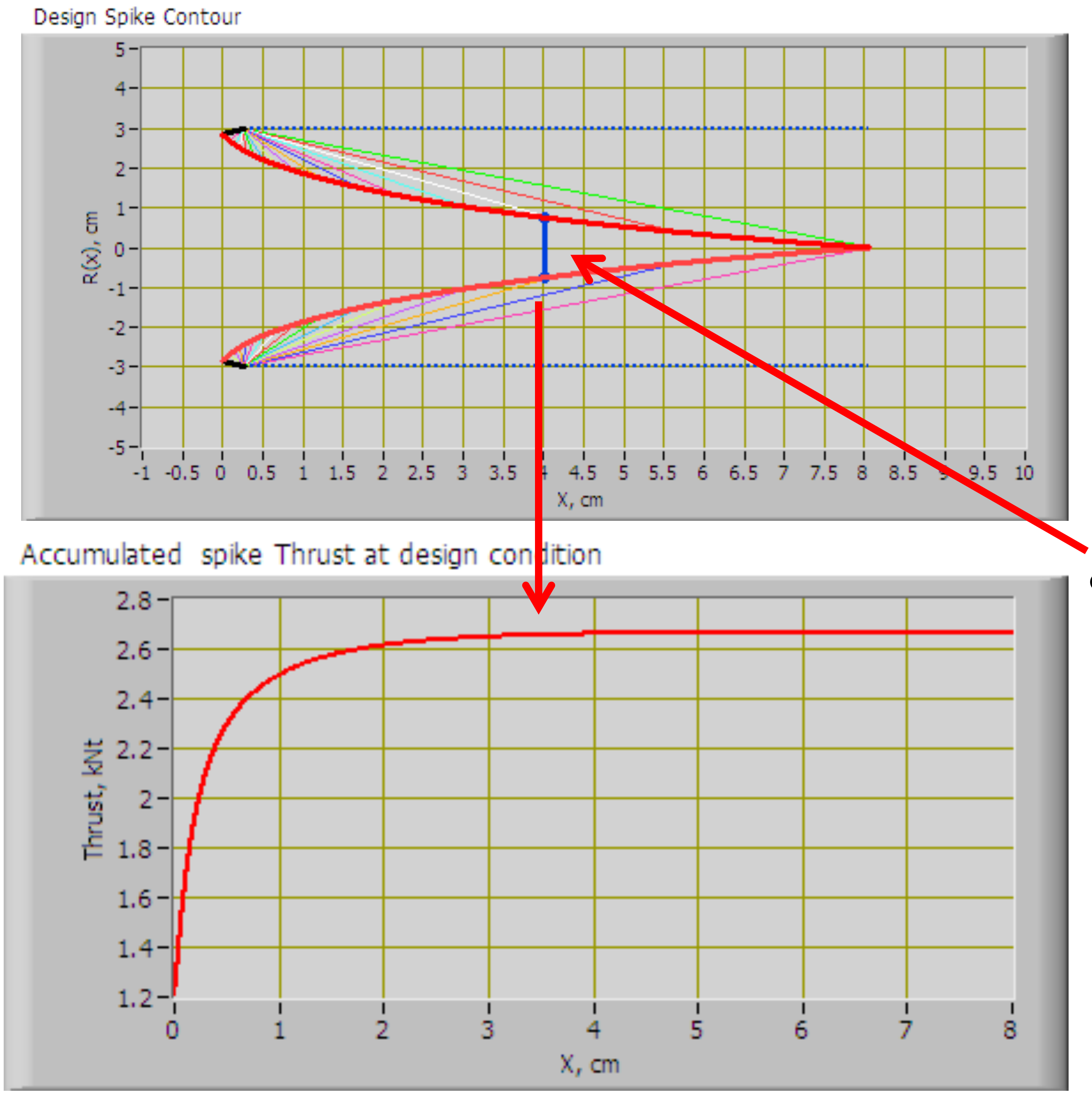

- Primary Loss is base drag

Effects of Spike Truncation (3)

Lift off

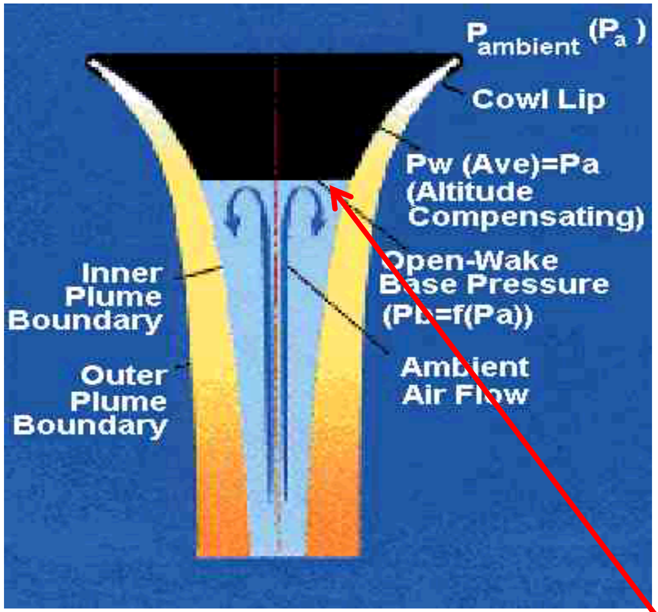

Vacuum (Space)

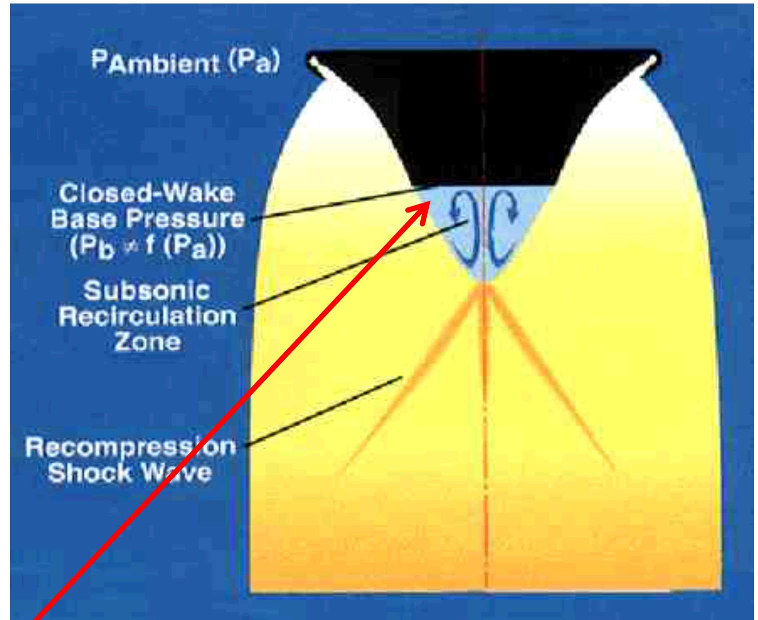

$$F_{base} = \left(p_{base} - p_{\infty}\right) \cdot \pi \cdot R_{base}^2$$

$$\nu_{base} = \nu_{trun} + \left(90^{\circ} - \theta_{trun}\right) \rightarrow M_{base} \rightarrow p_{base}$$

Effects of Spike Truncation (2)

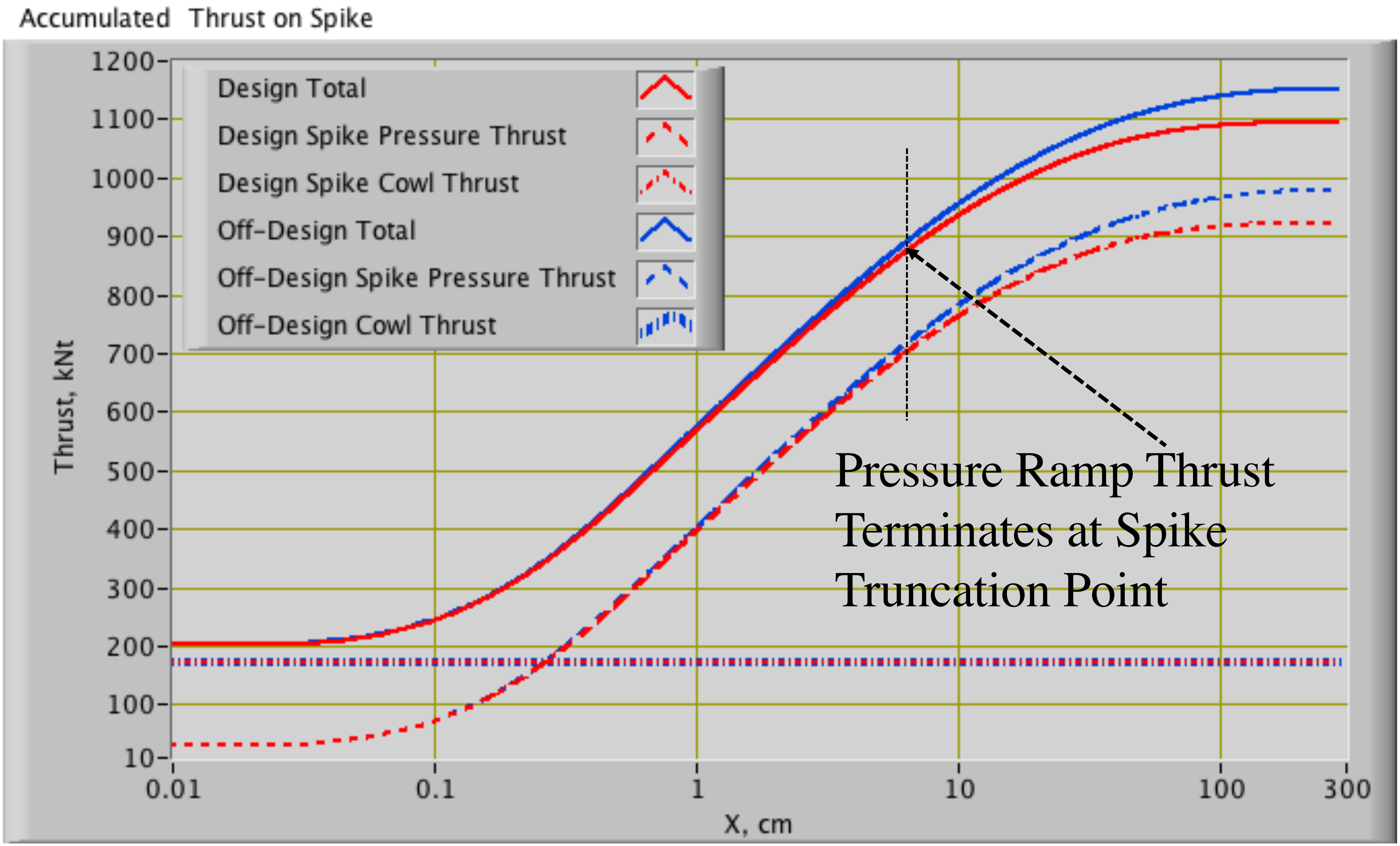

PLUG NOZZLES: SUMMARY OF FLOW FEATURES AND ENGINE PERFORMANCE

Marcello Onofri
University of Rome "La Sapienza", Roma, Italy
Chairperson of RTO/AVT WG 10 – Subgroup 1

The text is provided, as originally formatted, on the following pages.

PLUG NOZZLES: SUMMARY OF FLOW FEATURES AND ENGINE PERFORMANCE

Marcello Onofri
University of Rome "La Sapienza", Roma, Italy Chairperson of RTO/AVT WG 10 – Subgroup 1
AIAA 2002-0584
Onofri

terms of base pressure insensitivity to ambient pressure - can even occur when a closed recirculation bubble forms downstream of the base.

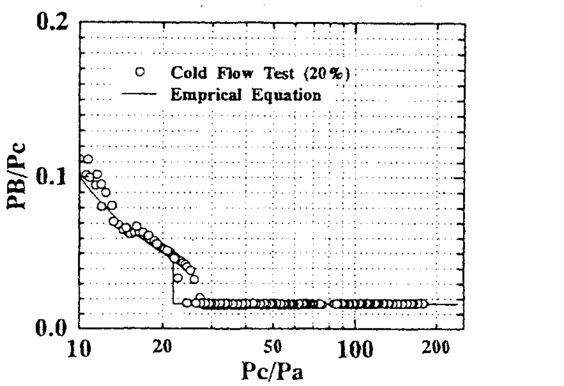

Fig. 5.2: Normalised base pressure versus PR. Experimental data from a linear aerospike nozzle cold gas model[21] compared with Hagemann's assumption[8].

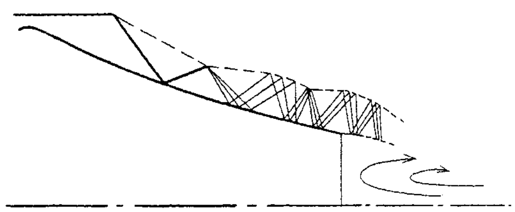

Text

Fig. 5.3: Subsonic open wake flow pattern downstream of a truncated plug nozzle base.

Furthermore, it is also possible that the separated inner shear layer does not reattach itself downstream of the base surface. This could be the case of a truncated plug nozzle with a large base surface comparatively to the annular section of the incoming supersonic jet, see Fig. 5.3. In such a base flow pattern, there is a ***subsonic open wake*** -really opened this time in terms of fluid mechanics-, and the base pressure is close to the ambient pressure. Thus, in that case, the problem is not to determine the base pressure, but to predict at which value of p_c/p_a the transition 'opening-closing' of the recirculation bubble occurs.

If the base flow pattern is a closed recirculation bubble, whatever the plug nozzle wake regime -closed or open-, then the determination of the base pressure in supersonic regime is submitted to the same flow physics, namely the physics of the ***'Supersonic Turbulent Flow Reattachment'***. Motivated by the base drag prediction not only for truncated plug nozzles but mainly for projectile and missile applications, the supersonic base flow physics have been extensively investigated in the world since the 50's. Thanks to many investigations performed downstream of the base of two-dimensional backward-facing steps, it has been derived analytical, pure-empirical and theoretico-empirical models as those presented below.

BASE PRESSURE PREDICTION

Pure empirical relationships

Fick et al.[20] have evaluated empirical relations of the base pressure versus constant incoming Mach number M_e and specific heat ratio. A comparison with the few available measurements showed that the two empirical relations issued from Ref. 30, see Eqs (5.1) and (5.2) below, failed to produce reliable results.

$$p_b = \frac{0.846 p_e}{M_e^{1.3}}, \qquad (5.1)$$

$$p_b = p_c\left(1 - 0.715\gamma\frac{M_e^{2.3} - 0.92 M_e^{2} - 0.03}{M_e^{2.7}}\right). \qquad (5.2)$$

A slighly better agreement was found[20] notably for 12-16% plug lengths if it was assumed that the base pressure results from a very simple averaging between pressure p_e at the truncated nozzle exit and pressure p_d at the exit of the hypothetical design full-length plug, as written below :

$$p_b = k(p_e + p_d); \quad with\ k = 0.5. \qquad (5.3)$$

When applied to linear aerospike nozzles, it was found[21] that the constant k had to be changed from 0.5 to 0.3 according to measured data.

Derived from cylinders and cones, an original empirical base-pressure model[31] has been changed in Ref. 20 by setting an exponent which should take into account the negative angle of the flow incoming the base region. For cold flow tests, and setting the exponent at 0.35, agreement with measured base pressure has been attainable with the "conical-approximation" equation below,

$$p_b = p_e\left(0.025 + \frac{0.906}{1 + \frac{\gamma - 1}{2} M_e^{2}}\right)^{0.35}. \qquad (5.4)$$

The empirical model derived in Re. 20 from a cylinder embedded in supersonic flow also gives a good agreement if Mach number M_e and a sonic pressure ratio are introduced, thus we obtain the "cylindrical-approximation" equation below,

$$p_b = p_e M_e\left(\frac{2}{\gamma + 1}\right)^{\frac{\gamma}{(\gamma - 1)}}\left(0.05 + \frac{0.967}{1 + \frac{\gamma - 1}{2} M_e^{2}}\right) \qquad (5.5)$$

Onofri et al.[32] have also evaluated Eqs. (5.4) and (5.5), and another plug nozzle base model proposed by

Rocketdyne, see Eq. (5.6) below*, and compared them with a new formula, see Eq. (5.7) below, applied to a clustered plug nozzle.

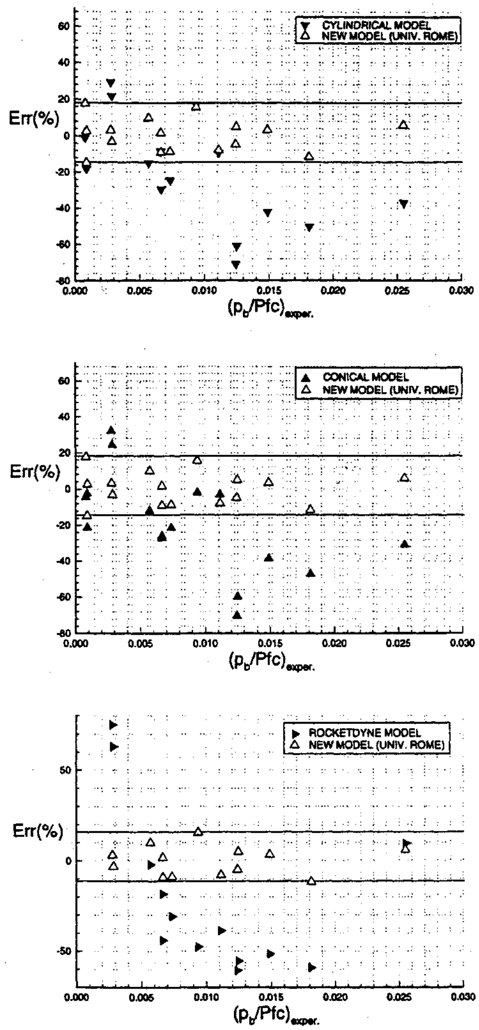

Fig. 5.4: Comparisons between base pressure purely-empirical relationships.

$$\frac{p_b}{p_c} = 0.58\frac{C_{F,\max,d} - C_{F,core}}{\varepsilon_b} \qquad (5.6)$$

$$p_b = p_e\left(0.05 + \frac{0.967}{1+\frac{\gamma-1}{2}M_e^{\,2}}\right)^{\Phi}, with \qquad (5.7)$$

$$\Phi = \frac{-0.2\phi^4 - 5.89\phi^2 + 20179.84}{\phi^4 + 20179.84}$$

* In eq. (5.6) $C_{F,max,d}$ indicates the ideal thrust coefficient at the design PR, $C_{F,core}$ the ideal thrust coefficient corresponding to the expansion ratio achieved at the transition point and ε_b the ratio between base and throat areas.

The results of this comparison, see Fig. 5.4, conclude that the model proposed by Univ. of Rome gives the smallest percentage of error [+19%,-15%] relatively to measured data.

The multi-component base-flow model

Preliminary remark

This theoretical approach is based on the flow partition into several regions or subdomains (viscous or inviscid) which are determined thanks to analytical and integral relationships. Flow subdomains are physically linked by semi-empirical relations, and the unicity of the solution is insured thanks to the using of a reattachment criterion. Such methods are able to predict the base pressure in various base configurations[24-26], and notably in case of truncated plug nozzles[26], with the two following reservations: 1) the computed configurations are two-dimensional, planar or axisymmetric, and 2) the base flow region is a closed recirculating-flow bubble. The following chapter is devoted to a brief description of these theoretical approaches, called multi-component methods.

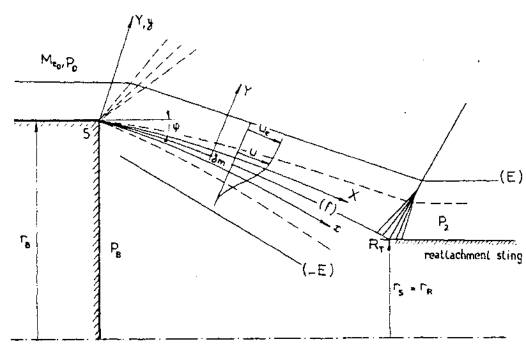

Fig. 5.5: Multi-component base flow model.

Model description

This model is derived from the well-known Korst model[22] for the supersonic separated flow reattaching behind a rearward facing step. As shown in Fig. 5.1a, the basic situation is that of a supersonic turbulent flow separating at a base shoulder S and reattaching further downstream on a wall or a sting in the vicinity of a point F. Mass injection at low velocity (base-bleed) can be performed in the dead air region.

In the spirit of this so-called Multi-Component approach, the flow is divided into four components or domains, Fig. 5.5:

a - The ***outer inviscid flowfield*** bounded by the isobaric boundary (f) along which the pressure is equal to the base pressure p_b. This boundary intersects the reattachment surface at the "ideal" reattachment point R_T. This supersonic outer inviscid flow can be computed by the Euler equations solved by the Method of Characteristics.

Calculations Using Prandtl/Meyer Expansion Theory

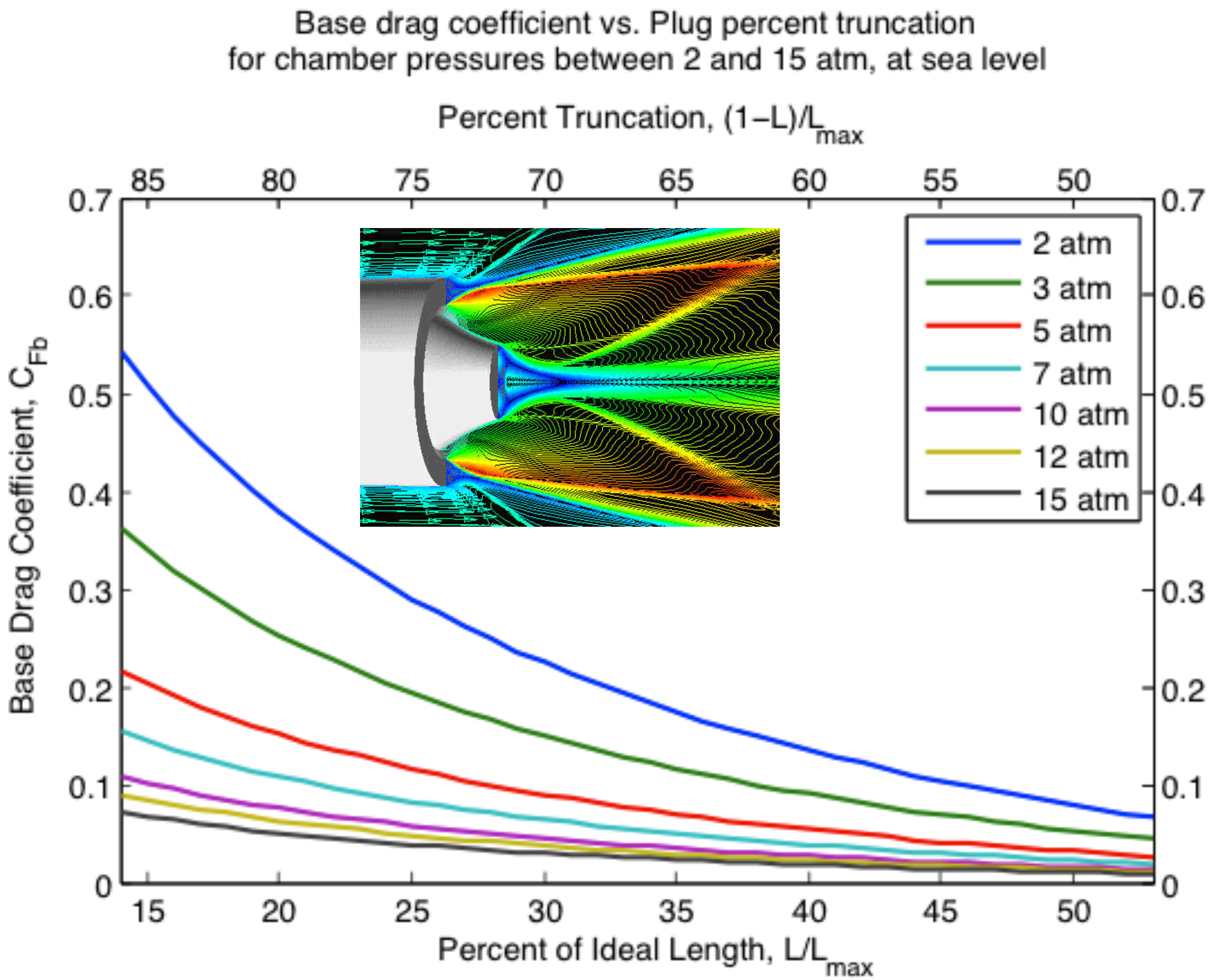

Thanks Matthew Wilson!

Calculations Using Prandtl/Meyer Expansion Theory (2)

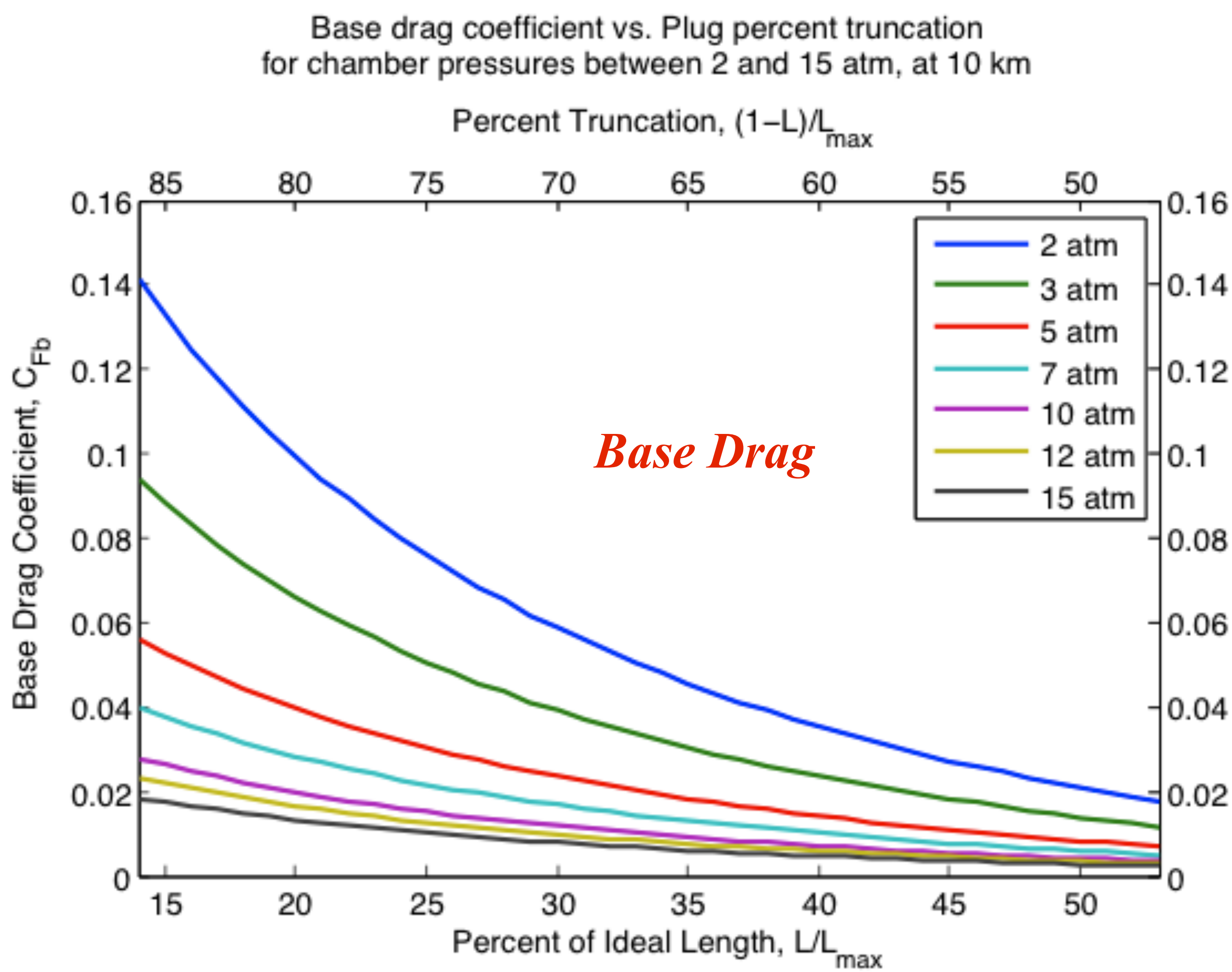

Thanks Matthew Wilson!

Truncated Spike Comparison to Minimum Length Nozzle

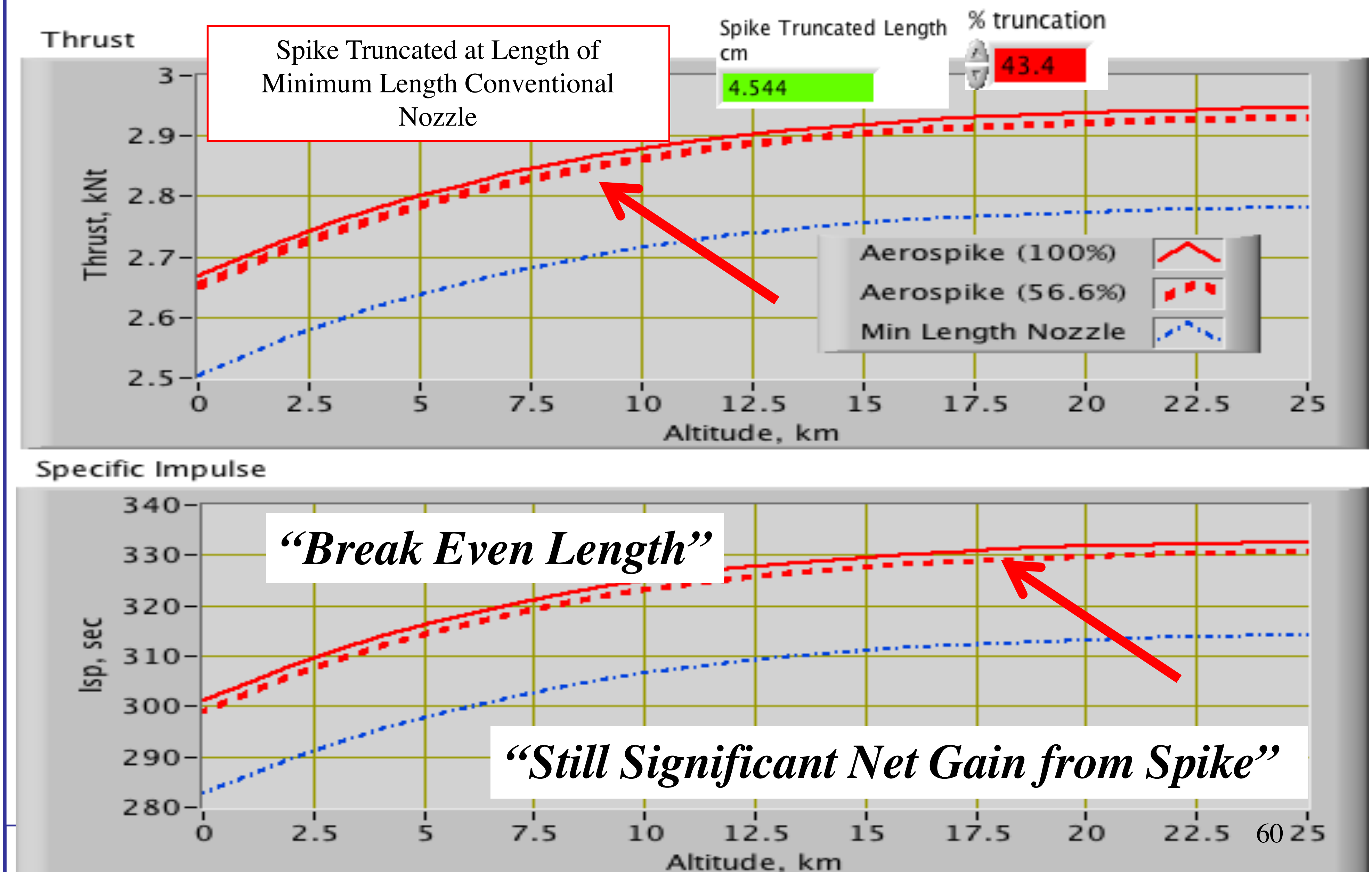

Utah State University

Mechanical & Aerospace Engineering

Truncated Spike Comparison to Minimum Length Nozzle(2)

Spike is Significantly Shorter Than Minimum Length Conventional Nozzle

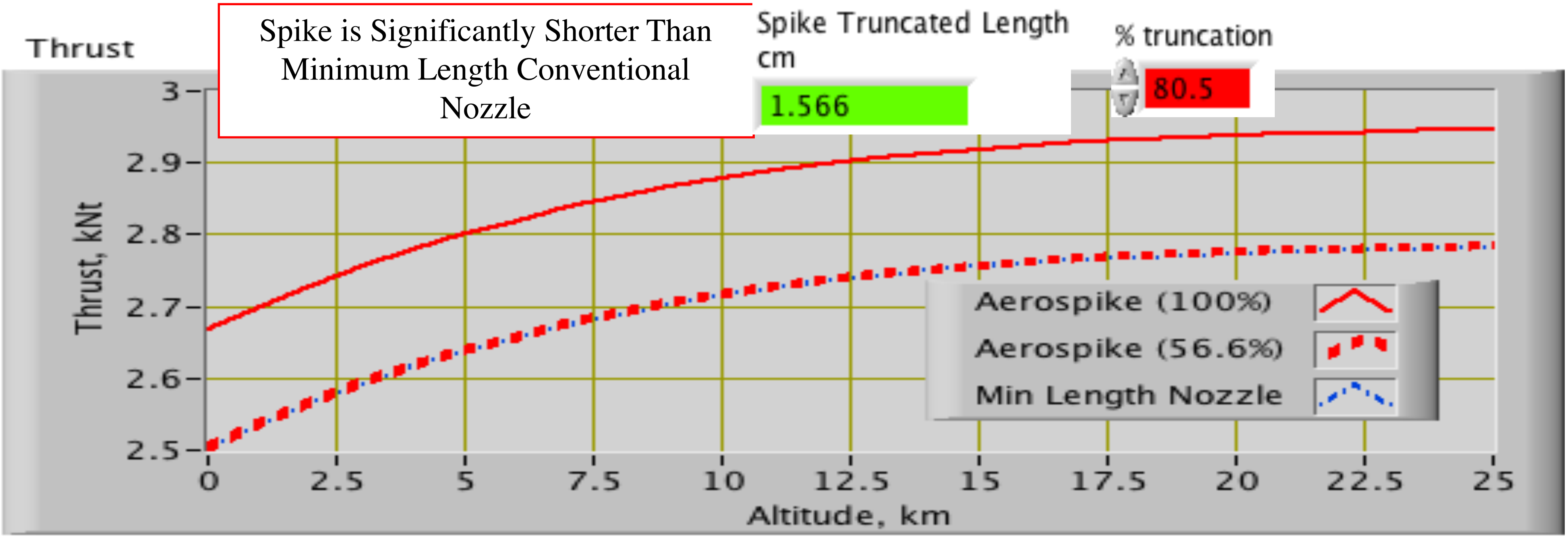

"Break Even Performance"

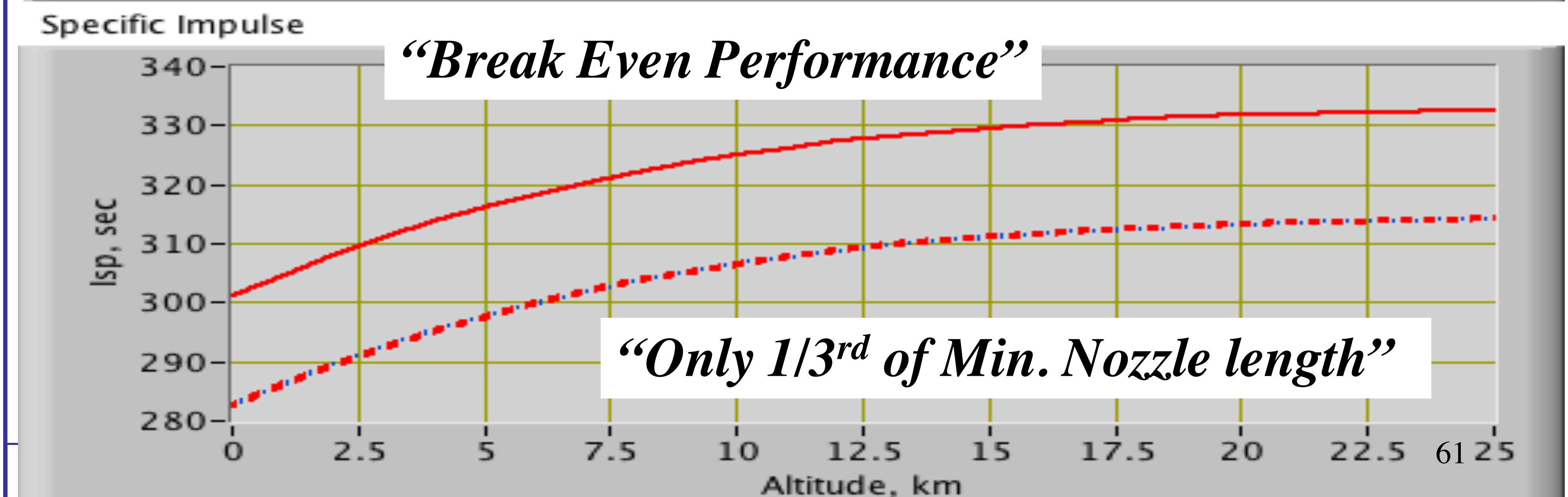

"Only 1/3rd of Min. Nozzle length"

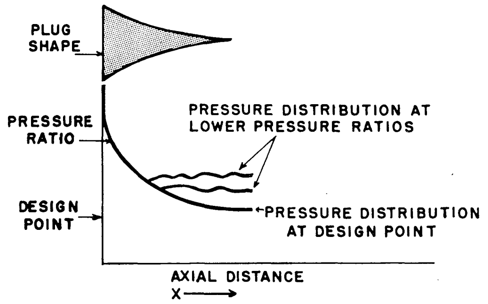

Fig. 6 Schematic illustration of pressure distribution along a fixed plug nozzle at various operating pressure ratios

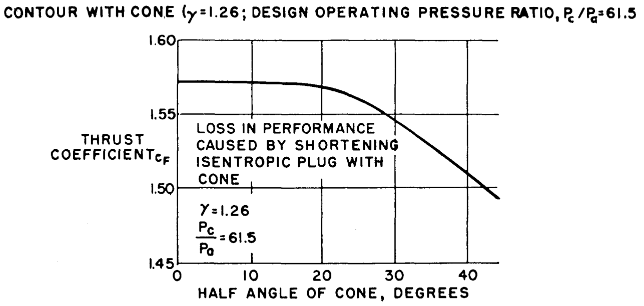

Fig. 7 Theoretical loss in performance caused by replacement of lower plug

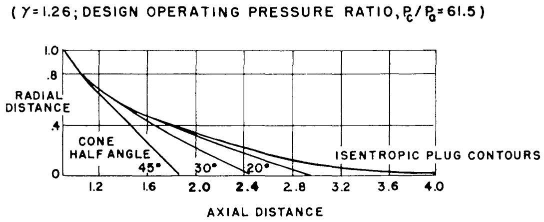

Fig. 8 Plug profiles for isentropic expansion and for shortened versions terminating with conical contours

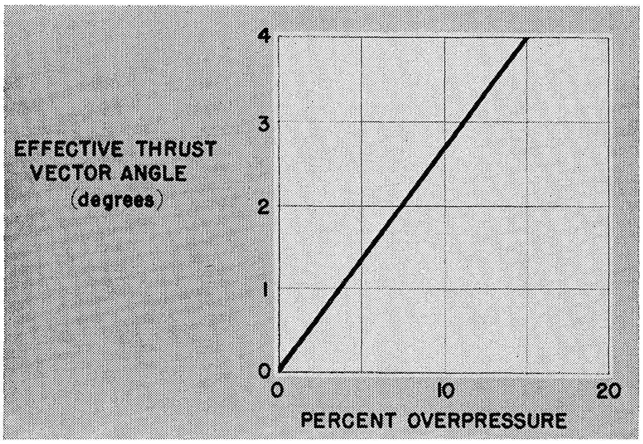

Fig. 9 Effect of per cent overpressure on effective thrust vector angle

thrust vector is concerned, can be shown to be additive. A typical set of data showing the variation of effective thrust vector angle with overpressure in the higher pressure combustor cell is shown in Fig. 9.

Application to Liquid Propellant Engine Design

The plug nozzle can be combined with annular combustors to form attractive liquid propellant propulsion system configurations. Fig. 10 represents an example of a plug-type turbopumped liquid propellant engine. The combustors are located around the base of the nozzle, and, in this particular unit, the turbine exhaust is brought out through the center of the nozzle. Such engines can be designed extremely short and compact to produce a well-packaged propulsion system. In fact, studies indicate that for identical thrust levels, the plug-type engines would be about half the length of conventional configurations as shown in Fig. 11 for a 1,500,000-lb thrust level. This makes them attractive not only for first-stage booster applications, but also for medium thrust size upper-stage propulsion systems. Similarly, the weight of the plug-type engine compares favorably with that of the conventional unit.

Application to Solid Rocket Engines

The problems and advantages of plug nozzle application to solid rocket engines differ considerably from those of liquid engines. Not all of the major advantages of liquid propellant plug nozzle engines such as thrust vector control, scaling, combustion stability and thrust structure simplification can be directly transposed to solid engine application. Gains unique to the application of plug nozzles to solid engines exist, but are generally not as compelling. Consequently, the advisability of converting to the plug from the cluster of four DeLaval nozzles typically employed in modern solid propellant rockets is not particularly clear-cut and depends to a large extent on the specific missile application intended.

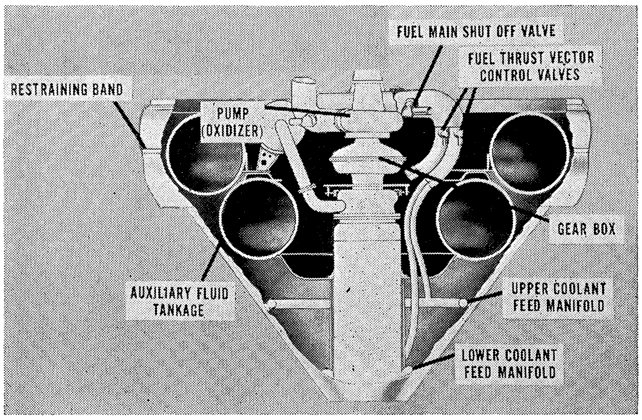

Fig. 10 Plug nozzle engine assembly

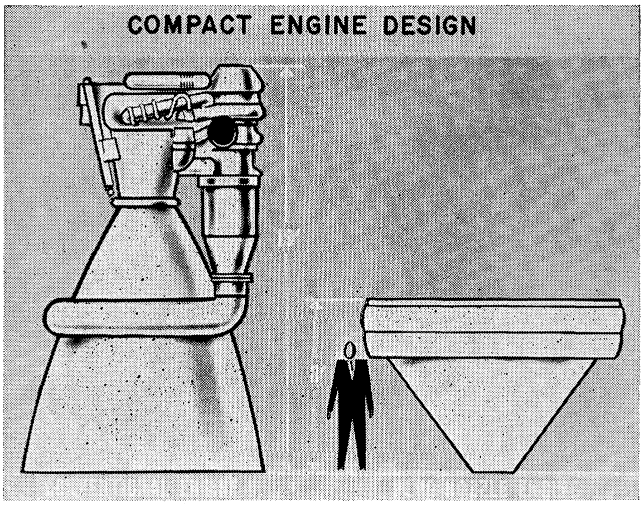

Fig. 11 Size of plug nozzle engine compared with that of conventional engine

Very High Expansion Ratio Spike Nozzles

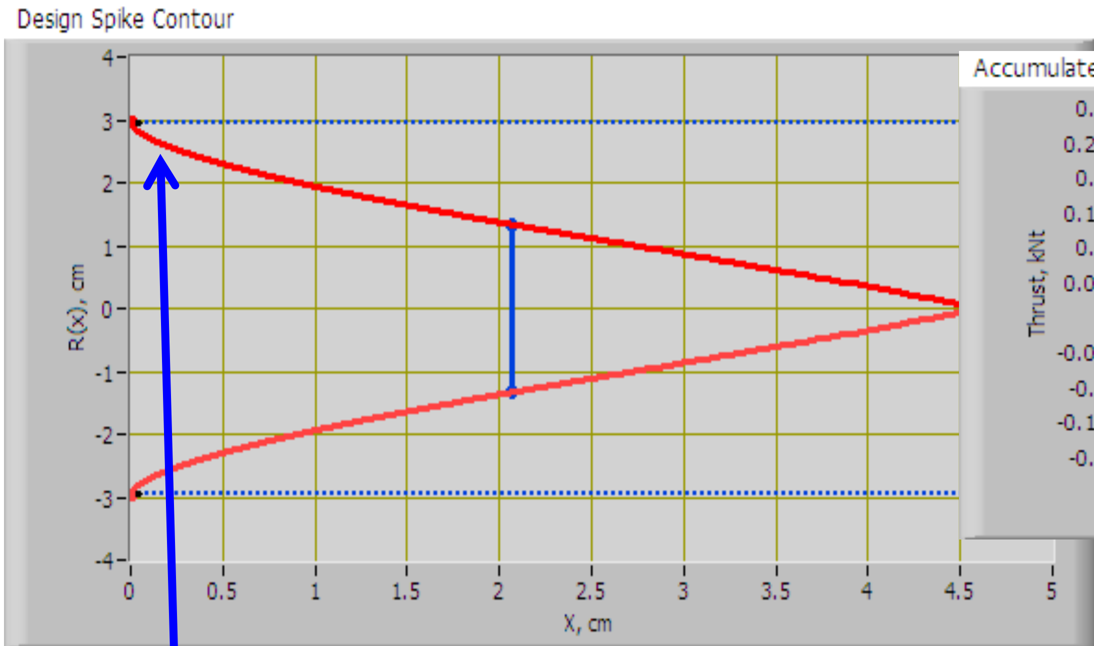

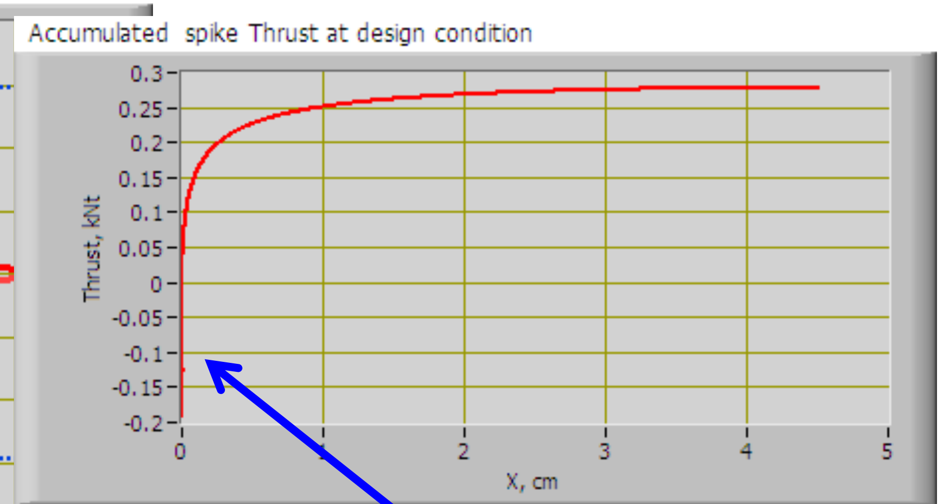

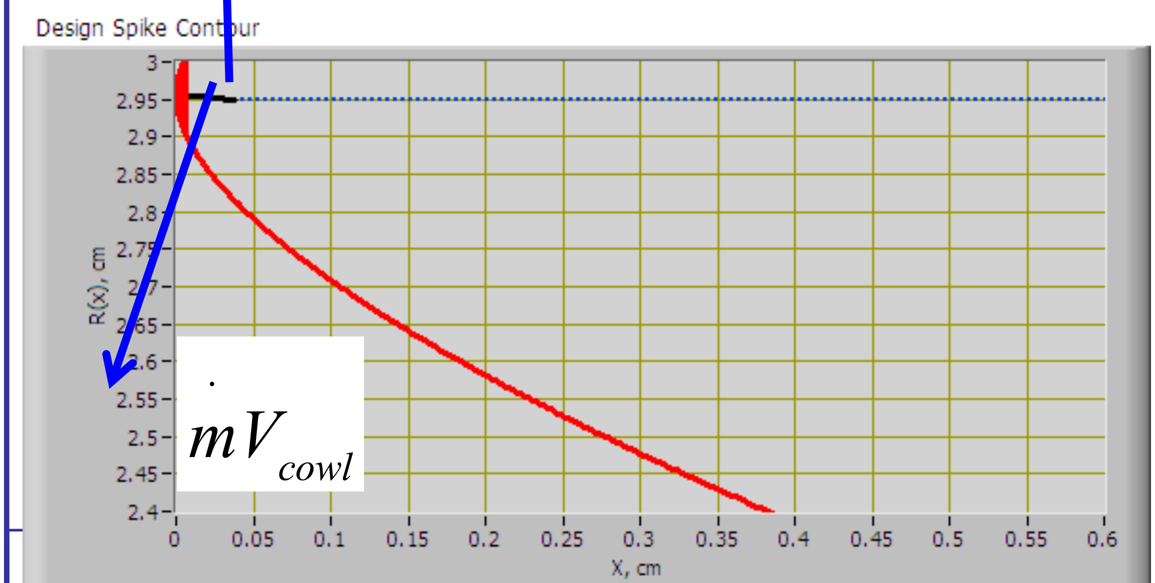

- Characteristic Line “bends backward” Near sonic line (cowl exit)
- Cowl exit momentum-thrust is *negative!*
- Very inefficient approach

Very High Expansion Ratio Spike Nozzles (2)

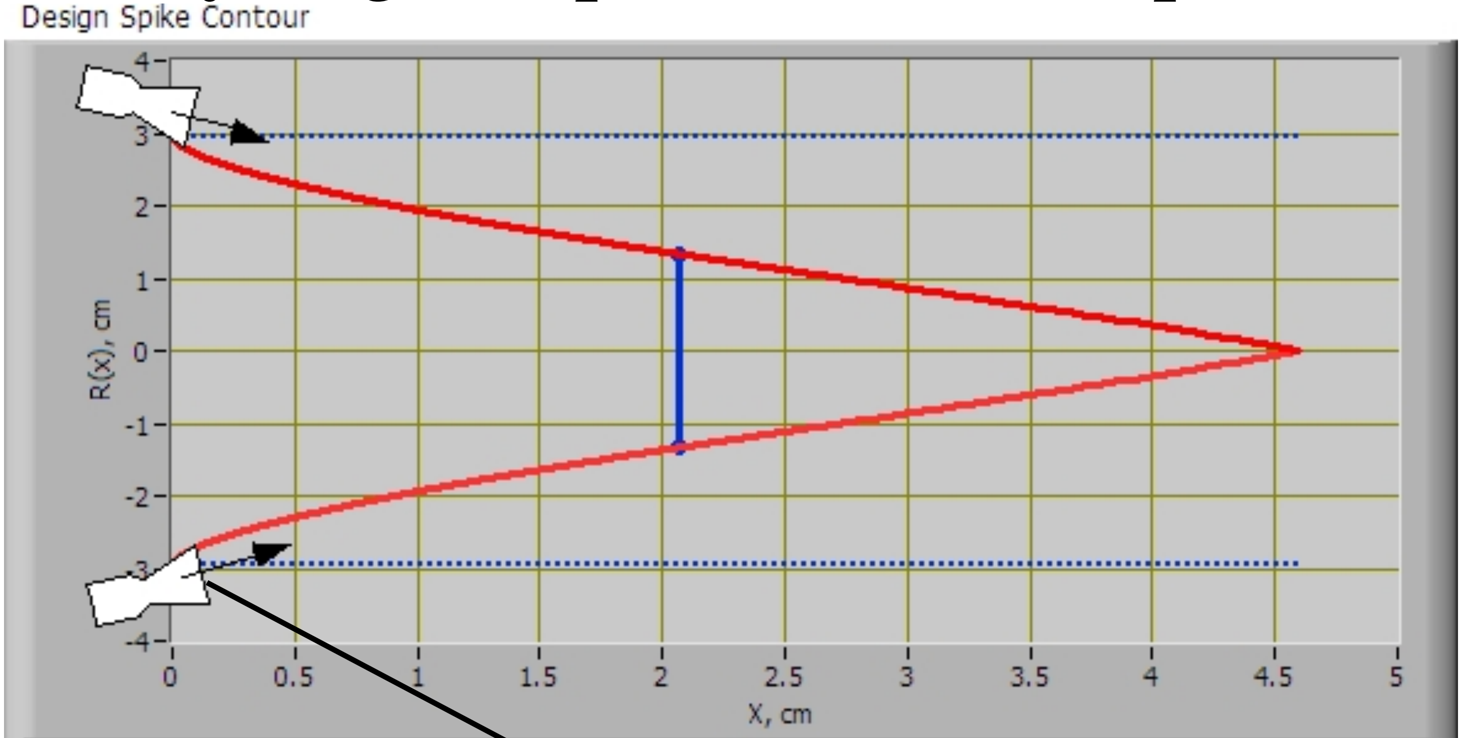

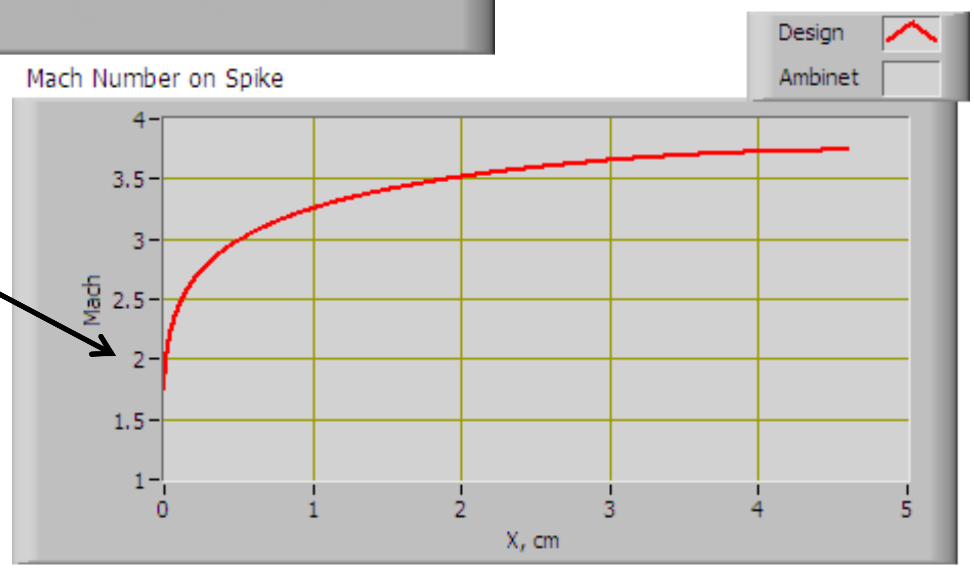

- Better Approach is to use supersonic cowl nozzle and position so exit mach and angle lines along spike characteristic line

Very High Expansion Ratio Spike Nozzles (3)

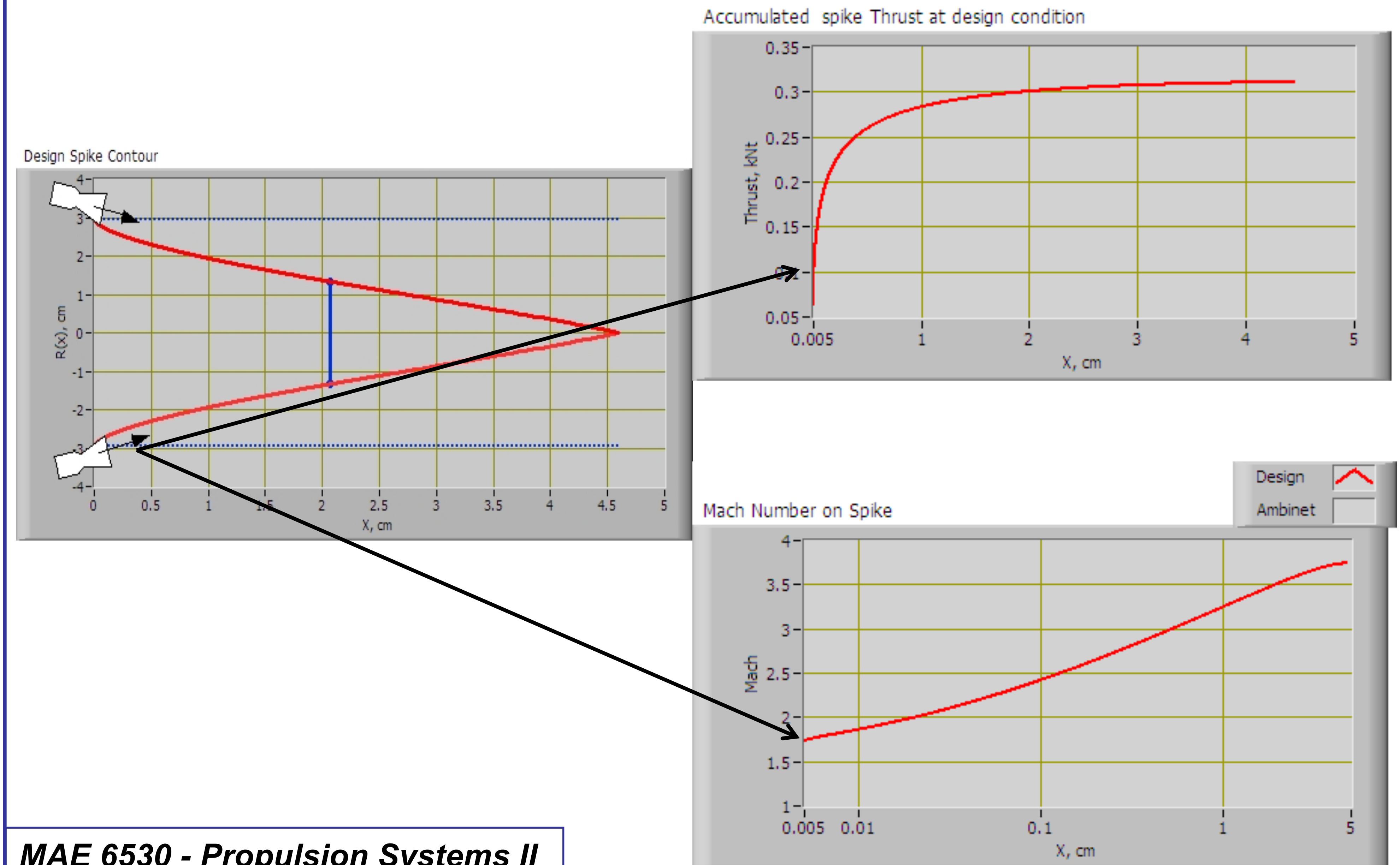

UtahState UNIVERSITY

Mechanical & Aerospace Engineering

Very High Expansion Ratio Spike Nozzles (4)

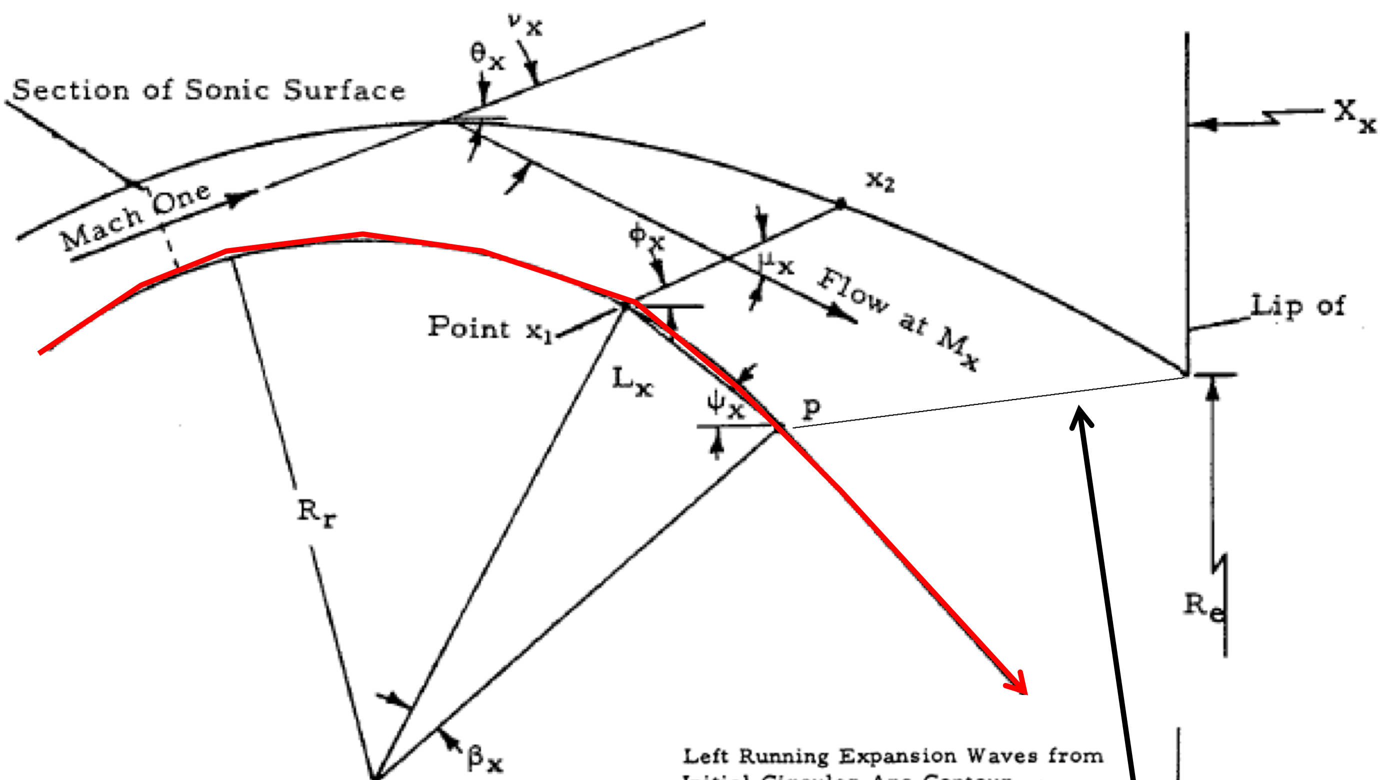

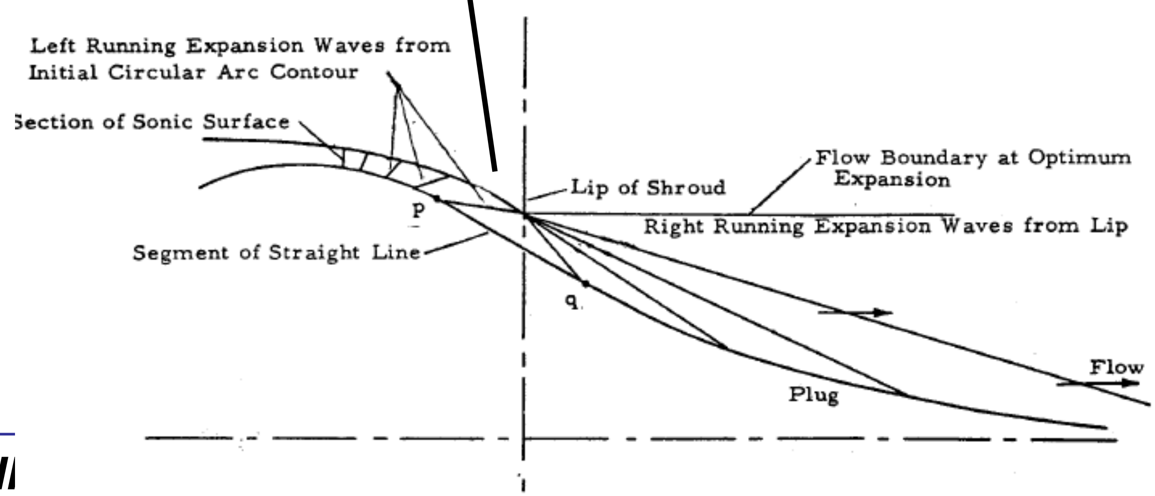

- Axi-symmetric supersonic cowl design

Very High Expansion Ratio Spike Nozzles (5)

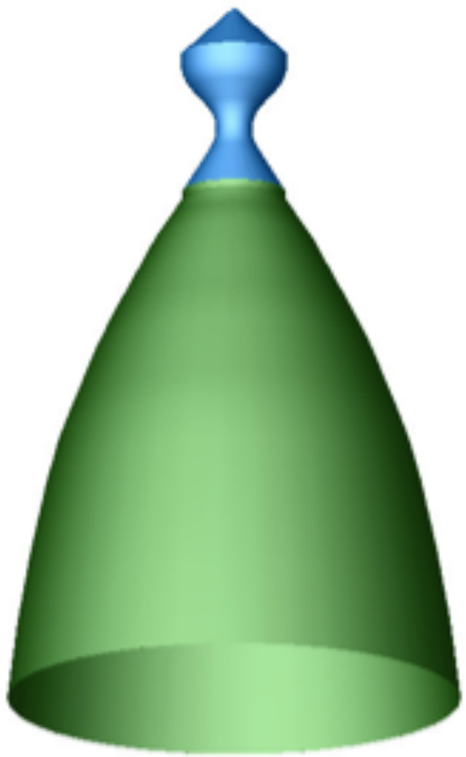

NOFB37 200:1 5500lbf Monopropellant Engine

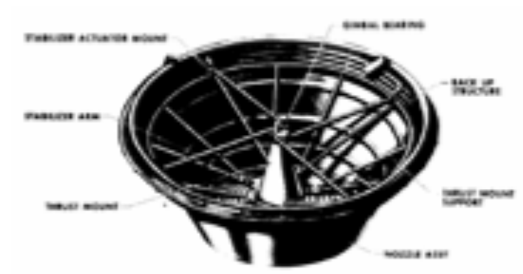

NOFB37 12 x 500 lbf (6000lbf) Monopropellant Engine

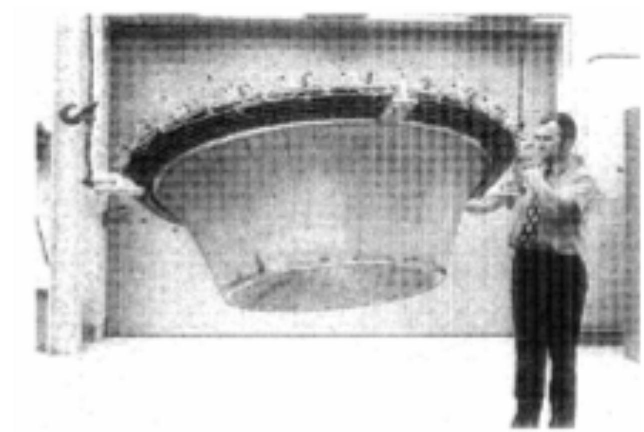

Figure 1 - Size comparison of a recently studied NOFB monopropellant lunar lander ascent engine for Altair program using a conventional bell nozzle vs. a 12-clustered aerospike plug. Far right is the original 15,000 lbf H_2/O_2 aerospike plug engine developed and tested by Rocketdyne in 1974 [2,4].